Cellular and Molecular Mechanisms Underlying Vulnerability and Resilience to Noise-Induced Tinnitus

by

Shuang Li

B.S. in Biomedical Engineering, Tsinghua University, 2009

Submitted to the Graduate Faculty of

School of Medicine in partial fulfillment

of the requirements for the degree of

Doctor of Philosophy

University of Pittsburgh

2014

UNIVERSITY OF PITTSBURGH

SCHOOL OF MEDICINE

This dissertation was presented

by

Shuang Li

It was defended on

Dec 16th, 2014

and approved by

Dr. Karl Kandler, Professor, Otolaryngology and Neurobiology

Dr. Elias Aizenman, Professor, Neurobiology

Dr. Brent Doiron, Associate Professor, Mathematics

Dr. Alison Barth, Professor, Department of Biological Sciences, Carnegie Mellon University

Dr. John Huguenard, Professor, Department of Neurology and Neurological Sciences, Stanford University

Dissertation Advisor: Dr. Thanos Tzounopoulos, Associate Professor, Otolaryngology and Neurobiology

Cellular and Molecular Mechanisms Underlying Vulnerability and Resilience to Noise-Induced Tinnitus

Shuang Li, PhD

Tinnitus, the perception of phantom sound, is often a debilitating condition that affects many millions of people. Little is known, however, about the molecule that underlies vulnerability and resilience to tinnitus. We investigated these mechanisms in the dorsal cochlear nucleus (DCN), an auditory brainstem nucleus that is essential for the induction of tinnitus. In DCN principal neurons (fusiform cells), we reveal a tinnitus-specific increase in the spontaneous firing rate (hyperactivity). We show that a reduction in Kv7.2/3 (KCNQ2/3) channel activity is essential for tinnitus induction and for the tinnitus-specific hyperactivity. This reduction is due to a shift in the voltage-dependence of KCNQ channel activation to more positive voltages. Importantly, *in vivo* pharmacological manipulation that shifts the voltage-dependence of KCNQ channels to more negative voltages prevents the development of tinnitus and provides an important link between the biophysical properties of the KCNQ channel and the vulnerability to tinnitus. Fusiform cells from noise-exposed mice that show resilience to tinnitus (non-tinnitus mice) display normal levels of spontaneous firing, but have more hyperpolarized subthreshold dynamics and more hyperpolarized resting membrane potential. These differences are due to a reduction in hyperpolarization-activated cyclic nucleotide-gated (HCN) channel activity. Longitudinal study reveals that 4 days after noise exposure, noise-exposed mice display non-tinnitus behavior, no fusiform cell hyperactivity, but reduced KCNQ2/3 currents. Importantly, while the preservation of reduced KCNQ2/3 currents 7 days after noise exposure gives rise to tinnitus behavior, the recovery of KCNQ2/3 currents to pre-exposed control levels is associated

with non-tinnitus behavior, and is accompanied by a decrease in HCN channel activity. *In vivo* pharmacological opening of KCNQ2/3 channels prevented the development of tinnitus and decreased HCN currents, suggesting that KCNQ2/3 plasticity determines vulnerability and resilience to tinnitus and drives the reduction in HCN channel activity. Reduced HCN channel activity in non-tinnitus mice, by hyperpolarizing the resting membrane potential, may further prevent fusiform cell hyperactivity and contribute to tinnitus resilience. Together, our results highlight KCNQ2/3 and HCN channels as potential targets for designing therapeutics that may reduce vulnerability and promote resilience to tinnitus.

TABLE OF CONTENTS

LIST OF TABLES

LIST OF FIGURES

LIST OF SUPPLEMENTAL FIGURES

LIST OF ABBREVIATIONS

ABR: auditory brainstem response

ACSF: artificial cerebral spinal fluid

ASR: acoustic startle reflex

AU: arbitrary unit

BFNC: benign familial neonatal convulsion

C terminus: carboxy terminal

cAMP: cyclic adenosine monophosphate

CaM: calmodulin

CNS: central nervous system

CS: conditioned stimulus

dB: decibel

DCN: dorsal cochlear nucleus

DRG: dorsal root ganglion

EC: entorhinal cortex

EMG: electromyography

HPA: hypothalamus-pituitary-adrenal

ICR: imprinting control region

IC50: half maximal inhibitory concentration

P-: Postnatal

PIP_2: phosphatidylinositol 4,5-bisphosphate

PMT: pontomesencephalic tegmentum

PnC: reticularis pontis caudalis

PPI: prepulse inhibition

RMP: resting membrane potential

SEM: standard error of the mean

SPL: sound pressure level

US: unconditioned stimulus

PREFACE

I would first like to thank my advisor, Dr. Thanos Tzounopoulos, for providing the exceptional support and advice throughout my PhD study. He continuously motivates and encourages me to push forward during my dissertation research. I will always remember the days when we discussed about scientific questions, designed extremely telling experiments, as well as made better and better versions of our manuscripts. I would also like to thank members of my Advisory Committee: Drs. Karl Kandler, Elias Aizenman, Brent Doiron, and Alison Barth. They have given me so many prudent advices from all different perspectives. I would like to express special gratitude to Dr. Karl Kandler for serving as my committee chair. I would also like to thank Dr. Brent Doiron for giving me a solid foundation on neural computation and modeling skills during my research project, and for our numerous great conversations. I am grateful to Dr. Elias Aizenman and Dr. Alison Barth, their challenging questions and discussion motivated me to do better. Finally, I would like to thank my outside examiner, Dr. John Huguenard, for taking time to participate in my defense.

I would also like to thank all the members of Tzounopoulos laboratory. In particular, I would like to thank Dr. Yanjun Zhao, Dr. Tamara Perez-Rosello, and Dr. Charles Anderson for their support both professionally and personally in the lab. Finally, I would like to dedicate my dissertation to my parents, for their continual and unwavering support. I thank you all for supporting me throughout this wonderful journey in Pittsburgh.

1.0 INTRODUCTION

Tinnitus, perceptions of sounds in the absence of sound stimulus, is a common auditory disorder that can be detrimental to the quality of life for millions of tinnitus sufferers. An estimated 5 – 15% of the population experiences chronic tinnitus; many millions of those have incapacitating symptoms (Axelsson and Ringdahl, 1989; Heller, 2003; Roberts et al., 2010; Shargorodsky et al., 2010). With an even higher prevalence of chronic tinnitus in recent war veterans (Yankaskas, 2012), the personal and financial costs of tinnitus have expanded dramatically. Despite the high prevalence of the disorder, the mechanisms that lead to tinnitus remain poorly understood. As a result, there is no generally accepted treatment, cure or preventive method for tinnitus. Therefore, to improve therapeutic methods for treating tinntius, it is critical to understand the pathophysiology that is causally linked to the development of tinnitus.

1.1.1 Central origin of noise-induced tinnitus

Tinnitus is frequent sequelae of acoustic overexposure (noise-induced tinnitus)(Tyler et al., 2007; Shargorodsky et al., 2010). Noise exposure primarily damages the auditory periphery (cochlea) and causes hair cell loss (Wang et al., 2002), ganglion cell degeneration (Kujawa and Liberman, 2006) and reduces auditory nerve activty (Liberman and Kiang, 1978; Schaette and

McAlpine, 2011). For many years, the peripheral auditory system was assumed to be the anatomical location where the pathology that led to tinntius was generated. However, as tinnitus can occur in deaf individuals and after sectioning of the auditory nerve (House and Brackmann, 1981; Berliner et al., 1992), it is now evident that the pathology that causes tinnitus is mostly in the central nervous system (CNS)(Tonndorf, 1987; Jastreboff, 1990). Therefore, a fundamental question is what is the abnormality of CNS that leads to the phantom perception of sound.

1.1.2 Behavioral models for evaluating tinnitus in animals

To investigate the cellular and molecular mechanisms underlying noise-induced tinnitus, successful assessment of tinnitus in animal is critical. Behavioral approaches to test tinnitus in animal models have adopted three major paradigms: Pavlovian conditioning, operant conditioning, and reflexes (von der Behrens, 2014). In Pavlovian conditioning, animals perform a preferable behavior (e.g. water licking) while a continuous sound is played. Ceasing of the sound (no sound, conditioned stimulus, CS) is followed by a punishment signal (unconditioned stimulus, US, e.g. footshock), leading to suppression of the preferable behavior during the CS stimulus (Jastreboff et al., 1988b; Jastreboff et al., 1988a; Heffner and Harrington, 2002). By measuring suppression of the preferable response, the ability to perceive no sound can be evaluated. After tinnitus induction, conditioned suppression that is related to perception of no sound reduced, indicating the spontaneous hearing of a sound, i.e. tinnitus (Heffner and Harrington, 2002). The relatively fast training process of Pavlovian paradigm enables a large number of animals to be assessed. However, as the association of no sound perception and suppression of the preferable behavior is dependent on the establishment of fear, and that CS is given only during the training period, the suppression of preferable response extinguishes

overtime and prevents the assessment of tinnitus over a long time (von der Behrens, 2014). Operant conditioning addresses this limitation. Operant conditioning is based on the training of the animal to take a special action (e.g. pressing a lever) to achieve a desirable stimulus (e.g. obtaining a food pellet). Punishment stimulus is given to suppress the operant behavior during no sound stimulus. Different from Pavlovian conditioning where the punishment signal is given only during the training session, the operant model also applies punishment during the testing session, which eliminates the extinguishment of the suppression behavior and enables the assessment of tinnitus behavior over extended periods. The disadvantage of this approach, however, is the requirement for repeated long-lasting training to reach the criteria for performing the behavioral testing (Bauer and Brozoski, 2001).

In 2006, Turner et al. introduced the gap startle paradigm as a high throughput method for screening tinnitus in animals that does not require training. This paradigm is based on the acoustic startle reflex (ASR) system. The ASR is elicited by acoustic stimuli more than 80-decibel sound pressure level (dB SPL) and with a steep onset (Kehne and Davis, 1984; Pilz et al., 1987). The acoustic stimuli excite neurons in the cochlear root nucleus and the auditory brainstem nucleus, which further project to the nucleus reticularis pontis caudalis (PnC) in the brainstem. Neurons in PnC in relay excite spinal interneurons and motor neurons that initiate a startle response (Kehne and Davis, 1984; Lee et al., 1996). A sound gap embedded in the otherwise continuous background sound that is delivered 10 - 300 ms before the startle stimulus inhibits the amplitude of the startle response (Leitner et al., 1993). Therefore, perception of tinnitus could be evaluated based on the inability of animals to show inhibition of ASR that is normally elicited by the silent gap. Previous study revealed that in normal rats, a pre-startle sound gap suppressed the startle amplitude (Turner et al., 2006b). However, after salicylate

(Turner and Parrish, 2008) or acoustic trauma (Turner et al., 2006b), animals display reduced inhibition of startle stimulus by the sound gap, ostensibly indicating that the gap is filled by a sound perception and is considered a perception of tinnitus. The ASR-based gap detection paradigm is not dependent on learning. Therefore, it could be applied to a large amount of animals with a short amount of time for behavioral measurements. The disadvantage of the ASR-based paradigm is that damage of the auditory and/or startle reflex system may lead to a false positive assessment of the tinnitus behavior (Lobarinas et al., 2013). Therefore, measurement of hearing ability through auditory brainstem response (ABR) and evaluation of ASR function is important for the interpretation of tinnitus behavior.

1.1.3 Application of gap detection paradigm to test tinnitus in humans

Due to the subjectivity of tinnitus perception in humans, evaluation of tinnitus in human patients has been relient on self-reporting, visual analog scale and questionnaires (Fournier and Hebert, 2013). Objectification of tinnitus measurements in humans is highly demanded. Given the development of ASR-based assessment of tinnitus in animals (Turner et al., 2006b), attempts have been made to apply similar methods to measure tinnitus in humans. Instead of measuring muscle twitching, electromyography (EMG) activity of the eye blink in human subjects is recorded as the indication for the strength of the startle response (Blumenthal et al., 2006). Similar to the gap effect in suppressing startle response in animals, introduction of a sound gap 30 - 500 ms before the startle stimulus led to a significant suppression of the startle response in human subjects with normal hearing and no tinnitus (Fournier and Hebert, 2013). Patients with high frequency tinnitus, however, show reduced suppression of the eye blinking by a sound gap. Importantly, although tinnitus patients report high frequency tinnitus (16 kHz and 11.3 kHz),

they show reduced gap-mediated suppression of eye blinking with both low (500 Hz) and high (4 kHz) background noise. This contradiction indicates that deficit of gap detection may not reveal purely the filling effect of tinnitus into the gap. Instead, it may reveal changes in the functional activity of one or more central neural structures that compose the gap detection circuit. Given that inhibition of the startle response by a prepulse sound (prepulse inhibition, PPI) is intact in tinnitus patients, and that gap detection but not PPI is dependent on cortical activation (Ison et al., 1991), it is probable that changes in the cortical processing lead to gap detection deficits in tinnitus patient. This possibility is consistent with previous findings that auditory cortex plays an essential role underlying tinnitus generation (Eggermont and Roberts, 2004) and that numerous neural correlates of tinnitus haven been detected in auditory cortex, including cortical reorganization, neuronal hyperactivity and hyper synchrony (Muhlnickel et al., 1998; Weisz et al., 2005; Engineer et al., 2011b; Shetake et al., 2012).

1.1.4 Neural correlates for noise-induced tinnitus

Study on noise-induced tinnitus has been focused on chronic phase, when symptom of tinnitus stabilizes. Significant progress has been made revealing that decrease in auditory nerve inputs leads to pathogenic neuronal plasticity and results in hyperexcitability of dorsal cochlear nucleus (auditory brainstem) and hyperexcitability of inferior colliculus (auditory midbrain) (Kaltenbach and Afman, 2000; Brozoski et al., 2002a; Ma et al., 2006), increased spontaneous activity, increased neural synchrony and tonotopical reorganization of primary auditory cortex (Norena and Eggermont, 2003; Roberts et al., 2008; Engineer et al., 2011b), and ultimately to stimulus-independent perception of sound (Yang et al., 2011). However, little is known about the plasticity mechanisms that initiate tinnitus. Elucidation of these mechanisms will lead to the

development of drugs and therapies that can be applied soon after acoustic trauma, thus preventing tinnitus from becoming permanent and irreversible.

1.1.5 Heterogeneous susceptibility to noise-induced tinnitus

Although the development of tinnitus is strongly correlated with acoustic trauma and noise-induced hearing loss (Liberman, 1990; Henderson and Hamernik, 1995), the absence of tinnitus after exposure to loud sounds -- resilience to tinnitus -- has been observed in a significant percentage of the population both in humans and in tinnitus animal models (Li et al., 2013; Yankaskas, 2013). Unlike other disorders where genetic and epigenetic factors play essential roles in determining vulnerability (Taylor et al., 2011; Bell et al., 2014b; Denk et al., 2014), vulnerability to noise-induced tinnitus cannot be explained by genetic factors (Kvestad et al., 2010), suggesting that the boundary between susceptibility and resilience to tinnitus may be malleable. Therefore, elucidating the molecular mechanisms underlying resilience to tinnitus could be vital for both developing natural ways to prevent and treat tinnitus, and understanding the mechanisms that differentiate pathogenic plasticity that leads to tinnitus from homeostatic plasticity that prevents the induction of tinnitus.

1.1.6 Dorsal cochlear nucleus is critical for the induction of noise-induced tinnitus

The dorsal cochlear nucleus (DCN) is an auditory brainstem nucleus that receives direct input from the auditory nerves (Oertel and Young, 2004). It processes the complex spectral pattern of the acoustic signal after the filtering effect of the pinna, and determines the sound

localization in the vertical plane (Young et al., 1992; Imig et al., 2000). Though previous study revealed that DCN is not necessary for the maintenance of tinnitus (Brozoski and Bauer, 2005), DCN is indispensible in the induction of tinnitus: bilateral DCN lesions before noise exposure prevents the development of tinnitus (Brozoski et al., 2012a). This inability to induce tinnitus is not due to a disruption in the afferent pathway that one might expect in case of cochlear ablation. In one hand, DCN does not participate in determining the hearing threshold (Masterton et al., 1994; Sutherland et al., 1998). More importantly in another, unilateral DCN lesion ipsilateral to the noise exposure side, in which case similar disruption on afferent pathway has been made, could not prevent tinnitus (Brozoski et al., 2012b). Therefore, DCN is the important link that enables the noise-induced peripheral trauma to trigger pathogenic plasticity in the central nervous system.

1.1.7 General mechanisms underlying the induction of tinnitus and the induction of neuropathic pain

The fact that tinnitus sufferers detect sound in the absence of acoustic stimulation leads to the conclusion that tinnitus is a phantom perception of sound (House and Brackmann, 1981; Berliner et al., 1992). A similar phantom perception-related neural disorder is neuropathic pain. Normally after damage in peripheral sensory tissue, inflammatory mediators are released (von Hehn et al., 2012). Those inflammatory mediators excite unmyelinated (C-) and thinly myelinated (Aδ-) primary afferent neurons and lead to change in neuronal activity of sensory fibers that are frequently accompanied by a decrease of in pain threshold as well as an increase in pain sensitivity (Scholz and Woolf, 2007; Basbaum et al., 2009). Those stimulus-driven pain sensations are reversible, serving as a protection mechanism and promoting tissue healing.

However, in neuropathic pain the nervous system itself is damaged and causes a decrease in pain threshold and an increase of pain sensitivity that does not depend on appearance of the pain-eliciting stimulus. Perception of pain in this case is input-independent and becomes a chronic phantom perception -- neuropathic pain (Baron, 2000).

Tinnitus is frequently generated following damage into the peripheral auditory system that leads to reduced auditory nerve inputs into the central auditory system (Liberman and Kiang, 1978; Schaette and McAlpine, 2011). Decreased auditory nerve inputs is followed by hyperactivity of principle cells in the DCN, which is a consistent neural correlate for tinnitus (Kaltenbach and Afman, 2000; Brozoski et al., 2002a; Kaltenbach et al., 2005; Middleton and Tzounopoulos, 2012). Similarly, neuropathic pain is initiated by injury of the peripheral sensory nerve, leading to neuronal death, degeneration of nerve terminals, loss of peripheral axons, damage in central terminals etc. (von Hehn et al., 2012). Peripheral nerve injury further triggers continuous or burst firing in the primary sensory neuron in the dorsal root ganglion (DRG) (Costigan et al., 2009). The fact that a normally quiet sensory neuron begins to initiate action potential is likely to be a causative agent in the continuous pain, allodynia and hyperalgesia (Kajander et al., 1992; Sheen and Chung, 1993). Moreover, previous studies revealed the crucial role of hyperactivity of DRG neurons in triggering central sensitization and neuropathic pain in the early stage (within 1 week of injury) (Sun et al., 2005; Xie et al., 2007). Therefore, hyperactivity of DRG neurons and the hyperactivity of DCN have extreme similarity in their roles underlying the induction of neuropathic pain and tinnitus respectively. The connection between peripheral deafferentation and development of central hyperactivity also composes a key factor shared by tinnitus and neuropathic pain. Although the event cascade and molecular mechanisms are still to be explored, a compensatory mechanism seems to play a role targeting

for homeostasis of a firing rate-related signal (O'Leary et al., 2014). Given that DRG neurons generate spontaneous activity without synaptic inputs, changes in ionic conductances of the neurons have been explored as a crucial mechanism underlying the induction of neuropathic pain.

1.1.8 Synaptic and intrinsic mechanisms underlying tinnitus-related DCN hyperactivity

Consistent with its key role in tinnitus generation, the DCN is a site where robust tinnitus-related neuronal hyperactivity has been identified (Kaltenbach and Afman, 2000; Brozoski et al., 2002a; Kaltenbach et al., 2005; Middleton and Tzounopoulos, 2012). Therefore, identifying the mechanisms underlying DCN hyperactivity is key to understanding the induction of tinnitus, and to providing important links between changes in the operation of cochlea and a phantom perception generated in the central nervous system.

Firing activity of DCN principle cells, fusiform cells, is determined both intrinsically and synaptically. Fusiform cell displays tonic spontaneous firing activity with a firing rate between 0 to 50 Hz (Manis, 1990; Leao et al., 2012). It integrates two sources of glutamatergic synaptic inputs - auditory nerve fibers and parallel fibers - and receives feed-forward glycinergic as well as GABAergic inhibition (Oertel and Young, 2004) . Severance of ascending (Zacharek et al., 2002) or descending (Zhang et al., 2006) inputs did not significantly affect the magnitude of spontaneous firing rate in the DCN, suggesting that tinnitus-related DCN hyperactivity is a phenomenon either generated by a self-regulated neural network, or caused by change in intrinsic neuronal properties. Although previous studies have suggested that synaptic disinhibition contributes to the increase in the spontaneous firing rate of principal neurons in the DCN (hyperactivity) (Wang et al., 2009; Middleton et al., 2011; Zeng et al., 2012), direct evidence is

lacking that these synaptic changes are crucial for the induction of tinnitus. Moreover, the principle neurons in the DCN, fusiform cells, display spontaneous firing activity that is independent of synaptic inputs (Leao et al., 2012). Therefore, it is possible that noise-induced DCN hyperactivity is caused by change in intrinsic membrane property of fusiform cells, which finally leads to the development of noise-induced tinnitus.

1.1.9 Summary of dissertation research

The goal of this dissertation is to unravel the cellular and molecular mechanisms in DCN fusiform cell that lead to the vulnerability and resilience to noise-induced tinnitus. We first improved a mouse model of noise-induced tinnitus (Turner et al., 2006b; Longenecker and Galazyuk, 2011), and established statistical criteria for behaviorally separating noise-exposed mice with tinnitus behavior (tinnitus mice) and noise-exposed mice without tinnitus behavior (non-tinnitus mice). With *in vitro* slice recording on DCN fusiform cells from sham-exposed (control) mice, noise-exposed tinnitus mice and noise-exposed non-tinnitus mice, we revealed a hyperactivity of fusiform cells that is specific to tinnitus mice and is independent of excitatory or inhibitory synaptic transmission. We then investigated intrinsic membrane property of DCN fusiform cells. We revealed that the tinnitus-specific fusiform cell hyperactivity and vulnerability to tinnitus is caused by a reduction in KCNQ2/3 channel activity. The lack of fusiform cell hyperactivity and resilience to tinnitus is mediated by recovery of KCNQ2/3 channel activity after an initial reduction, together with a decrease in HCN channel activity. Collectively, our studies reveal that noise-induced plasticity of KCNQ2/3 and HCN channels in DCN fusiform cells contribute to the vulnerability and resilience to tinnitus.

2.0 CHAPTER 1. PATHOGENIC PLASTICITY OF KV7.2/3 CHANNEL ACTIVITY IS ESSENTIAL FOR THE INDUCTION OF TINNITUS

2.1 ABSTRACT

Tinnitus, the perception of phantom sound, is often a debilitating condition that affects many millions of people. Little is known, however, about the molecules that participate in the induction of tinnitus. In brain slices containing the dorsal cochlear nucleus, we reveal a tinnitus-specific increase in the spontaneous firing rate of principal neurons (hyperactivity). This hyperactivity is observed only in noise-exposed mice that develop tinnitus and only in the dorsal cochlear nucleus regions that are sensitive to high frequency sounds. We show that a reduction in Kv7.2/3 (KCNQ2/3) channel activity is essential for tinnitus induction and for the tinnitus-specific hyperactivity. This reduction is due to a shift in the voltage dependence of KCNQ channel activation to more positive voltages. Our *in vivo* studies demonstrate that a pharmacological manipulation that shifts the voltage dependence of KCNQ to more negative voltages prevents the development of tinnitus. Together, our studies provide an important link between the biophysical properties of the KCNQ channel and the generation of tinnitus. Moreover, our findings point to previously unknown biological targets for designing therapeutic drugs that may prevent the development of tinnitus in humans.

2.2 INTRODUCTION

Tinnitus is a common auditory disorder that is often the result of extreme sound exposure. An estimated 5 – 15% of the population experiences chronic tinnitus, with many millions of those sufferers disabled by this condition (Axelsson and Ringdahl, 1989; Roberts et al., 2010; Shargorodsky et al., 2010). With an even higher prevalence of chronic tinnitus in recent war veterans (Yankaskas, 2012), the personal and financial costs of tinnitus have expanded dramatically. Despite the high prevalence of tinnitus, the neuronal mechanisms that mediate the initiation (induction) and the maintenance (expression) of the disorder remain poorly understood. As a result, there is no generally accepted treatment, cure or preventive method for tinnitus.

Tinnitus is usually initiated by noise-induced cochlear damage that causes hair cell loss, ganglion cell degeneration and reduced auditory nerve input to the central auditory system (Schaette and McAlpine, 2011). Decreased peripheral input leads to pathogenic neuronal plasticity that results in subcortical hyperexcitability, increased neural synchrony, cortical reorganization, and ultimately stimulus-independent perception of sound (Melcher et al., 2000; Salvi et al., 2000; Brozoski et al., 2002b; Eggermont and Roberts, 2004; Finlayson and Kaltenbach, 2009; Engineer et al., 2011a; Middleton et al., 2011; Schaette and McAlpine; Yang et al., 2011). However, little is known about the plasticity mechanisms that initiate tinnitus. Elucidation of these mechanisms will lead to the development of drugs and therapies that can be applied soon after the acoustic trauma, thus preventing tinnitus from becoming permanent and irreversible.

The dorsal cochlear nucleus (DCN) is an auditory brainstem nucleus that is indispensable to the induction of tinnitus: ablation of the DCN prior to noise exposure prevents the induction of

tinnitus (Brozoski et al., 2012b). Consistent with its key role in tinnitus generation, the DCN is a site where robust tinnitus-related neuronal plasticity has been identified (Kaltenbach et al., 2005). Studies in animal models of noise-induced tinnitus have revealed that DCN principal neurons, fusiform cells, exhibit elevated spontaneous firing frequency (hyperactivity) that is correlated with the behavioral evidence of tinnitus (Brozoski et al., 2002b; Kaltenbach et al., 2004; Middleton et al., 2011). Although previous studies have suggested that a shift in the excitatory/inhibitory synaptic balance contributes to the DCN hyperactivity (Wang et al., 2009; Middleton et al., 2011; Zeng et al., 2012), direct evidence is lacking that these synaptic changes are crucial for the induction of tinnitus. Here, we reveal that pathogenic plasticity of Kv7 (KCNQ) potassium channel establishes DCN hyperactivity and triggers the development of tinnitus. This significant role of KCNQ channels makes them promising targets for the development of therapeutic approaches for preventing the induction of tinnitus.

2.3 RESULTS

2.3.1 Changes in the Intrinsic Properties of Fusiform Cells Mediate Tinnitus-Specific, DCN Hyperactivity

To determine the cellular mechanisms underlying the induction of tinnitus, we used an animal model that allows us to assess whether a mouse experiences tinnitus one week after being exposed to a loud sound (noise exposure, see Materials and Methods 2.5.1 and Figure S 1). This animal model is based on the inhibition of an acoustic startle response by a silent gap that is embedded in a constant background sound (Turner et al., 2006a); the silent gap is placed 130 ms

before the startle stimulus (gap detection, Figure 1a). Control mice and mice that do not experience tinnitus after noise exposure (non-tinnitus mice) detect the gap and show inhibition of the startle response; mice with behavioral evidence of tinnitus after noise exposure (tinnitus mice) show reduced inhibition of the startle response, as their tinnitus fills the gap. One week after noise exposure, 51.4% (18/35) of noise-exposed mice showed behavioral evidence of tinnitus, with significantly increased gap startle ratio (startle response to gap and startle stimulus / response to startle stimulus alone) revealed only by high (≥ 20 kHz), but not low frequency background sounds (Figure 1b, sham-exposed mice (control): n = 16, p = 0.55; tinnitus: n = 18, p < 0.001; non-tinnitus: n = 17, p = 0.20; Figure 1c, control: n = 16, p = 0.47; tinnitus: n = 18, p = 0.17; non-tinnitus: n=17, p = 0.14; Figure S 2). The development of the high-frequency tinnitus is consistent with previous studies that have used similar noise exposure (Wang et al., 2009; Middleton et al., 2011). Importantly, gap detection deficits of tinnitus mice are not due to temporal processing impairment or inability to hear the background sounds, because prepulse inhibition (PPI, inhibition of startle response by a preceding non-startling sound, Figure 1d) was identical among control, tinnitus and non-tinnitus mice (Figure 1e, control: n = 18, p = 0.72; tinnitus: n = 16, p = 0.61; non-tinnitus: n = 17, p = 0.32; Figure 1f, control: n = 18, p = 0.62; tinnitus: n = 18, p = 0.26; non-tinnitus: n = 17, p = 0.83; Figure S 3, Figure S 4, Figure S 5). The behavioral distinction of tinnitus from non-tinnitus mice enables us to identify the induction mechanisms that are tinnitus-specific and that are not general markers of noise exposure or hearing loss.

Previous studies have shown that DCN fusiform cells exhibit elevated spontaneous firing frequency (hyperactivity) that could underlie the triggering of tinnitus (Brozoski et al., 2002b; Kaltenbach et al., 2004). Given that spontaneous firing of fusiform cells is dependent on

their intrinsic ionic conductances (Leao et al., 2012), we blocked excitatory and inhibitory synaptic transmission to study the role of intrinsic conductances on the observed tinnitus-related DCN hyperactivity. Using whole-cell and cell-attached recordings in DCN slices, we recorded from fusiform cells in control, tinnitus and non-tinnitus mice one week after noise exposure. We revealed that when synaptic transmission is blocked, only fusiform cells from tinnitus mice showed increased spontaneous activity (Figure 1h, control: 9.7 ± 1.8 Hz, n = 14, tinnitus: 15.9 ± 1.0 Hz, n = 16, non-tinnitus: 8.4 ± 0.9 Hz, n = 12, $p = 0.0004$). Moreover, this hyperactivity is observed only in DCN areas that represent high (~ ≥ 20 kHz, dorsal part), but not low sound frequencies (Parham et al., 2000) (< 20 kHz, ventral part) (Figure 1g, i, control: 10.0 ± 1.5 Hz, n = 17, tinnitus: 7.9 ± 1.1 Hz, n = 7, non-tinnitus: 9.5 ± 1.9 Hz, n = 8, $p = 0.71$). Thus, our results suggest that noise-induced DCN hyperactivity is tinnitus-specific and is mediated by changes in the intrinsic ionic conductances of fusiform cells.

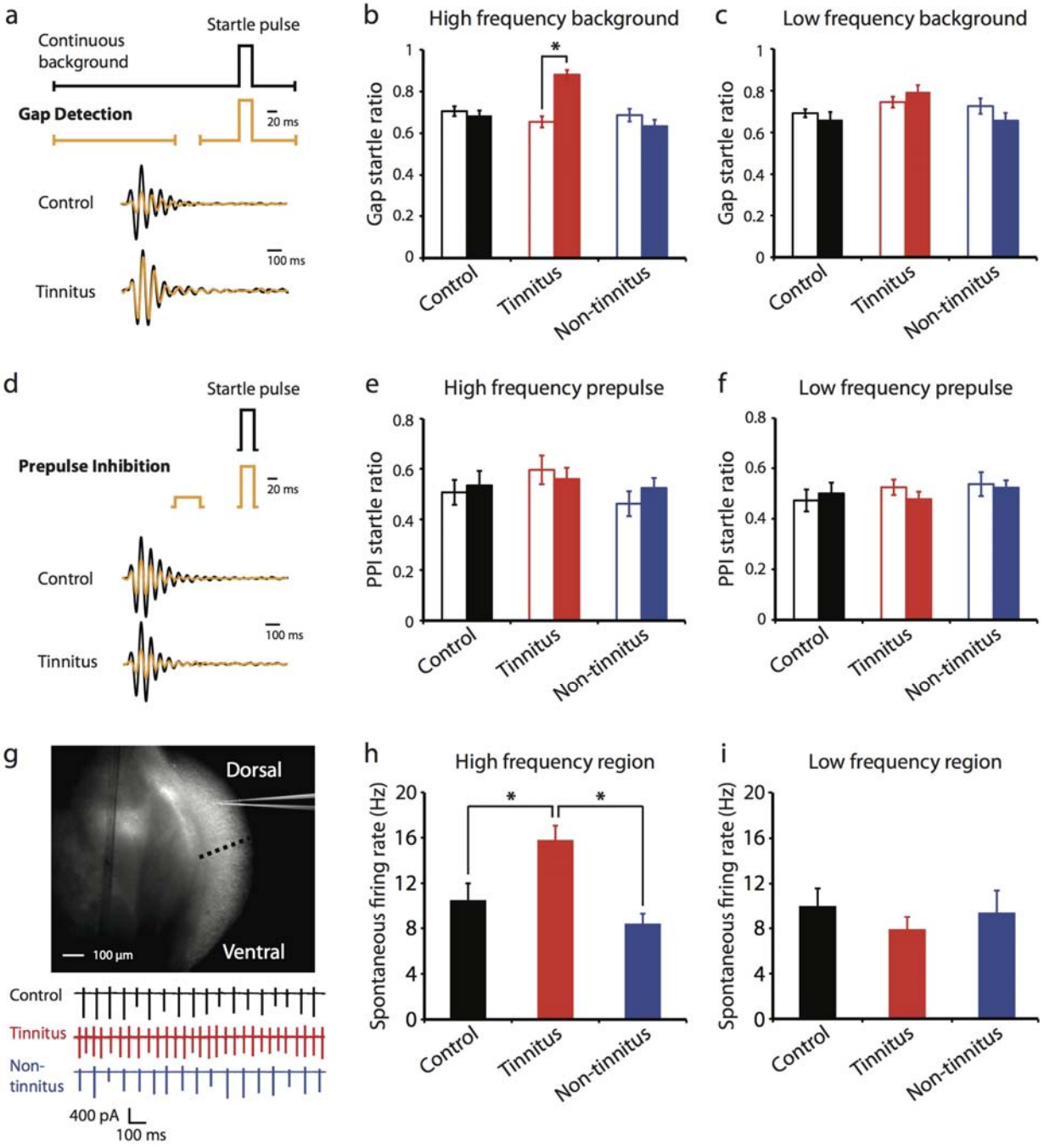

Figure 1. Fusiform cells recorded from DCN areas representing high frequency sounds display increased spontaneous firing frequency in mice with tinnitus.

Legends for Figure 1.

a. Top, diagram illustrating the gap detection protocol (black trace: a startle sound stimulus preceded by a constant background sound; yellow trace: a startle sound stimulus preceded by a constant background sound with a brief gap). Bottom, startle responses elicited by gap detection protocol were recorded as a downward pressing force on a mechanical platform.

b, c. Summary graph of gap startle ratio (response to gap and startle stimulus / response to startle stimulus alone) for high- and low-frequency background sounds (high frequency background, 20 - 32 kHz, control: n = 18, tinnitus: n = 18, non-tinnitus: n = 17; low frequency background, 10 - 16 kHz, control: n = 17, tinnitus: n = 17, non-tinnitus: n = 15). Open bars represent gap startle ratio before sham- or noise exposure, filled bars represent gap startle ratio one week later.

d. Top, diagram illustrating the prepulse inhibition protocol (PPI); Bottom, startle responses elicited by a loud sound (black trace) or by a loud sound preceded by a brief non-startling sound (yellow trace).

e, f. Summary graph of prepulse startle ratio (response to prepulse and startle stimulus / response to startle stimulus alone) for high- and low-frequency prepulse (high frequency prepulse, control: n = 18, tinnitus: n = 16, non-tinnitus: n = 17; low frequency prepulse, control: n = 17, tinnitus: n = 17, non-tinnitus: n = 15).

g. Top, light microscopic image of a coronal section of DCN from a P25 ICR mouse. The dotted line indicates the boundary that was used for dividing DCN areas that respond to high (~ ≥ 20 kHz, dorsal) or low frequency sounds (ventral). Bottom, representative cell-attached recordings from fusiform cells in the high frequency region of the DCN from control (black), tinnitus (red) and non-tinnitus mice (blue).

h, i. Summary graph of spontaneous firing rate of fusiform cells from control, tinnitus and non-tinnitus in the presence of excitatory and inhibitory receptor antagonists (10 μM NBQX, 20 μM SR95531 and 0.5 μM strychnine) (high frequency region, control: n = 14, tinnitus: n = 16, non-tinnitus: n = 12; low frequency region, control: n = 17, tinnitus: n = 7, non-tinnitus: n = 8).

Asterisk, $p < 0.05$. Error bars indicate SEM.

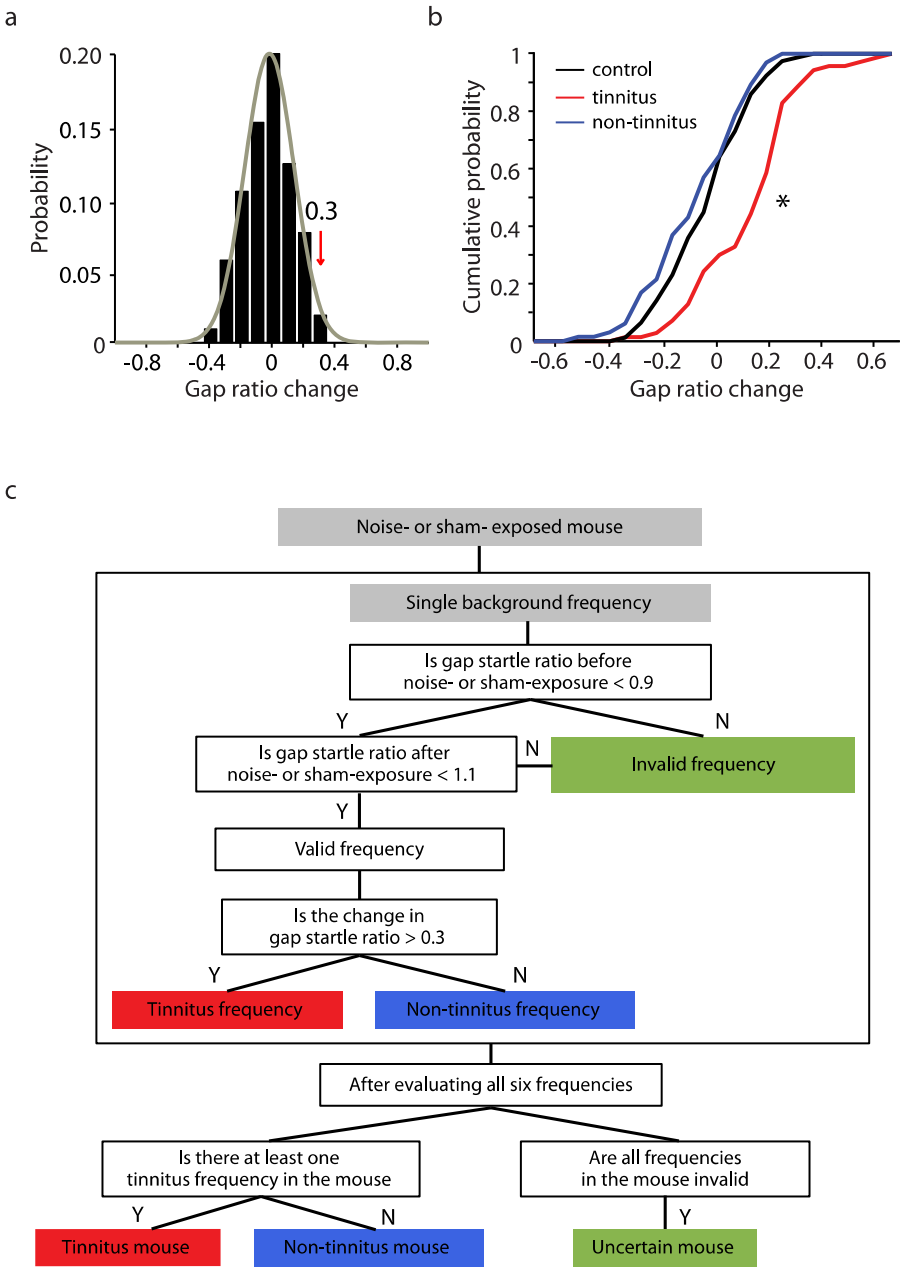

Figure S 1. Noise-induced increase in gap startle ratio for more than 0.3 is a criterion for separating tinnitus from non-tinnitus mice.

Legends for Figure S 1.

a. Probability distribution of changes in gap startle ratio (response to gap and startle stimulus/response to startle alone) (gap ratio change) before and 1 wk after sham exposure in control mice. Changes in gap ratios represent changes in control mice between postnatal day (P) 17–P20 and P24–P27 (age matched to pre- and post-noise-exposed mice). Data were fitted by a normal distribution (gray curve, $\mu = -0.01$, $\delta = 0.15$, $n = 77$). Gap ratio changes less than 0.3 (red arrow) represent 96.1% of the population in experiment and 97.8% in fitted distribution.

b. Cumulative probability distribution for changes in gap ratio before and after sham- or noise exposure for control (black), tinnitus (red), and non-tinnitus mice (blue) (control: -0.01 ± 0.02, $n = 75$, tinnitus: 0.14 ± 0.02, $n = 70$, non-tinnitus: -0.06 ± 0.02, $n = 65$, $P < 0.0001$). *$P < 0.05$.

c. Diagram illustrating the criteria for assessing the behavioral evidence of tinnitus.

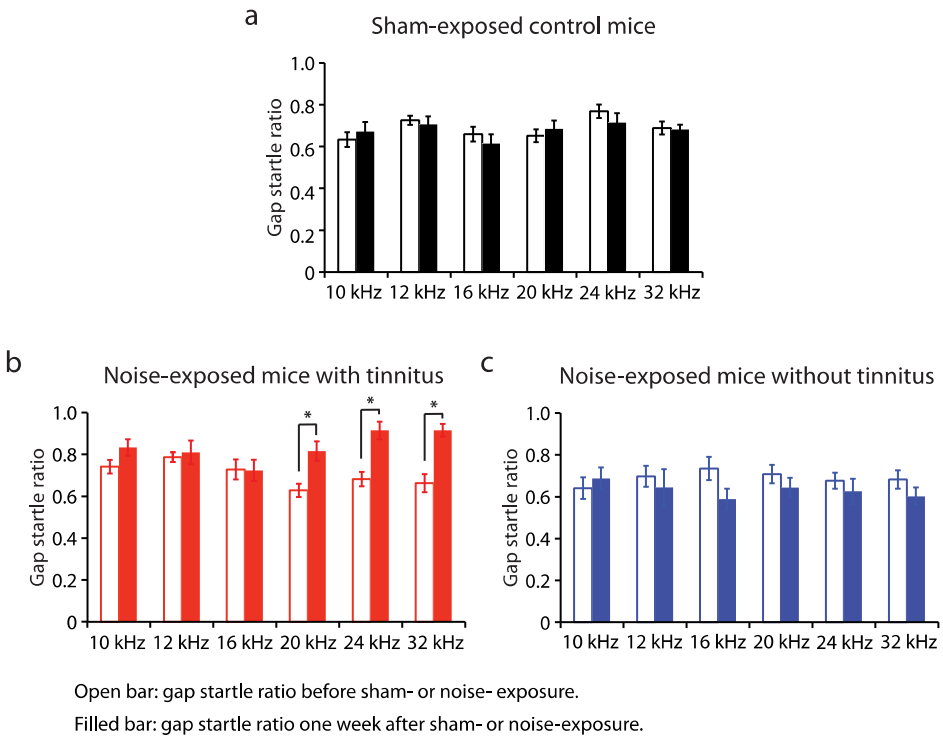

Figure S 2. Tinnitus behavior (gap detection deficit) is detected with high-frequency background sounds.

Legends for Figure S 2.

Summary graph of gap startle ratio (response to gap and startle stimulus/response to startle alone) for different frequencies of background for:

a. Control (10 kHz, before: 0.63 ± 0.03, after: 0.67 ± 0.04, n = 13, P = 0.37; 12 kHz, before: 0.73 ± 0.02, after: 0.71 ± 0.04, n = 13, P = 0.64; 16 kHz, before: 0.66 ± 0.04, after: 0.61 ± 0.04, n = 13, P = 0.44; 20 kHz, before: 0.65 ± 0.03, after: 0.68 ± 0.04, n = 13, P = 0.46; 24 kHz, before: 0.77 ± 0.03, after: 0.71 ± 0.04, n = 12, P = 0.19; 32 kHz, before: 0.69 ± 0.03, after: 0.68 ± 0.02, n = 16, P = 0.87);

b. Tinnitus (10 kHz, before: 0.74 ± 0.03, after: 0.83 ± 0.04, n = 13, P = 0.11; 12 kHz, before: 0.79 ± 0.02, after: 0.81

± 0.06, n = 9, P = 0.67; 16 kHz, before: 0.73 ± 0.05, after: 0.72 ± 0.05, n = 9, P = 0.93; 20 kHz, before: 0.63 ± 0.03, after: 0.82 ± 0.05, n = 16, P < 0.001; 24 kHz, before: 0.68 ± 0.03, after: 0.92 ± 0.04, n = 12, P = 0.004; 32 kHz, before: 0.66 ± 0.04, after: 0.92 ± 0.03, n = 12, P < 0.0001);

c. Non-tinnitus mice (10 kHz, before: 0.64 ± 0.05, after: 0.69 ± 0.05, n = 10, P = 0.37; 12 kHz, before: 0.70 ± 0.05, after: 0.64 ± 0.09, n = 7, P = 0.39; 16 kHz, before: 0.74 ± 0.06, after: 0.59 ± 0.05, n = 9, P = 0.06; 20 kHz, before: 0.71 ± 0.04, after: 0.64 ± 0.05, n = 13, P = 0.16; 24 kHz, before: 0.68 ± 0.04, after: 0.63 ± 0.06, n = 13, P = 0.29; 32 kHz, before: 0.68 ± 0.04, after: 0.60 ± 0.04, n = 15, P = 0.12).

*P < 0.05. Error bars indicate SEM.

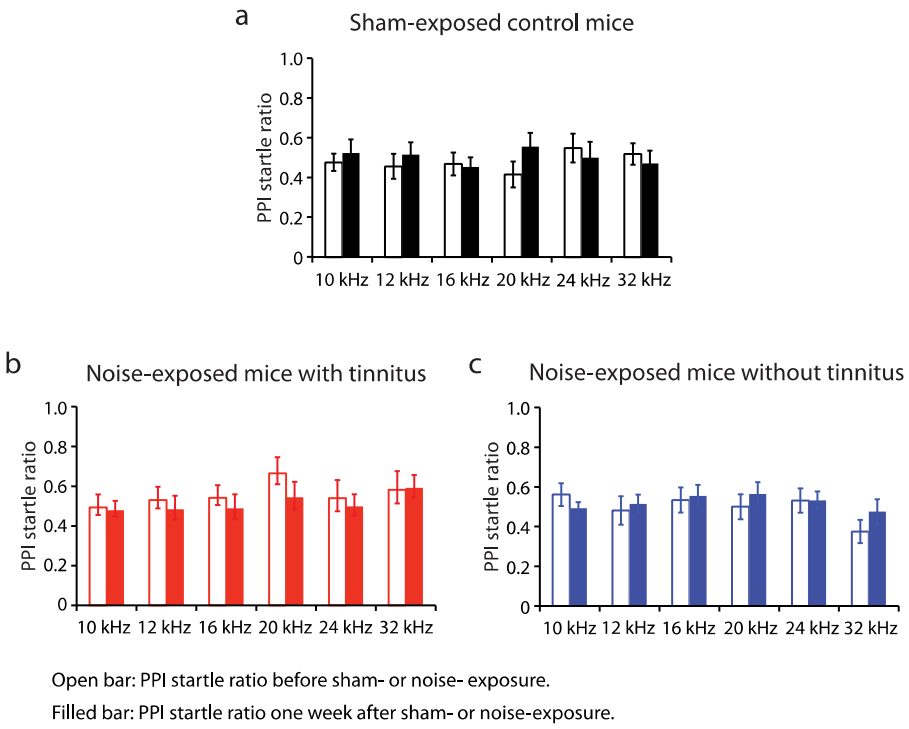

Figure S 3. PPI is not affected by noise exposure.

Legends for Figure S 3.

Summary graph of PPI startle ratio (response to prepulse and startle stimulus/response to startle alone) with different frequencies of prepulse for:

a. Control (10 kHz, before: 0.48 ± 0.04, after: 0.52 ± 0.07, n = 15, P = 0.52; 12 kHz, before: 0.46 ± 0.06, after: 0.52 ± 0.06, n = 16, P = 0.52; 16 kHz, before: 0.47 ± 0.06, after: 0.45 ± 0.05, n = 18, P = 0.06; 20 kHz, before: 0.42 ± 0.07, after: 0.56 ± 0.07, n = 15, P = 0.12; 24 kHz, before: 0.55 ± 0.07, after: 0.50 ± 0.07, n = 16, P = 0.61; 32 kHz, before: 0.52 ± 0.05, after: 0.50 ± 0.08, n = 16, P = 0.61);

b. Tinnitus (10 kHz, before: 0.49 ± 0.05, after: 0.47 ± 0.04, n = 17, P = 0.79; 12 kHz, before: 0.53 ± 0.05, after: 0.48 ± 0.06, n = 15, P = 0.49; 16 kHz, before: 0.54 ± 0.05, after: 0.48 ± 0.07, n = 14, P = 0.51; 20 kHz, before: 0.66 ± 0.07, after: 0.54 ± 0.07, n = 12, P = 0.28; 24 kHz, before: 0.54 ± 0.08, after: 0.49 ± 0.05, n = 11, P = 0.64; 32 kHz,

before: 0.58 ± 0.09, after: 0.59 ± 0.06, n = 14, P = 0.69) and;

c. Non-tinnitus mice (10 kHz, before: 0.56 ± 0.06, after: 0.49 ± 0.03, n = 16, P = 0.31; 12 kHz, before: 0.48 ± 0.07, after: 0.51 ± 0.05, n = 14, P = 0.75; 16 kHz, before: 0.53 ± 0.06, after: 0.55 ± 0.06, n = 15, P = 0.84; 20 kHz, before: 0.50 ± 0.06, after: 0.55 ± 0.06, n = 15, P = 0.50; 24 kHz, before: 0.53 ± 0.06, after: 0.53 ± 0.04, n = 15, P = 0.99; 32 kHz, before: 0.37 ± 0.06, after: 0.48 ± 0.06, n = 17, P = 0.13).

Error bars indicate SEM.

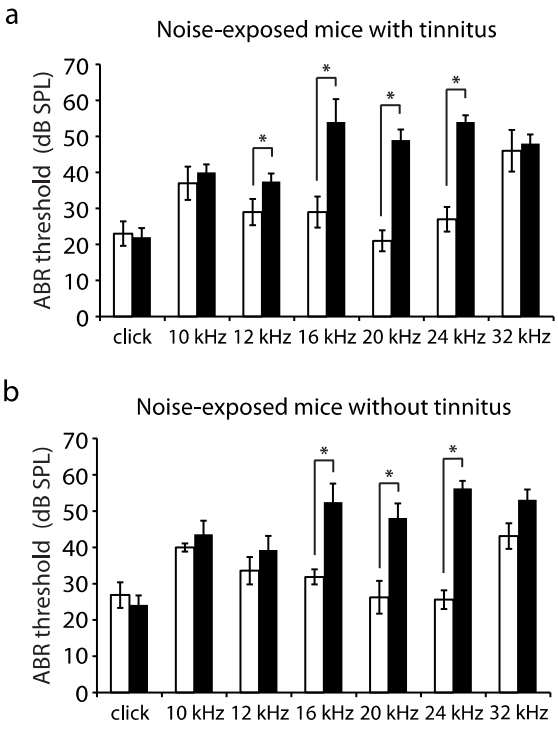

Open bar: ABR thresholds before noise exposure.
Filled bar: ABR thresholds one week after noise exposure.

Figure S 4. ABR thresholds are equally elevated one week after noise exposure in both tinnitus and non-tinnitus mice.

Legends for Figure S 4.

Summary graph showing ABR thresholds before (opens bars) and 1 wk after noise exposure (filled bars) in:

a. Tinnitus (click, before: 23.0 ± 3.4 dB, after: 22.0 ± 2.5 dB, n = 5, P = 0.28; 10 kHz, before: 37.0 ± 4.6 dB, after: 40.0 ± 2.2 dB, n = 5, P = 0.41; 12 kHz, before: 29.0 ± 3.7 dB, after: 37.5 ± 2.2 dB, n = 5, P = 0.04; 16 kHz, before: 29.0 ± 4.3 dB, after: 54.0 ± 6.4 dB, n = 5, P = 0.01; 20 kHz, before: 21.0 ± 2.9 dB, after: 49.0 ± 2.9 dB, n = 5, P < 0.001; 24 kHz, before: 27.0 ± 3.4 dB, after: 54.0 ± 1.9 dB, n = 5, P < 0.001; 32 kHz, before: 46.0 ± 5.8 dB, after: 48.0 ± 2.5 dB, n = 5, P = 0.73); and

b. Non-tinnitus mice (click, before: 26.9 ± 3.5 dB, after: 24.2 ± 2.6 dB, n = 7, P = 0.2; 10 kHz, before: 40.0 ± 1.1 dB, after: 43.6 ± 3.8 dB, n = 7, P = 1.00; 12 kHz, before: 33.6 ± 3.8 dB, after: 39.9 ± 3.9 dB, n = 7, P = 0.22; 16

kHz, before: 31.8 ± 2.1 dB, after 52.5 ± 5.1 dB, n = 7, P = 0.04; 20 kHz, before: 26.3 ± 4.5 dB, after: 48.1 ± 4.0 dB, n = 7, P = 0.005; 24 kHz, before: 25.6 ± 2.6 dB, after: 56.3 ± 2.1 dB, n = 7, P < 0.001; 32 kHz, before: 43.1 ± 3.5 dB, after: 53.1 ± 2.8 dB, n = 18, P = 0.07).

*P < 0.05. Error bars indicate SEM.

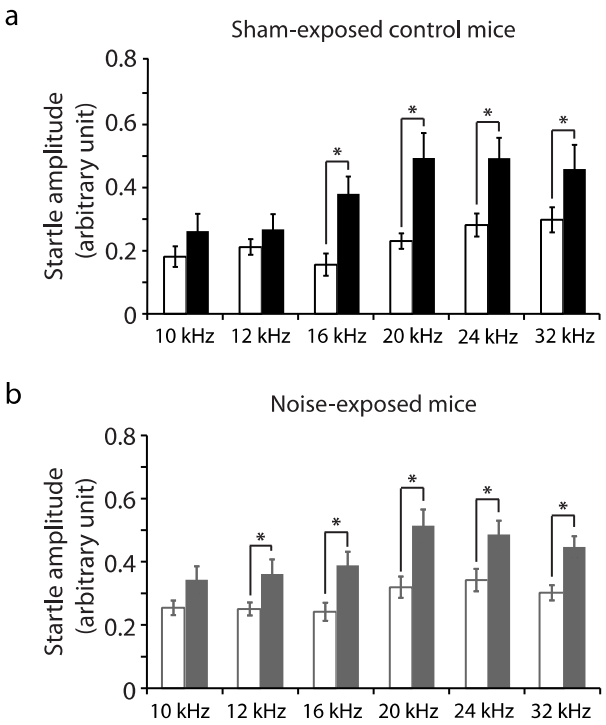

Figure S 5. Acoustic startle amplitude is increased in mice between P17–P20 and P24–P27 in an age-dependent manner, but the increase is unaffected by noise exposure.

Legends for Figure S 5.

Acoustic startle amplitude before and 1 wk after sham- or noise exposure for:

a. Control (10 kHz, before: 0.18 ± 0.03, after: 0.26 ± 0.05, n = 11, P = 0.21; 12 kHz, before: 0.21 ± 0.03, after: 0.27 ± 0.05, n = 11, P = 0.26; 16 kHz, before: 0.15 ± 0.04, after: 0.38 ± 0.05, n = 11, P = 0.01; 20 kHz, before: 0.23 ± 0.02, after: 0.49 ± 0.08, n = 11, P = 0.007; 24 kHz, before: 0.28 ± 0.04, after: 0.49 ± 0.06, n = 11, P = 0.01; 32 kHz, before: 0.30 ± 0.03, after: 0.46 ± 0.08, n = 11, P = 0.03); and

b. Noise-exposed mice (10 kHz, before: 0.25 ± 0.02, after: 0.34 ± 0.04, n = 17, P = 0.06; 12 kHz, before: 0.25 ± 0.02, after: 0.36 ± 0.05, n = 17, P = 0.04; 16 kHz, before: 0.24 ± 0.03, after: 0.38 ± 0.04, n = 17, P = 0.006; 20 kHz, before: 0.32 ± 0.03, after: 0.51 ± 0.05, n = 17, P = 0.004; 24 kHz, before: 0.34 ± 0.04, after: 0.48 ± 0.04, n = 17, P = 0.005; 32 kHz, before: 0.30 ± 0.02, after: 0.45 ± 0.03, n = 17, P = 0.001).

*P < 0.05. Error bars indicate SEM.

2.3.2 Decreased KCNQ Channel Activity Causes Tinnitus-Specific, DCN Hyperactivity

To determine the ionic conductances that are associated with the tinnitus-specific hyperactivity, we examined the intrinsic properties of fusiform cells. Our studies revealed that reduction in KCNQ (M) current -- a subthreshold, non-inactivating K^+ current (Brown and Adams, 1980; Delmas and Brown, 2005) -- is responsible for the detected DCN hyperactivity. To quantify KCNQ channel activity we held fusiform cells at -30 mV for 5 seconds and then stepped the voltage to -50 mV for 1 sec to unmask their slow deactivation (Figure 2a). In agreement with previous studies, this protocol revealed a slowly deactivating current that is blocked by XE991 (10 μM), a specific KCNQ channel blocker (Figure 2a). Given the voltage-independence of XE991 blocking on KCNQ1 (Wang et al., 2000) and similar IC50s (~ 1 μM) of KCNQ currents tested by different voltages (Wang et al., 1998; Koyama and Appel, 2006; Cavaliere and Hodge, 2011), we use the XE991-sensitive deactivation current tested from -30 mV to -50 mV to represent the KCNQ currents activity. By recording from control, tinnitus and non-tinnitus mice, we found that XE991-sensitive KCNQ currents are specifically reduced in tinnitus mice (Figure 2b, control: 68.6 ± 9.6 pA, n = 7, tinnitus: 27.0 ± 3.7 pA, n = 8, non-tinnitus: 72.4 ± 8.2 pA, n = 7, p = 0.004). Importantly, the reduction of KCNQ currents in tinnitus mice is observed only in fusiform cells that represent high, but not low sound frequencies (Figure 2c, control: 80.9 ± 12.0 pA, n = 6; tinnitus: 62.8 ± 6.2 pA, n = 6, non-tinnitus: 73.4 ± 10.7 pA, n = 6, p = 0.45). Thus, the frequency-dependent reduction of KNCQ currents corresponds to the frequency-dependence of tinnitus-specific hyperactivity (Figure 2h, i), as well as to the frequency-dependence of tinnitus behavior (Figure 2b, c). Together, these results suggest that the reduction of KCNQ channel activity is associated with the tinnitus behavior and the tinnitus-specific DCN hyperactivity.

Next we examined whether the decrease of KCNQ channel activity is causally linked to the tinnitus-specific hyperactivity. If hyperactivity of fusiform cell in tinnitus mice is caused by decreases in KCNQ channel activity, then the pharmacological blockade of KCNQ channel activity is expected to have a smaller effect on increasing the spontaneous firing activity in tinnitus mice compared to control mice. Moreover, we expect to observe this occluding effect in recordings from the high frequency, but not the low frequency region of the DCN. Indeed, in cell-attached recordings from high frequency DCN regions, XE991 did not affect spontaneous firing rates of fusiform cells in tinnitus mice, but it significantly increased spontaneous firing rates of fusiform cells in control mice (Figure 2d, at 15 - 20 mins after XE991 application, control: 184.9 ± 1.9 % of baseline, n = 6, tinnitus: 111.3 ± 1.1 % of baseline, n = 7, $p < 0.05$). Moreover, application of XE-991 equalizes the spontaneous firing rate of fusiform cells of control and tinnitus mice (Figure S 6), which further supports the hypothesis that a decrease in KCNQ channel activity is responsible for the tinnitus-specific hyperactivity. Consistent with our hypothesis, in recordings from low frequency DCN regions, blockade of KCNQ channels with XE991 revealed a similar enhancing effect on the spontaneous firing frequency of fusiform cells in control and tinnitus mice (Figure 2e, control: 199.8 ± 1.6 % of baseline, n = 6, tinnitus: 208.8 ± 3.0 % of baseline, n = 6, $p > 0.05$). The lack of effect of XE991 on fusiform cells in tinnitus mice is not due to a "ceiling" effect, as XE991 had a similar effect in fusiform cells with both low (< 12 Hz, n = 2) and high (> 12 Hz, n = 5) spontaneous firing frequency (Figure 2f, middle and right traces). Together, these results demonstrate that reduction of KCNQ channel activity is correlated, and causally linked to the DCN, tinnitus-specific hyperactivity. This previously unknown plasticity of KCNQ channels reveals the importance of KCNQ channels in the generation of the neural correlates of tinnitus.

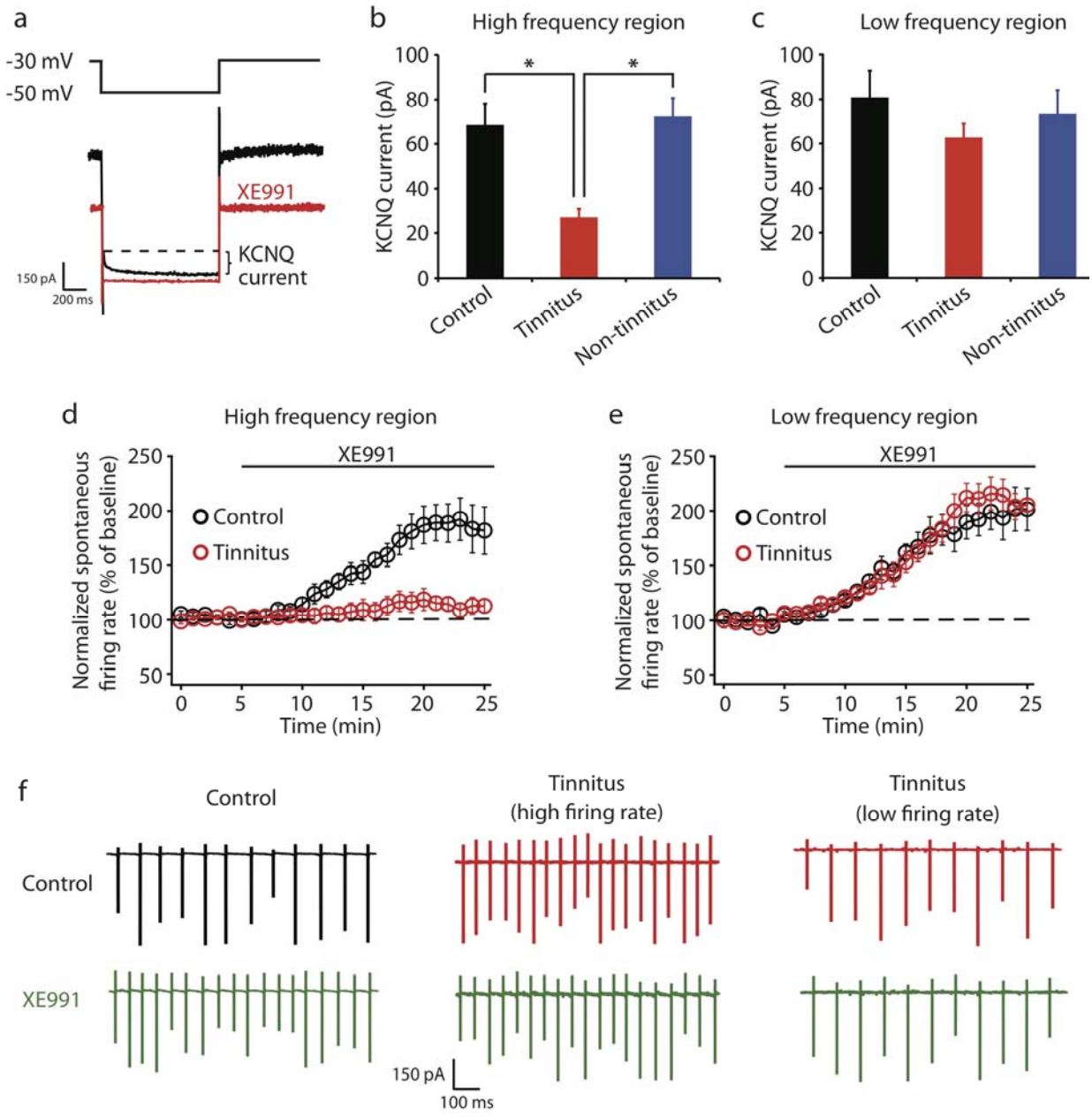

Figure 2. Decreased KCNQ channel activity is responsible for tinnitus-specific DCN hyperactivity.

Legends for Figure 2.

a. Current elicited by 1 s hyperpolarization to −50 mV from a holding potential of −30 mV before (black) and after XE991 (10 μM) (red). Curly bracket indicates the XE991-sensitive, slowly deactivating, KCNQ current.

b, c. Summary graphs showing KCNQ currents as measured by protocol in A (high-frequency region, control: n = 7, tinnitus: n = 8, non-tinnitus: n = 7; low-frequency region, control: n = 6, tinnitus: n = 6, non-tinnitus, n = 6).

d, e. Summary graphs showing the time course of normalized spontaneous firing frequency of fusiform cells before and after XE991 in high- (control: n = 6, tinnitus: n = 7) and low-frequency DCN region (control: n = 6, tinnitus: n = 6).

f. Representative cell- attached recordings showing spontaneous firing of fusiform cell in high-frequency region of the DCN before (control: black; tinnitus: red) and after XE991 (green). All experiments were performed in the presence of excitatory and inhibitory receptor antagonists as in Figure 1 H and I.

Asterisk, $p < 0.05$. Error bars indicate SEM.

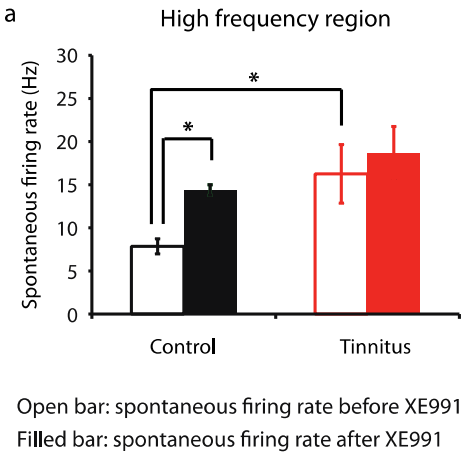

Figure S 6. XE991 equalizes the spontaneous firing rate between control and tinnitus mice.

Legends for Figure S 6.

Summary graph of spontaneous firing rate of fusiform cells recorded from high-frequency DCN regions in control (black) and in tinnitus mice (red), before and after XE991 application (before XE991: control, 7.9 ± 0.9 Hz, n = 6, tinnitus, 16.3 ± 3.4 Hz, n = 7, P = 0.049; after XE991: control, 14.3 ± 0.6 Hz, n = 6, P < 0.001 compared with control before XE991; after XE991: tinnitus, 18.6 ± 3.1 Hz, n = 7, P = 0.232 compared with control after XE991). *P < 0.05. Error bars indicate SEM.

2.3.3 Reduced KCNQ Channel Activity Enhances Subthreshold Excitability in Tinnitus Mice

Previous studies in hippocampal neurons have shown that KCNQ channel activity reduces neuronal excitability by modulating resting membrane potential (RMP), action potential

threshold, spike afterdepolarization, and subthreshold excitability (Yue and Yaari, 2004; Peters et al., 2005; Hu et al., 2007; Tzingounis and Nicoll, 2008). To investigate the mechanism via which KCNQ channels modulate fusiform cell excitability, we examined these parameters in control and tinnitus mice. Our results show that RMP, spike threshold and other suprathreshold parameters are not different either between control and tinnitus mice or in control mice before and after XE991 application (Figure 3a, RMP, control: n = 6, tinnitus: n = 11, p = 0.87; control: n = 6, XE991: n = 6, p = 0.74; Figure 3b, spike threshold, control: n = 11, tinnitus: n = 11, p = 0.26; control: n = 6; XE991: n = 6, p = 0.85, Table 1). However, we observed a significant increase in the subthreshold excitability of tinnitus mice (Figure 3c, depolarization rate from -60 mV to spike threshold, control: 0.32 ± 0.05 V/s, n=11, tinnitus: 0.75 ± 0.16 V/s, n = 12, p = 0.02). Moreover, application of XE991 in control mice mimics the effect of reduced KCNQ channel activity in tinnitus mice (Figure 3d, left): XE991 speeds up the rate of subthreshold depolarization and reduces the threshold current ($I_{threshold}$) needed to elicit a spike (Figure 3d, $I_{threshold}$, control: 0.13 ± 0.05 nA, n = 5, after XE991: 0.10 ± 0.04 nA, n = 5, p = 0.045). Together, our results suggest that the reduced KCNQ channel activity in tinnitus mice increases spontaneous firing rate of fusiform cells by increasing subthreshold excitability.

2.3.4 Plasticity of KCNQ2/3 Channels Is Crucial for the Induction of Tinnitus

The KCNQ family of K^+ channels comprises five members (KCNQ1 - 5). Given that mutations of KCNQ2 and KCNQ3 genes cause hyperexcitable epileptic states (Jentsch, 2000), and the expression of these subunits in the DCN (Cooper et al., 2001; Saganich et al., 2001), we investigated whether KCNQ2/3 subunits mediate KCNQ currents in fusiform cells. We employed TEA and UCL2077, two pharmacological agents that provide differential block to

KCNQ currents mediated by different subunits. Compatible with the sensitivity of KCNQ2/3-mediated currents to these blockers (Wang et al., 1998; Soh and Tzingounis, 2010), application of TEA blocked KCNQ currents with an IC50 of 1.8 mM (Figure 3e, n = 4 - 6 for each TEA concentration) and application of UCL2077 (3 μM) blocked KCNQ currents by 23 % (Figure 3f, 77.3 ± 0.5 % of baseline, n = 5). Given that KCNQ5-mediated currents are potentiated by UCL2077 (Soh and Tzingounis, 2010; Huang and Trussell, 2011) and neither KCNQ1 nor KCNQ4 subunits are expressed in the DCN (Kharkovets et al., 2000; Goldman et al., 2009), our findings suggest that KCNQ2/3 heteromers mediate the KCNQ currents in fusiform cells. Together, our results suggest that it is the plasticity of KCNQ2/3 channels that leads to the reduction of KCNQ channel activity in tinnitus mice.

2.3.5 Depolarizing Shift of $V_{1/2}$ Causes Reduced KCNQ Channel Activity in Tinnitus Mice

The reduction of KCNQ channel activity in tinnitus mice suggests a reduction of channel expression, a shift in the voltage-dependence of channel activation or both. To examine these possibilities, we compared maximal conductance (G_{max}) and half-maximal activation voltage ($V_{1/2}$) of KCNQ channels in control and tinnitus mice. Voltage ramps evoked an outward current that was partially suppressed by XE991 (Figure 3g); by subtracting the trace after application of XE991 from the control trace, we determined the conductance–voltage relationship for KCNQ currents (Figure 3h). Through fitting with a Boltzmann relationship, we revealed that G_{max} in tinnitus mice is not reduced (Figure 3i), but the $V_{1/2}$ of KCNQ currents is shifted to more depolarized potentials (Figure 3i, $V_{1/2}$, control: -32.8 ± 1.7 mV, n = 6, tinnitus: -25.1 ± 1.7 mV, n = 6, p = 0.009; G_{max}, control: 54.7 ± 14.2 nS, n = 6, tinnitus: 53.1 ± 12.9 nS, n = 6, p = 0.93). While the Boltzmann fits -- especially, for determining maximal conductance -- are limited by

the range of voltages over which we were able to maintain voltage clamp, our results suggest that a depolarizing shift in $V_{1/2}$ in tinnitus mice is important for the reduction in KCNQ currents that, in turn, leads to tinnitus-specific hyperactivity.

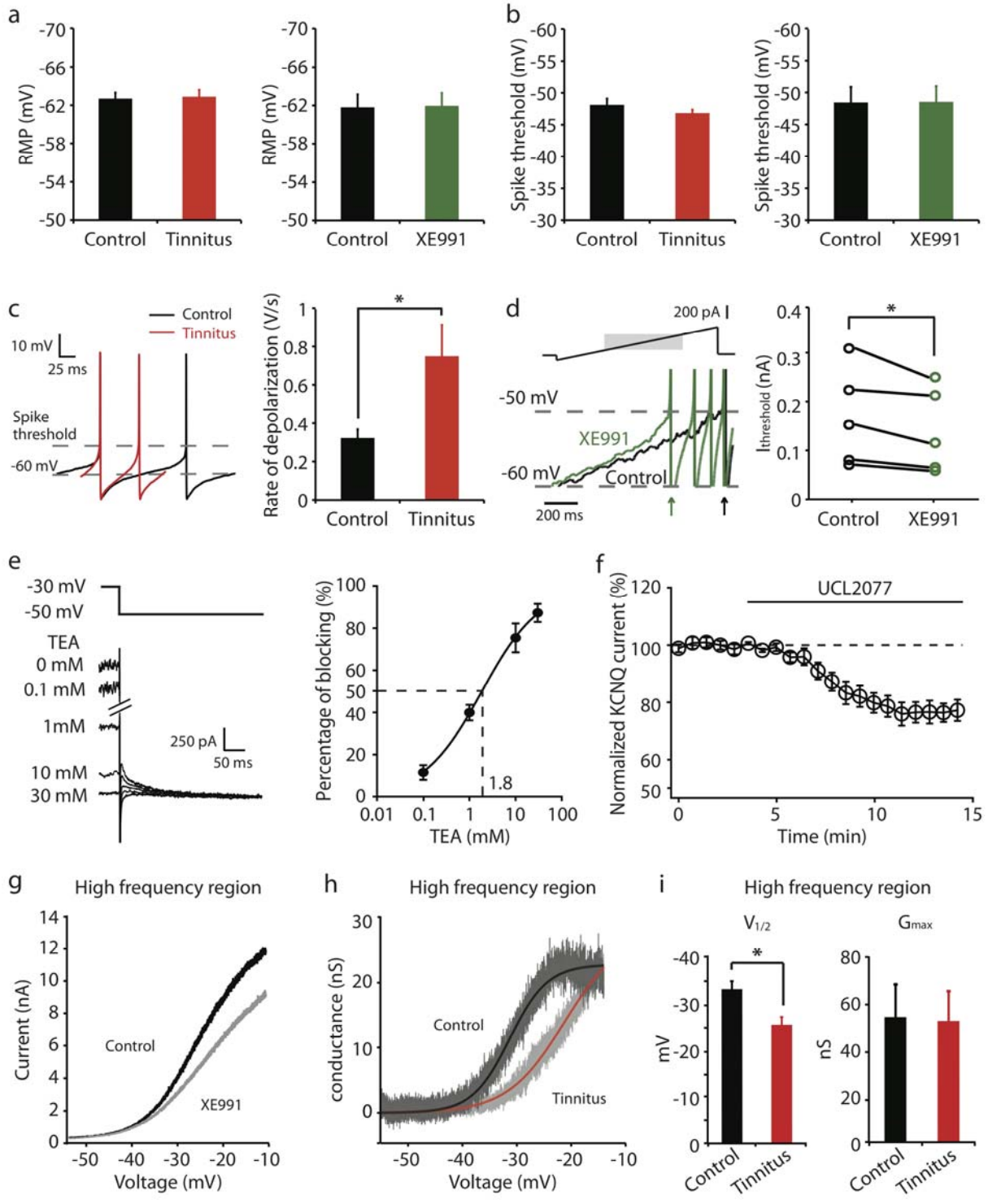

Figure 3. Reduced KCNQ2/3 channel activity leads to increased subthreshold excitability in tinnitus mice; this reduction is due to a depolarizing shift of $V_{1/2}$.

Legends for Figure 3.

a. (Left) RMP of fusiform cells from control and tinnitus mice (control: n = 11; tinnitus: n = 11). (Right) RMP of fusiform cells from control mice before and after the effect of XE991 (10 μM) (n = 6).

b. (Left) Spike threshold of fusiform cells from control and tinnitus mice (control: n = 11; tinnitus: n = 11). (Right) Spike threshold of fusiform cells from control mice before and after the effect of XE991 (n = 6).

c. Representative traces (Left) and summary graph (Right) of rate of subthreshold depolarization (from −60 mV to spike threshold) during spontaneous firing of fusiform cell in control (black: n = 11) and tinnitus mice (red: n = 12).

d. (Left) Representative traces of voltage response of fusiform cell (Lower) to injection of a current ramp (top, 0.2 nA/s) before (black) and after the effect of XE991 (green) (only response to shadowed region of stimulus is shown). Arrows indicate the times of the peak of the first spike response in each case. (Right) Currents needed to evoke the first spike during the current ramp ($I_{threshold}$) before (black, n = 5) and after XE991 application (green, n = 5).

e. Representative traces (Left) and summary graph (Right) showing block of KCNQ currents by 0.1, 1, 10, and 30mM TEA (0.1 mM: n = 5, 1 mM: n = 6; 10 mM: n = 6; 30 mM: n = 4). The voltage protocol is the same as in Figure 2A.

f. Summary graph showing the time course of UCL2077 (3 μM) effect on KCNQ currents elicited at −30 mV (n = 5).

g. Voltage ramp (10 mV/s) reveals an outward current that is partially blocked by XE991.

h. Representative conductance– voltage relationship of XE991-sensitive current in control (dark gray) and tinnitus mice (light gray). Black and red lines represent Boltzmann fits.

i. Summary graph for Boltzmann fit parameters V1/2 and G_{max} (control: n = 6, tinnitus: n = 6). All experiments were performed in the presence of excitatory and inhibitory receptor antagonists as in Figure 1 H and I.

Asterisk, $p < 0.05$. Error bars indicate SEM.

Table 1. Spike parameters of fusiform cells from high-frequency region of DCN in control and tinnitus mice

	Input resistance	Spike amplitude	Depolarization slope	Hyperpolarization slope	Half height width	fAHP
Control	63.61 ± 4.28 MΩ	38.92 ± 1.29 mV	161.05 ± 5.80 V/s	-156.06 ± 5.45 V/s	0.30 ± 0.01 ms	22.36 ± 1.37 mV
Tinnitus	67.55 ± 2.40 MΩ	38.28 ± 1.02 mV	147.32 ± 4.59 V/s	-136.75 ± 4.88 V/s	0.34 ± 0.02 ms	22.11 ± 1.08 mV

* fAHP: fast afterhyperpolarization;
* Depolarization slope: maximum depolarizing slope;
* Hyperpolarization slope: minimum hyperpolarizing slope;

Legends for Table 1.

All recordings were performed in fusiform cells in the high-frequency region of the DCN (input resistance, control: n = 8, tinnitus: n = 12, P = 0.62; spike amplitude, control: n = 11, tinnitus: n = 11, P = 0.67; depolarization slope, control: n = 11, tinnitus: n = 11, P = 0.07; hyperpolarization slope, control: n = 11, tinnitus, n = 11, P = 0.07; half height width, control: n = 11, tinnitus: n = 11, P = 0.67; fAHP, control: n = 11, tinnitus: n = 11, P = 0.88). Depolarization slope: maximum depolarizing slope; hyperpolarization slope: minimum hyperpolarizing slope; fAHP: fast afterhyperpolarization.

2.3.6 Retigabine, a KCNQ Channel Activator, Prevents the Development of Tinnitus.

The critical role of the voltage-dependence of KCNQ channels on generating tinnitus-specific hyperactivity, suggests the provocative link between the biophysical properties of KCNQ channels and the development of perception of phantom sound. This hypothesis predicts that pharmacological shift in the voltage-dependence of KCNQ channel activity to more hyperpolarized potentials will inhibit the development of tinnitus behavior. To test this hypothesis, we injected noise-exposed mice (starting 30 min after noise exposure and continuing injections twice a day for 5 days) with retigabine: retigabine specifically enhances KCNQ channel activation by causing a hyperpolarizing shift in the voltage-dependence of the channel activation (Tatulian et al., 2001; Xiong et al., 2008). IP injection of retigabine (as its dihydrochloride salt) reduced the percentage of noise-exposed mice that develop tinnitus to the same level as for control mice (Figure 4a, control: 11.1% (2/18, see Materials and Methods 2.5.1 and Figure S 1), noise-exposed: 51.4% (18/35), noise-exposed + retigabine: 18.8% (3/16), noise-exposed + saline: 43.8% (7/16)). Retigabine does not affect temporal processing or hearing, as it did not affect prepulse inhibition or hearing thresholds (Figure 4b, PPI, control: n = 16, noise-exposed: n = 33, noise-exposed + retigabine: n = 16, noise-exposed + saline: n = 16, p = 0.55; Figure 4c, ABR threshold, control: n = 7, noise-exposed: n = 18, noise-exposed + retigabine: n = 7, noise-exposed + saline: n = 7, p = 0.35; Figure S 7, Figure S 8). Although IP injection of retigabine affects KCNQ channels throughout the brain, these results, in combination with our physiological studies (Figure 1, Figure 2, Figure 3) and the key role of DCN in tinnitus induction (Brozoski et al., 2012b), support the notion that the pathogenic plasticity of subcortical KCNQ channel activity is crucial for the induction of tinnitus. Importantly, these results link the

voltage-dependence of KCNQ channel opening with the development of the perception of phantom sound.

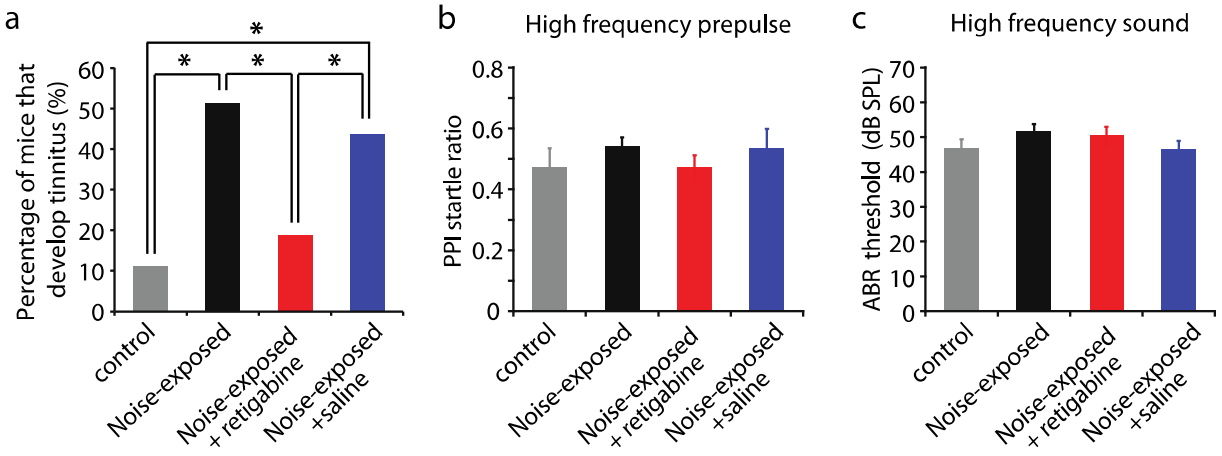

Figure 4. Pharmacological enhancement of KCNQ channel activity prevents the development of tinnitus.

Legends for Figure 4.

All data were recorded 1 week after sham- or noise exposure.

a. Percentage of mice that develop tinnitus (control: n = 18, noise-exposed: n = 35, noise-exposed + retigabine: n = 16, noise-exposed + saline: n = 16).

b, c. PPI and ABR thresholds for high-frequency testing sounds (20–32 kHz) (PPI startle ratio, control: n = 16, noise-exposed: n = 33, noise-exposed + retigabine: n = 16, noise-exposed + saline: n = 16; ABR thresholds, control: n = 7, noise-exposed: n = 18, noise-exposed + retigabine: n = 7, noise-exposed + saline: n = 7).

Asterisk, $p < 0.05$. Error bars indicate SEM.

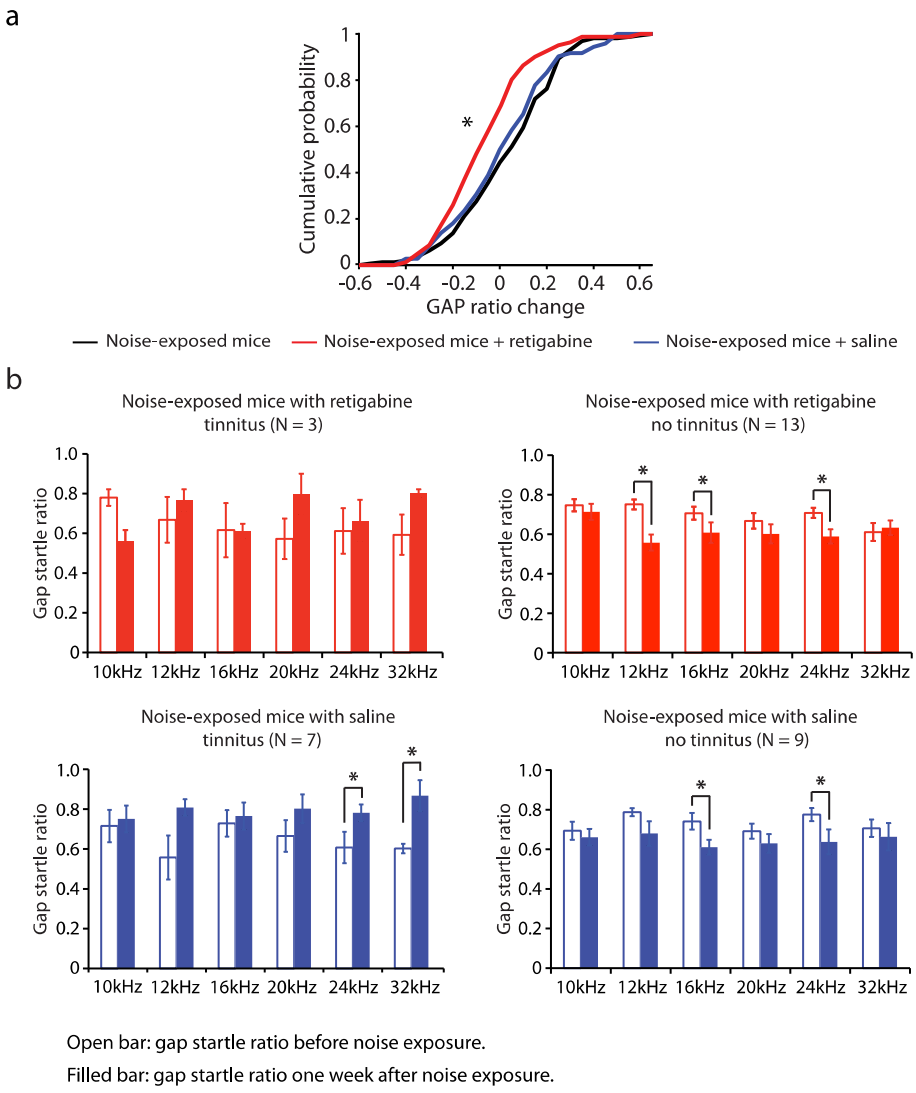

Figure S 7. Retigabine administration prevents the development of tinnitus.

Legends for Figure S 7.

a. Cumulative probability distribution for changes in gap startle ratio before and 1 wk after noise exposure (gap ratio change) for noise-exposed only mice (black), noise-exposed mice with retigabine injection (red), and noise-exposed mice with saline injection (blue) (noise-exposed: 0.04 ± 0.02, n = 135, noise-exposed + retigabine: −0.05 ± 0.02, n = 81, noise-exposed + saline: 0.03 ± 0.03, n = 72, P = 0.002).

b. Summary graph of gap startle ratio (response to gap and startle stimulus/response to startle alone) for different frequencies of background for: noise-exposed mice treated with retigabine that showed tinnitus (Upper Left, 10 kHz,

before: 0.78 ± 0.04, after: 0.56 ± 0.05, n = 3; 12 kHz, before: 0.67 ± 0.11, after: 0.77 ± 0.06, n = 2; 16 kHz, before: 0.62 ± 0.14, after: 0.61 ± 0.04, n = 3, 20 kHz, before: 0.57 ± 0.10, after: 0.80 ± 0.10, n = 3; 24 kHz, before: 0.61 ± 0.11, after: 0.66 ± 0.11, n = 3; 32 kHz, before: 0.59 ± 0.10, after: 0.80 ± 0.02, n = 3), noise-exposed mice treated with retigabine that did not show tinnitus (Upper Right, 10 kHz, before: 0.75 ± 0.03, after: 0.71 ± 0.04, n = 13, P = 0.37; 12 kHz, before: 0.75 ± 0.03, after: 0.56 ± 0.04, n = 9, P < 0.001; 16 kHz, before: 0.71 ± 0.03, after: 0.61 ± 0.05, n = 11, P = 0.03; 20 kHz, before: 0.67 ± 0.04, after: 0.60 ± 0.05, n = 10, P = 0.21; 24 kHz, before: 0.71 ± 0.03, after: 0.59 ± 0.04, n = 11, P = 0.02; 32 kHz, before: 0.61 ± 0.05, after: 0.63 ± 0.04, n = 11, P = 0.71), noise-exposed mice treated with saline that showed tinnitus (Lower Left, 10 kHz, before: 0.72 ± 0.08, after: 0.75 ± 0.07, n = 6, P = 0.76; 12 kHz, before: 0.56 ± 0.11, after: 0.81 ± 0.04, n = 4, P = 0.08; 16 kHz, before: 0.73 ± 0.07, after: 0.77 ± 0.09, n = 6, P = 0.55; 20 kHz, before: 0.67 ± 0.08, after: 0.80 ± 0.07, n = 7, P = 0.13; 24 kHz, before: 0.61 ± 0.08, after: 0.78 ± 0.04, n = 6, P = 0.04; 32 kHz, before: 0.60 ± 0.02, after: 0.87 ± 0.8, n = 6, P = 0.02) and noise-exposed mice treated with saline that did not show tinnitus (Lower Right, 10 kHz, before: 0.69 ± 0.05, after: 0.66 ± 0.04, n = 11, P = 0.52; 12 kHz, before: 0.79 ± 0.02, after: 0.68 ± 0.06, n = 8, P = 0.14; 16 kHz, before: 0.74 ± 0.04, after: 0.61 ± 0.04, n = 11, P = 0.01; 20 kHz, before: 0.69 ± 0.04, after: 0.63 ± 0.05, n = 11, P = 0.18; 24 kHz, before: 0.78 ± 0.03, after: 0.64 ± 0.06, n = 11, P = 0.02; 32 kHz, before: 0.71 ± 0.04, after: 0.66 ± 0.07, n = 10, P = 0.49).

*P < 0.05. Error bars indicate SEM.

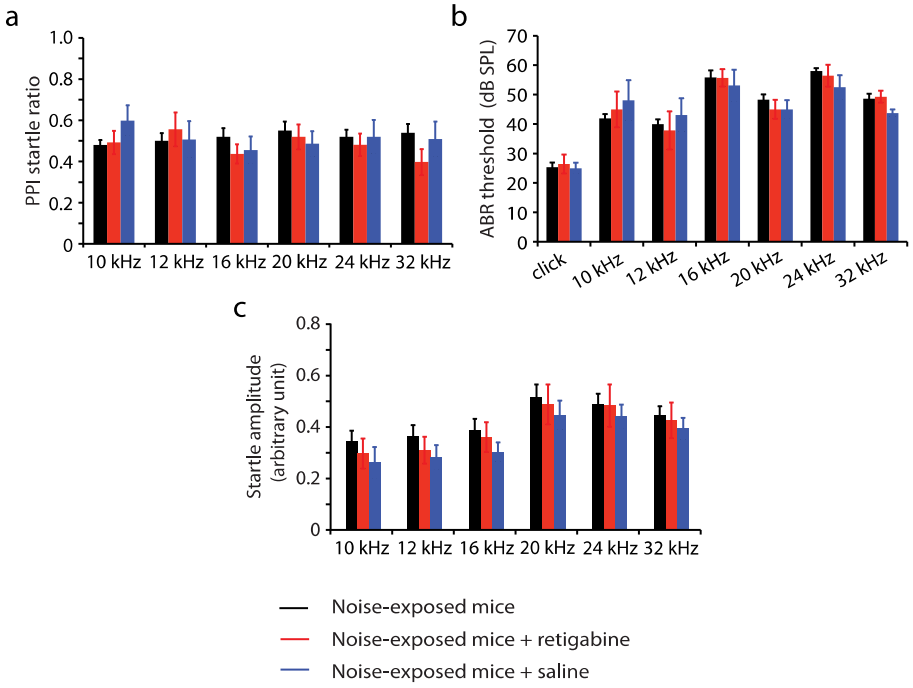

Figure S 8. Retigabine administration does not affect PPI; auditory brainstem response (ABR) thresholds; startle reflex amplitude.

Legends for Figure S 8.

a. Summary graph of PPI startle ratio (response to prepulse and startle stimulus/response to startle alone) for different frequencies of prepulse 1 wk after noise exposure in noise- exposed only mice (black), noise-exposed mice with retigabine injection (red), and noise-exposed mice with saline injection (blue) (10 kHz, noise-exposed: 0.48 ± 0.02, n = 33, noise-exposed + retigabine: 0.49 ± 0.06, n = 15, noise-exposed + saline: 0.60 ± 0.07, n = 13, P = 0.13; 12 kHz, noise-exposed: 0.50 ± 0.04, n = 29, noise-exposed + retigabine: 0.56 ± 0.08, n = 14, noise-exposed + saline: 0.51 ± 0.09, n = 11, P = 0.77; 16 kHz, noise-exposed: 0.52 ± 0.04, n = 29, noise-exposed + retigabine: 0.44 ± 0.05, n = 15, noise-exposed + saline: 0.46 ± 0.07, n = 16, P = 0.49; 20 kHz, noise-exposed: 0.55 ± 0.04, n = 27, noise-exposed + retigabine: 0.52 ± 0.06, n = 14, noise-exposed + saline: 0.49 ± 0.06, n = 12, P = 0.70; 24 kHz, noise-exposed: 0.52 ± 0.03, n = 26, noise-exposed + retigabine: 0.48 ± 0.05, n = 14, noise-exposed + saline: 0.52 ± 0.08, n = 13, P = 0.82; 32 kHz, noise-exposed: 0.54 ± 0.04, n = 30, noise-exposed + retigabine: 0.40 ± 0.06, n = 16, noise-

exposed + saline: 0.51 ± 0.09, n = 14, P = 0.21).

b. Summary graph showing ABR thresholds 1 wk after noise exposure for noise-exposed only mice, noise-exposed mice with retigabine injection and noise-exposed mice with saline injection (click, noise-exposed: 25.3 ± 1.6 dB, n = 15, noise-exposed + retigabine: 26.4 ± 3.2 dB, n = 7, noise-exposed + saline: 25.0 ± 1.9 dB, n = 7, P = 0.9; 10 kHz, noise-exposed: 41.9 ± 1.5 dB, n = 18, noise-exposed + retigabine: 45.0 ± 6.1 dB, n = 7, noise- exposed + saline: 48.1 ± 6.8 dB, n = 7, P = 0.5; 12 kHz, noise-exposed: 40.0 ± 1.6 dB, n = 18, noise-exposed + retigabine: 37.9 ± 6.4 dB, n = 7, noise-exposed + saline: 43.1 ± 5.7 dB, n = 7, P = 0.69; 16 kHz, noise-exposed: 55.8 ± 2.4 dB, n = 18, noise-exposed + retigabine: 55.7 ± 3.0 dB, n = 7, noise-exposed + saline: 53.1 ± 5.3 dB, n = 7, P = 0.86; 20 kHz, noise-exposed: 48.3 ± 1.8 dB, n = 18, noise-exposed + retigabine: 45.0 ± 3.3 dB, n = 7, noise-exposed + saline: 45.0 ± 3.2 dB, n = 7, P = 0.50; 24 kHz, noise-exposed: 58.1 ± 1.0 dB, n = 18, noise-exposed + retigabine: 56.4 ± 3.7 dB, n = 7, noise-exposed + saline: 52.5 ± 4.11 dB, n = 7, P = 0.26; 32 kHz, noise-exposed: 48.6 ± 1.65 dB, n = 18; noise-exposed + retigabine: 49.3 ± 2.0 dB, n = 16, noise-exposed + saline: 43.7 ± 1.3 dB, n = 7, P = 0.17).

c. Summary graph showing acoustic startle amplitude 1 wk after noise exposure for noise-exposed only mice, noise-exposed mice with retigabine injection and noise- exposed mice with saline injection (noise-exposed: 0.34 ± 0.04, n = 17, noise-exposed + retigabine: 0.30 ± 0.06, n = 14, noise-exposed + saline: 0.26 ± 0.06, n = 14, P = 0.57; 12 kHz, noise-exposed: 0.36 ± 0.05, n = 17, noise-exposed +retigabine: 0.31 ± 0.05, n = 14, noise-exposed + saline: 0.30 ± 0.04, n = 14, P = 0.53; 16 kHz, noise-exposed: 0.39 ± 0.04, n = 17, noise-exposed + retigabine: 0.36 ± 0.06, n = 14, noise-exposed + saline: 0.30 ± 0.04, n = 14, P = 0.39; 20 kHz, noise- exposed: 0.51 ± 0.05, n = 17, noise-exposed + retigabine: 0.49 ± 0.08, n = 14, noise-exposed + saline: 0.45 ± 0.06, n = 14, P = 0.75; 24 kHz, noise-exposed: 0.49 ± 0.04, n = 18, noise-exposed + retigabine: 0.48 ± 0.08, n = 14, saline: 0.44 ± 0.05, n = 14, P = 0.81; 32 kHz, noise-exposed: 0.45 ± 0.03, n = 17, noise-exposed + retigabine: 0.43 ± 0.07, n = 14, noise-exposed + saline: 0.40 ± 0.04, n = 14, P = 0.7).

Error bars indicate SEM.

2.4 DISCUSSION

2.4.1 Tinnitus is a KCNQ channelopathy.

KCNQ channels are slowly activating, non-inactivating potassium channels that open at subthreshold membrane potentials. The time- and voltage-dependent properties of KCNQ channels enable them to function as effective "brakes" that control excitability in neuronal, sensory and muscular cells (Delmas and Brown, 2005; Soldovieri et al., 2011). The importance of KCNQ channels is emphatically illustrated by the finding that mutations in KCNQ genes underlie multiple neurological diseases that are characterized by membrane hyperexcitability, such as epilepsy (Jentsch, 2000; Maljevic et al., 2010). Here, we report that tinnitus is a KCNQ channelopathy: a reduction in KCNQ2/3 channel activity leads to the DCN tinnitus-specific hyperactivity and initiates the development of tinnitus.

2.4.2 Up-regulation of mAChR signaling may underlie the reduced KCNQ channel activity in tinnitus mice.

KCNQ channels, often KCNQ2 and KCNQ3, mediate the native neuronal M-type currents (Brown and Adams, 1980; Wang et al., 1998). M currents are strongly inhibited by activation of muscarinic acetylcholine receptors (mAChRs) and other G-protein coupled receptors that reduce membrane PIP_2 levels (Marrion, 1997; Suh and Hille, 2002; Zhang et al., 2003). Given the important role of cholinergic activity in DCN synaptic plasticity (Zhao and Tzounopoulos, 2011) and that noise exposure increases cholinergic activity in the DCN (Jin et

al., 2006; Kaltenbach and Zhang, 2007), our results suggest that noise-induced up regulation of mAChR signaling may underlie the reduced KCNQ channel activity in tinnitus mice.

2.4.3 KCNQ-mediated subcortical hyperactivity plays a triggering role for development of tinnitus.

Given that ablation of the DCN does not eliminate tinnitus once developed (Brozoski and Bauer, 2005), we propose the existence of a "critical period" during which KCNQ channel enhancement is capable of preventing the development of tinnitus. Therefore, we suggest that plasticity of subcortical KCNQ2/3 channels is essential for the induction, but not the expression of tinnitus. Recent studies show that cortical reorganization (Eggermont and Roberts, 2004; Engineer et al., 2011a) and aberrant thalamocortical rhythms (Llinas et al., 2005) (thalamocortical dysrythmia) may underlie the expression of tinnitus; thalamocortical dysrythmia, by promoting stimulus-independent gamma oscillations could maintain the conscious perception. Moreover, while it is evident that auditory system dysfunction is necessary for the generation of tinnitus, the maintenance of chronic tinnitus may involve pathological interactions between auditory and non-auditory structures, such as the limbic system (Rauschecker et al., 2010; Leaver et al., 2011). Thus, our findings suggest that KCNQ-mediated, subcortical hyperactivity may be triggering cortical reorganization and thalamocortical dysrythmia, which, in combination with changes in the limbic system, lead to the maintenance of the perception of phantom sound.

2.4.4 Plasticity of KCNQ biophysical properties may underlie the induction of chronic neuropathic pain.

Chronic neuropathic pain is another phantom perception that is initiated by a peripheral trauma that results in subcortical hyperexcitability and cortical reorganization (Woolf, 1983; Vartiainen et al., 2009). Although changes in KCNQ channels have been associated with chronic neuropathic pain (Passmore et al., 2003; Brown and Passmore, 2009), a detailed mechanistic scheme for the role of KCNQ channels in pain has yet to emerge. Given the similarities between tinnitus and central neuropathic pain (Tonndorf, 1987; Moller, 2007; De Ridder et al., 2011), our studies suggest that plasticity of KCNQ biophysical properties is a promising site for investigating the induction mechanisms of chronic neuropathic pain.

2.4.5 KCNQ2/3 channel activators are promising therapeutic drugs for preventing the development of tinnitus.

While our studies do not exclude other synaptic and intrinsic plasticity mechanisms that may contribute to the tinnitus-related changes in DCN excitability (Wang et al., 2011; Pilati et al., 2012; Zeng et al., 2012), our results highlight KCNQ2/3 channels as key players in the induction of tinnitus. KCNQ channels have been attractive targets for treating diseases associated with hyper-excitability (Wulff et al., 2009); retigabine, a KCNQ channel activator, has been recently approved as an anticonvulsant. Our findings, by illustrating the role of reduced KCNQ channel activity in the induction of tinnitus, suggest that KCNQ2/3 channel activators are promising therapeutic drugs for preventing the development of tinnitus.

2.4.6 Spontaneous firing rate of fusiform cell is dependent but not linearly correlated with KCNQ channel activity

Our results revealed that reduction in KCNQ channel activity happen only in fusiform cells from tinnitus mice, and only in cells from high frequency region of the DCN (Figure 2). Although KCNQ currents amplitude reduced for around 60% comparing with cells from control mice, the effect of XE991 on increasing the spontaneous firing rate of fusiform cells were completely abolished for cells from high frequency DCN region of tinnitus mice (Figure 2d). Our results indicate that KCNQ currents amplitude is not linearly correlated with spontaneous firing rate of fusiform cells. The dissociation between the KCNQ amplitude and change in spontaneous firing rate of fusiform cell is possibly due to the dynamical interactions of membrane potential with various ionic conductances, including KCNQ channels, persistent sodium channels, HCN channels, low threshold calcium channels, A-type potassium channels etc. (Kanold and Manis, 1999; Leao et al., 2012), on regulating the spontaneous firing rate of DCN fusiform cell.

2.5 MATERIALS AND METHODS

2.5.1 Mouse model of tinnitus

Noise exposure ICR (CD-1) mice (postnatal day P17 - P20), both male and female, were used for this study. For the noise-exposed group, mice were anesthetized with 3% isoflurane in oxygen; after stabilization, anesthesia level was maintained at 1 - 1.5%. A pipette tip was fixed

onto the speaker (CF-1; Tucker Davis Technologies), and was inserted into left ear canal of the mouse (unilateral noise exposure). Narrow bandpass noise with a 1-kHz bandwidth centered at 16 kHz was presented at 116 dB SPL for 45 minutes. For sham-exposed (control) mice, the procedures were identical with the induced mice but no-noise was presented (sham exposure).

Gap Detection Gap detection paradigm (Turner et al., 2006a; Middleton et al., 2011) was used for detecting behavioral evidence of tinnitus. Gap detection of sham- or noise-exposed mice was assessed before exposure and one week (6 to 7 days) after exposure. Mice were confined in custom-made housing constructed of Lego parts and a small plastic container with cardboard plate and placed on a load-cell platform (E45-11; Coulbourn Instruments) inside of a sound-attenuating chamber (ENV-022SD; Med Associates). The ambient sound in the chamber was 46 dB SPL (4 kHz – 40 kHz). All sounds were presented through a planar isodynamic tweeter (RT2H-A; HiVi), which was positioned in front of the animal to reduce standing wave resonances. Testing was done using narrow bandpass sound with a 1-kHz bandwidth centered at 10, 12, 16, 20, 24, and 32 kHz presented at 70 dB SPL. For each trial, this background sound was presented randomly for 8 – 25 s. Testing sessions began with 20 startle-only trails (white noise burst at 104 dB SPL for 20 ms) to habituate the evoked startle response. The startle response represents the time course of the downward force (presented as arbitrary units, AU) that the mouse applies onto the platform in response to the startle stimulus. Gap detection was evaluated by the gap startle ratio, which is the ratio of the peak-peak value of the startle waveform in trials with gap over the peak-peak amplitude of the startle waveform in trials in the absence of the gap; startle-only trials and gap trials were presented in an alternating fashion (the gap detection trial was always before the startle-only trial). Gap detection trials were identical to startle-only trials except that a 50-ms silent gap was introduced; the startle stimulus was presented 80 ms after the

cessation of the silent gap. Background frequency was presented for three times in an ascending fashion in repeat of four trials. This allowed each frequency to be presented 12 times. For each frequency, 12 gap startle ratios were collected and averaged. Baseline movement (not induced by startle) was analyzed for the engagement level of a mouse to the startle dependent test. Only mice that showed the baseline under 0.1 AU were used.

Prepulse Inhibition. Prepulse inhibition (PPI) is the inverse of gap detection. PPI was tested in a quiet background, and a brief non-startling sound (prepulse) -- of similar intensity with the background sound used in the gap detection test -- was presented before the startle stimulus. PPI was performed together with gap detection right before and one week after noise- or sham-exposure. In PPI trials, a 50-ms, 70-dB SPL bandpass sound with 1-kHz bandwidth centered at 10, 12, 16, 20, 24, and 32 kHz was presented 130 ms before a startle stimulus (20 ms at 104 dB SPL). Testing sessions began with 20 startle-only trials. PPI trials and startle only trials were presented in an alternating fashion (the PPI trial was always presented before the startle-only trial). Frequencies were presented in an ascending fashion, with each frequency being presented five times. Prepulse inhibition was evaluated by PPI startle ratio, which is the ratio of the peak-peak value of the startle waveform in trials with prepulse, over the peak-peak value of the startle waveform in startle only trial.

Auditory Brainstem Response The hearing thresholds of left ear of sham- and noise-exposed mice were measured before and one week after exposure using auditory brainstem response (ABR) measurements. ABR thresholds were measured immediately after gap detection and prepulse inhibition test. Measurements were conducted in a sound-attenuating chamber (ENV-022SD; Med Associates) using sub dermal electrodes placed at the vertex; the ground electrode was placed ventral to the right pinna, and the reference electrode was placed ventral to

the left pinna. Mice were anesthetized initially with 3% isoflurane in oxygen, which was then maintained at 1 – 1.5%. The mice were placed on top of the heating pad with rectal thermometer to maintain the internal temperature at 36.5 - 38.5 $^{\circ}$C. To present the sound stimuli, a pipette tip was fixed to the end of a plastic tube (2.5 cm in length), which was attached to the speaker (CF-1; Tucker Davis Technologies), and was inserted into the left ear canal. ABR thresholds were obtained for 1-ms clicks and 3-ms tone bursts of 10, 12, 16, 20, 24, and 32 kHz presented at a rate of 18.56 per second. Stimuli were produced using the System 3 software package from Tucker Davis Technologies. Evoked potentials were averaged 1,024 times and filtered using a 300- to 3,000-Hz bandpass filter.

Criteria for behavioral evidence for tinnitus The first requirement is that the mouse is able to detect the gap in the background sound before noise- or sham-exposure; thus, the gap startle ratio for a single test frequency before exposure is required to be below 0.9. To control for potential prepulse excitation effects, the gap startle ratio for a single frequency after exposure is required to be below 1.1. The frequencies that meet the above requirements are considered as valid frequencies and are used for further analysis. Next, we established the criterion for determining whether a valid frequency is a tinnitus or a non-tinnitus frequency. To establish this criterion we determined the variability in changes of gap detection in sham-exposed (control) mice; we measured the change in gap detection ratios before sham exposure and one-week after sham exposure. In Figure S 1we plot the probability distribution of changes in gap startle ratio, we fit these data with a normal distribution with mean $\mu = -0.01$ and standard deviation $\delta = 0.15$. As 2δ point on the upper tail marked a gap ratio increase of 0.3, the probability that the gap ratio increases more than 0.3 in a sham-exposed mouse is less than 2.2%. Based on this analysis, we identified a valid frequency as tinnitus frequency only if we detect an increase in gap ratio for

more than 0.3 for this frequency; otherwise this frequency is a non-tinnitus frequency. After assesing all six background frequencies in each mouse, we consider this mouse as a tinnitus mouse, if it shows, at least, one tinnitus frequency. Mice that had valid frequencies, but did not have any tinnitus frequency were considered as non-tinnitus mice. Mice that did not have any valid frequency were not included for further analsysis/experiments (uncertain group, 7/42 (16.7%), see diagram below). Taking into consideration the number of valid frequencies for each control mouse (2 - 6), the probability of detecting a control mouse as tinnitus mouse, i.e., the false positive (or sponataneous, not noise-induced, tinnitus) rate is 9.2%, which is calculated by

$$P = \sum_{i=2}^{6} p_i \times (1 - 0.978^i)$$

where p_i is the probablity of having i valid frequency points in a tested mouse. This value matched our experimental findings, where 2 out of 18 (11.1%) control mice were considered as having tinnitus . Assessment for behavior evidence of tinnitus is described in the following diagram (Y = yes; N = No)

2.5.2 Retigabine experiments

ICR (CD-1) mice (P17 - P20), both male and female, were randomly assigned into two groups (16 mice for each group): noise-exposed treated with retigabine and noise-exposed treated with vehicle (0.9% saline) (referred to as retigabine group and saline group, respectively). All mice were first assessed for gap detection, PPI, as well as ABR threshold prior to noise exposure. For the retigabine group, retigabine (as its dihydrochloride salt, Santa Cruz Biotechnology, LKT lab) was dissolved in 0.9% saline and administered 30 minutes after noise exposure via intraperitoneal (IP) injection at a dose of 10 mg/kg. In the saline group, the same

dose of 0.9% saline was administered via IP injection. Both retigabine and saline were further administered twice a day for 5 days every 12 hrs. After the initial injection of retigabine dihydrochloride the mice showed slight motor impairment, tremor, and increase in appetite. These symptoms were diminished 2 – 3 hours later; by the third day, all of these behavior symptoms were not apparent after injection of retigabine. Gap detection, prepulse inhibition and ABR threshold were re-tested 24 - 48 hours after the final injection, at which time retigabine dihydrochloride was out of the body system (Luszczki, 2009).

2.5.3 Electrophysiology

Slice preparation Coronal slices of left DCN (210 μm) were prepared from control- and noise-exposed (P24 - 27). Animals were handled and sacrificed according to methods approved by the Institutional Animal Care and Use Committee of the University of Pittsburgh. Immediately after the slices were prepared, they were incubated in normal artificial cerebral spinal fluid (ACSF) at 36°C for one hour, and then at room temperature. Fusiform cells were visualized using an Olympus upright microscope (BX51w1, 40 × optics) under oblique illumination condenser equipped with a XC-ST30 CCD camera and analog monitor. Cells were identified based on their morphological and electrophysiological characteristics. The preparation of slices and the identification for fusiform cells have been described in detail (Tzounopoulos et al., 2004a). The incubation as well as external recording solution contained (in mM): 130 NaCl, 3 KCl, 1.2 KH_2PO_4, 2.4 $CaCl_2.2H_2O$, 1.3 $MgSO_4$, 20 $NaHCO_3$, 3 NaHEPES, and 10 D-glucose, saturated with 95% O_2 / 5% CO_2. KH_2PO_4 free external solution was used for studying the voltage-dependent property of KCNQ currents, to prevent precipitation with bath-applied $CdCl_2$ (200 μM, see below). NBQX (10 μM, Abcam) or DNQX (20 μM, Abcam), strychnine (0.5 μM,

Sigma-Aldrich), SR95531 (20 μM, Abcam) were used to block glutamatergic, glycinergic as well as GABAergic synaptic transmission. XE991 (10 μM, Abcam) was applied for blocking KCNQ currents. Tetrodotoxin (TTX, 0.5 μM, Abcam) was used to block spiking activity. Tetraethylammonium chloride (TEA, Abcam) and UCL2077 (3 μM, Sigma-Aldrich) were used for assessing the subunit composition of KCNQ currents. When applying the voltage-clamp ramp protocol, external $CsCl_2$ (1 mM) and $CdCl_2$ (200 μM) were used to block hyperpolarization-activated non-selective cation channels (HCN, Ih channel) and calcium channels, respectively. All the drugs were dissolved in de-ionized water, except for UCL2077, which used DMSO as vehicle; the final DMSO concentration was less than 0.5%. Drugs were prepared as stock solution, diluted to the final concentration immediately before using, and applied through bath perfusion. Recordings were performed with temperature controlled between 34 °C to 37 °C by an inline heating system (Warner Instruments, Hamden, CT) with perfusion speed maintained (4-6 ml min^{-1}).

Electrophysiological recordings For whole-cell voltage- and current-clamp experiments, pipettes (3 - 5 MΩ) were filled with a K-based internal solution containing (in mM): 113 K-gluconate, 4.5 $MgCl_2.6H_20$, 14 Tris-Phosphocreatine, 9 HEPES, 0.1 EGTA, 4 Na_2ATP, 0.3 Tris-GTP, 10 Sucrose, pH 7.3, and 300 mOsmol. Liquid junction potential of -11 mV was corrected. Access resistance was monitored throughout the experiment from the size and shape of the capacitive transient in response to a 5 mV depolarization step. Recordings with access resistance larger than 15 MΩ were eliminated. For loose cell-attached voltage-clamp recording, pipettes (1.5 – 2.5 MΩ) were filled with modified external solution containing (in mM): 125 NaCl, 2.5 KCl, 1.25 NaH_2PO4, 2 $CaCl_2.2H_2O$, 1 $MgCl_2$, 25 $NaHCO_3$, and 25 glucose. Seal resistance was maintained between 10 - 20 MΩ with command potential at 0 mV. Slight

adjustment (-5 mV to 5 mV) was given to ensure that the amplifier read 0 pA at the baseline potential. Spike peak-peak amplitudes smaller than 50 pA (background noise p-p amplitude is around 10 pA) were not included for the analysis, to eliminate potential contamination from nearby cells. Recordings were performed with Clampex 10.2 and Multiclamp 700B amplifier interfaced with Digidata 1440A data acquisition system (Axon Instruments). For whole-cell voltage clamp experiments, fast, slow capacitive currents as well as series resistance (Rs) were compensated (60 – 80%, bandwidth 15kHz). We did not perform Rs compensation for Figure 2a to monitor Rs throughout the experiment (more than 20% in Rs during the experiment led to the exclusion of the experiment; initial Rs was controlled to be between 8 - 12 MΩ for all these recordings). Cells with an average firing rate below than 1 Hz were not included, due to irregularity in firing rate. As spontaneous firing rate of fusiform cells is not affected by the recording mode (Leao et al., 2012), we used whole-cell or cell-attached mode to measure spontaneous firing rates in Figure 1h, i. All protocols, except for the gap-free recording in current clamp, were applied below 0.1 Hz to eliminate potential short-term plasticity effects. In voltage-clamp step protocol for measuring KCNQ currents, tail-current amplitude was measured as the difference between the initial peak amplitude and averaged response for the last 200 ms. Step and ramp protocols (whole-cell recording) for studying KCNQ currents were applied after obtaining 5 minutes of stable KCNQ currents amplitude before drug application and 5 minutes of stable amplitude after drug application (Figure 2 and Figure 3e-i). These recordings were routinely terminated within 30 minutes after breaking in. For current-clamp ramp protocols, hyperpolarization current was first applied to maintain stable membrane potential at -76 mV (Figure 3c,d). Threshold current ($I_{threshold}$) was measured as the ramp current at which peak of the first spike was detected (Figure 3d). For cell-attached recordings of the time course of the effect

of XE991 (10-20 μM) on the spontaneous firing of fusiform cell (Figure 2d-f), data was normalized to the mean firing rate of the 5 minutes before drug application. Firing frequency was measured every 1 min by averaging the firing rate of 10 consecutive spikes. Resting membrane potential was measured with whole-cell current clamp (0 pA holding current) 5 minutes after TTX (0.5 μM) application when a stable membrane potential was obtained. XE991 was applied on top of TTX for its effect on resting membrane potential (Figure 3a). Spike parameters were analyzed from spontaneous firing spikes with holding current I = 0 pA (synaptic transmission was pharmacologically blocked). For each fusiform cell, 20 consecutive spikes with standard deviation of instantaneous firing rate smaller than 2 Hz were aligned at the peak and averaged. Spike threshold was measured in phase plane as the membrane potential at which the depolarization slope shows the first abrupt change (Δslope > 10 V/s, Figure 3b). Input resistance was measured with small current steps at subthreshold potentials. Spike amplitude is the voltage difference between spike threshold and peak amplitude of the spike. Depolarization and hyperpolarization slope indicate the maximum slope during the depolarization and minimum slope during hyperpolarization phase of the spike. Half height width is the width of the spike when voltage equals to (spike threshold + spike amplitude/2). Fast afterhyperpolarization (fAHP) is the voltage difference between spike threshold and spike undershoot. For Figure 3c, rate of depolarization = [spike threshold (mV) - (-60 mV)] / time from -60 mV to spike threshold]. In voltage-clamp ramp experiments, XE991-sensitive KCNQ currents elicited by slow voltage ramp (10V/s) were converted to conductance (G, nS) based on Ohm's law: $G = I / (V - V_r)$. I (pA) is the current amplitude at the membrane potential V (mV), and V_r is the reversal potential of potassium (-85.5 mV, (Leao et al., 2012)). Conductance-voltage curves were then fitted with Boltzmann function to describe the voltage dependence of KCNQ activation (Figure 3h, i):

$$G = \frac{G_{\max}}{1 + e^{-(V - V_{half})/k}}$$

where G_{max} (nS) is the maximal conductance, V_{half} (mV) is the voltage for half-maximal activation and k is the slope factor (mV). To assess the concentration dependence TEA blockade, percentage of blocking (Y) with different concentration of TEA (x) was fitted with Hill equation (Figure 3e):

$$Y = \frac{B_{\max} x^h}{IC_{50}^h + x^h}$$

B_{max} is the maximum percentage of blocking, IC50 is the half-maximum blocking concentration and h is the Hill coefficient. Analysis was performed on Igor Pro Software 5.05A, GraphPad Prism 5 and Matlab 2011a.

2.5.4 Statistics

Mann-Whitney test was applied for behavioral data that didn't pass normality test. For electrophysiological data, we assumed that the population distribution follows normal distribution and applied Student's T-test as well as One-Way Analysis of Variance (ANOVA) for statistical analysis.

3.0 CHAPTER 2. NOISE-INDUCED PLASTICITY OF KCNQ2/3 AND HCN CHANNELS UNDERLIES VULNERABILITY AND RESILIENCE TO TINNITUS

3.1 ABSTRACT

Vulnerability to noise-induced tinnitus is associated with increased spontaneous firing rate (hyperactivity) in dorsal cochlear nucleus (DCN) principal neurons (fusiform cells). This hyperactivity is caused, at least in part, by decreased Kv7.2/3 (KCNQ2/3) potassium currents. However, the biophysical mechanisms underlying resilience to tinnitus, which is observed in noise-exposed mice that do not develop tinnitus (non-tinnitus mice), remain unknown. Our results show that noise exposure induces a reduction in KCNQ2/3 channel activity in DCN fusiform cells in noise-exposed mice by 4 days after exposure. Tinnitus is developed in mice that do not compensate for this reduction within the next 3 days. Resilience to tinnitus is developed in mice that show a re-emergence of KCNQ2/3 channel activity and a reduction in HCN (hyperpolarization-activated cyclic nucleotide-gated, non-selective cation) channel activity. Our results highlight KCNQ2/3 and HCN channels as potential targets for designing therapeutics that may promote resilience to tinnitus.

3.2 INTRODUCTION

Tinnitus, the perception of sound in the absence of acoustic stimulus, is frequently caused by exposure to loud sounds (Shargorodsky et al., 2010) and can be detrimental to the quality of life for millions of tinnitus sufferers (Roberts et al., 2010; Shargorodsky et al., 2010). Although the development of tinnitus is strongly correlated with acoustic trauma and noise-induced hearing loss, the absence of tinnitus after exposure to loud sounds -- resilience to tinnitus -- has been observed in a significant percentage of the population both in humans and in animal models (Zeng et al., 2012; Li et al., 2013; Yankaskas, 2013). Unlike other hyperexcitability-related disorders, such as neuropathic pain and epilepsy, where genetic and epigenetic factors play essential roles in determining susceptibility (Taylor et al., 2011; Bell et al., 2014a; Denk et al., 2014), the susceptibility to noise-induced tinnitus cannot be explained by genetic factors (Kvestad et al., 2010), suggesting that the boundary between susceptibility and resilience to tinnitus may be malleable. Therefore, elucidating the molecular mechanisms underlying resilience to tinnitus could be vital for both developing natural ways to prevent and treat tinnitus, and understanding the mechanisms that differentiate pathogenic plasticity that leads to tinnitus from homeostatic plasticity that prevents the induction of tinnitus.

Physiological properties associated with resilience to tinnitus have been detected in the DCN, an auditory brainstem nucleus that is essential for the induction of tinnitus (Brozoski et al., 2012b). Although all noise-exposed animals show similar shifts in their hearing thresholds, only a portion of them display DCN hyperactivity (increased spontaneous firing rate of fusiform cells) and develop tinnitus, termed tinnitus mice (Longenecker and Galazyuk, 2011; Koehler and Shore, 2013; Li et al., 2013; Longenecker et al., 2014). In tinnitus mice, KCNQ2/3 currents are reduced at hyperpolarized membrane potentials, due to a depolarizing shift in the voltage

dependence of KCNQ2/3 channel opening (Li et al., 2013). This reduction leads to DCN hyperactivity, which is crucial for the induction of tinnitus (Li et al., 2013). On the other hand, noise-induced mice that do not develop tinnitus (non-tinnitus mice) do not show fusiform cell hyperactivity after sound-exposure, and express normal levels of KCNQ2/3 currents (Li et al., 2013). Nonetheless, knowledge of the biophysical mechanisms associated with resilience to tinnitus is still in its infancy.

Because fusiform cell spontaneous firing is mediated by intrinsic, not synaptic, properties (Leao et al., 2012), we blocked excitatory and inhibitory synaptic transmission to investigate the intrinsic mechanisms underlying resilience to tinnitus in a mouse model of noise-induced tinnitus. We evaluated fusiform cell intrinsic excitability in control (sham-exposed), tinnitus and non-tinnitus mice. We then extended this analysis by pharmacologically and biophysically isolating the ion channels whose noise-induced plasticity was associated with fusiform cell spontaneous firing rates and tinnitus or non-tinnitus behavior. Our results highlight the importance of KCNQ2/3 and HCN channels in the resilience to tinnitus and illuminate therapeutic paths that may enhance natural resilience for tinnitus prevention.

3.3 RESULTS

3.3.1 Mouse model of tinnitus allows for behavioral separation of noise-exposed mice with either vulnerability or resilience to tinnitus

To study the neural mechanisms underlying resilience to noise-induced tinnitus, we employed an animal model of tinnitus that permits behavioral separation of tinnitus from non-

tinnitus mice. According to this model, behavioral evidence of tinnitus is evaluated based on the inability of tinnitus mice to detect a silent sound gap in a continuous background sound, for their tinnitus "fills in the gap" (Turner et al., 2006b; Longenecker and Galazyuk, 2011; Li et al., 2013). When introducing a silent gap in a constant background sound before a startle stimulus (gap trial), normal mice detect the gap and show reduced startle amplitude compared to their response to a startle stimulus preceded by the same background sound but without any gap. Noise-exposed mice that do not perceive the silent gap show similar startle amplitudes in gap and no-gap trials and are considered tinnitus mice. Noise-exposed mice that perceive the silent gap show reduced startle amplitudes in gap trials and are considered non-tinnitus mice. To evaluate the gap detection ability of sham- and noise-exposed mice, we quantified the gap startle ratio (before and after exposure), which is the maximum startle amplitude in gap trials divided by the maximum startle amplitude in no-gap trials (Figure 5B). Moreover, to evaluate the frequency-specificity of noise-induced tinnitus, we quantified the gap startle ratio for background sounds with different frequencies (Materials and Methods 3.5.1). Our results showed that one week after noise exposure, 52.4% (11/21) of the noise-exposed mice exhibited a significant gap detection deficit at high- (20 - 32 kHz) but not at low-frequency (10 - 16 kHz) background sounds. This deficit is indicated by an increase in gap startle ratios and is consistent with behavioral evidence of high-frequency tinnitus (Figure 5B middle, Figure S 9, Materials and Methods 3.5.1). Importantly, increases in gap startle ratios in tinnitus mice cannot be explained by noise-induced impairments in temporal processing or by noise-induced inability to hear the background sound, because prepulse inhibition (PPI, the inhibition of startle response by a preceding non startling sound of similar intensity as the background sound used in gap detection) was similar among control, tinnitus, and non-tinnitus. We conclude that our animal model

provides a clear separation of noise-exposed mice with and without behavioral evidence of tinnitus, and therefore enables us to investigate the mechanisms underlying vulnerability and resilience to tinnitus.

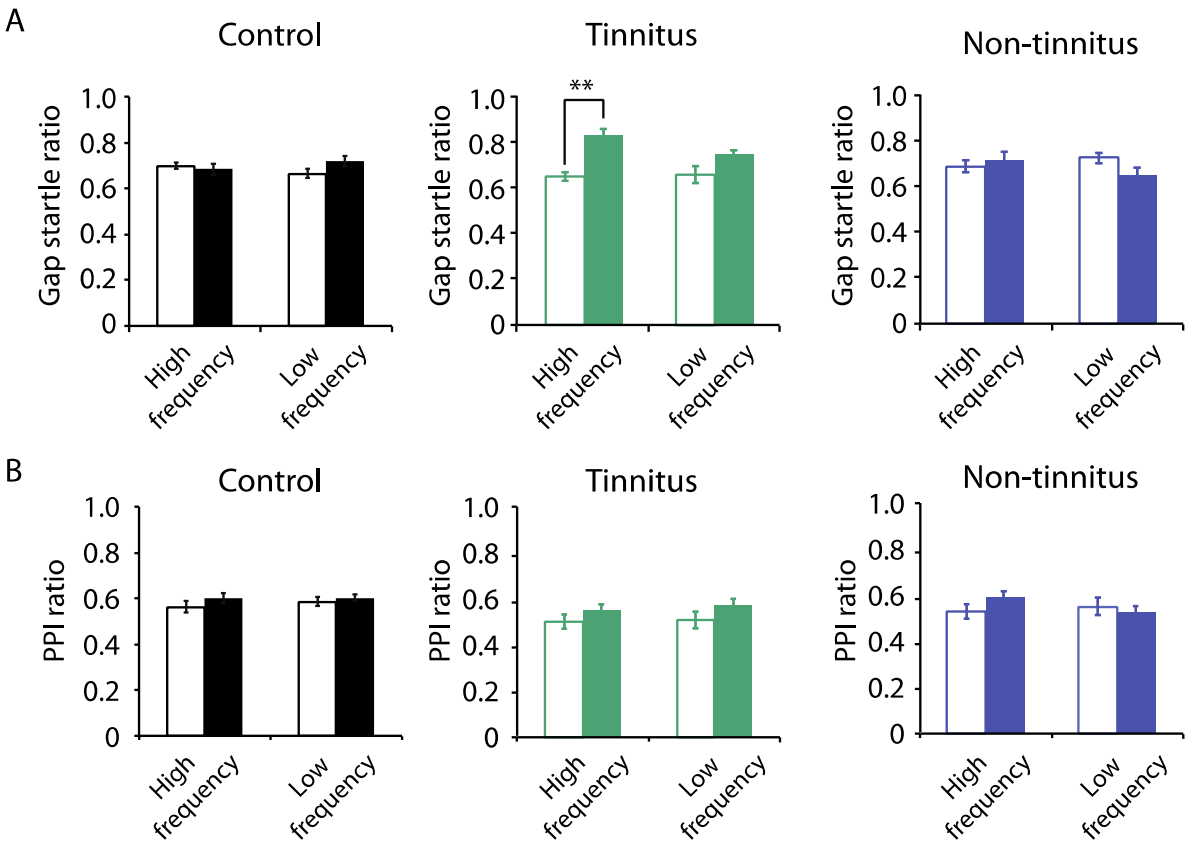

Figure 5. Mouse model of tinnitus allows for behavioral separation of noise-exposed mice with either vulnerability or resilience to tinnitus

Legends for Figure 5.

A. Summary graphs of gap startle ratio (response to gap-trial/ response to no-gap-trial) for high- and low-frequency background sounds (high-frequency background, 20–32 kHz, control: n = 22, tinnitus: n = 11, non-tinnitus: n = 10;

low frequency background, 10–16 kHz, control: n = 22, tinnitus: n = 11, non-tinnitus: n = 10). Open bars represent gap startle ratio before sham- or noise exposure; filled bars represent gap startle ratio 1 week later.

B. Summary graphs of prepulse inhibition ratio (PPI ratio, response to prepulse and startle stimulus/response to startle stimulus alone) for high- and low-frequency prepulse (control: n = 22, tinnitus: n = 11, non-tinnitus: n = 10).

Asterisk, $p < 0.001$. Error bars indicate SEM.

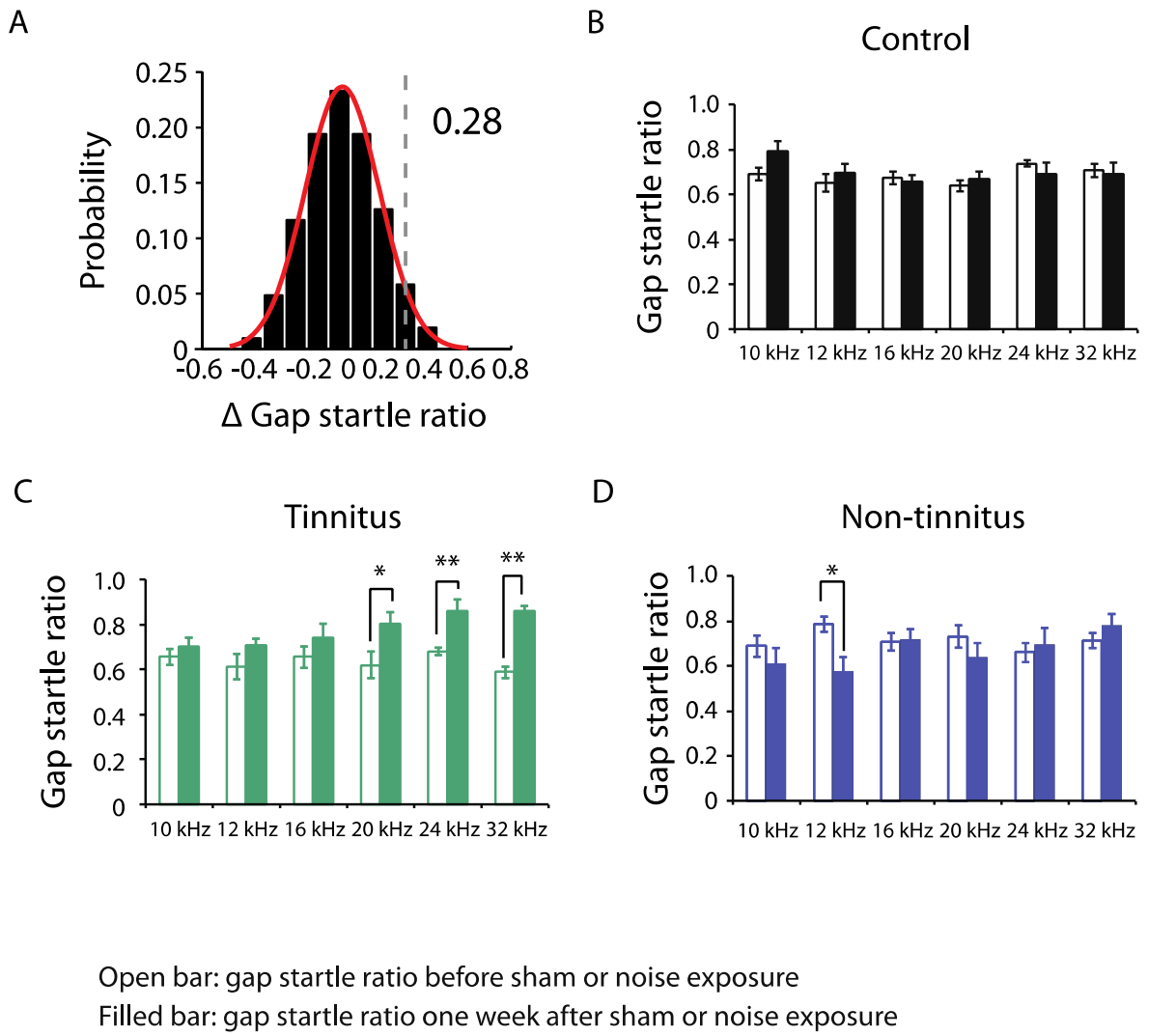

Figure S 9. Noise-Induced increases in gap startle ratio for more than 0.28 is a criterion for separating tinnitus from non-tinnitus mice

Legends for Figure S 9.

A. Probability distribution of changes in gap startle ratio (Δ gap startle ratio) in sham-exposed (control) mice. Δ gap startle ratio represents changes in control mice between postnatal day P17- P20 and P24 - P27. Data were fitted by a normal distribution (red curve, $\mu = -0.02$, $\delta = 0.15$, $n = 21$). Δ gap startle ratios smaller than 0.28 (dotted line, which is the point that is 2 standard deviations above the mean and used as the threshold for evaluating tinnitus) represent 98.6% of the experimental population and 98.5% of the fitted distribution.

B. Summary graph of gap startle ratio for different frequencies of background for control mice: 10 kHz, before: 0.69 ± 0.03, n = 13, after: 0.79 ± 0.04, n = 17, p = 0.08; 12 kHz, before: 0.65 ± 0.04, n = 8, after: 0.70 ± 0.04, n = 18, p = 0.47; 16 kHz, before: 0.67 ± 0.03, n = 15, after: 0.66 ± 0.03, n = 18, p = 0.67; 20 kHz, before: 0.64 ± 0.02, n = 14, after: 0.67 ± 0.03, n = 18, p = 0.47; 24 kHz, before: 0.74 ± 0.02, n = 17, after: 0.69 ± 0.05, n = 14, p = 0.34; 32 kHz, before: 0.71 ± 0.03, n = 19, after: 0.69 ± 0.05, n = 16, p = 0.78.

C. Summary graph of gap startle ratio for different frequencies of background for tinnitus mice: 10 kHz, before: 0.65 ± 0.04, n = 8, after: 0.70 ± 0.04, n = 10, p = 0.36; 12 kHz, before: 0.61 ± 0.06, n = 5, after: 0.71 ± 0.03, n = 10, p = 0.10; 16 kHz, before: 0.66 ± 0.05, n = 8, after: 0.74 ± 0.06, n = 10, p = 0.30; 20 kHz, before: 0.62 ± 0.06, n = 7, after: 0.80 ± 0.05, n = 11, p = 0.04; 24 kHz, before: 0.68 ± 0.02, n = 7, after: 0.86 ± 0.05, n = 9, p = 0.006; 32 kHz, before: 0.59 ± 0.03, n = 8, after: 0.86 ± 0.03, n = 12, $P < 0.0001$.

D. Summary graph of gap startle ratio for different frequencies of background for non-tinnitus mice: 10 kHz, before: 0.69 ± 0.05, n = 7, after: 0.61 ± 0.07, n = 10, p = 0.40; 12 kHz, before: 0.78 ± 0.03, n = 6, after: 0.58 ± 0.06, n = 8, p = 0.02; 16 kHz, before: 0.71 ± 0.04, n = 6, after: 0.72 ± 0.04, n = 9, p = 0.83; 20 kHz, before: 0.73 ± 0.05, n = 6, after: 0.64 ± 0.06, n = 9, p = 0.32; 24 kHz, before: 0.66 ± 0.04, n = 7, after: 0.70 ± 0.07, n = 9, p = 0.67; 32 kHz, before: 0.71 ± 0.03, n = 7, after: 0.78 ± 0.05, n = 6, p = 0.26.

Asterisk, $p < 0.05$. Double asterisk, $p < 0.01$. Error bars indicate SEM.

3.3.2 Fusiform cells from non-tinnitus mice show hyperpolarized subthreshold dynamics and hyperpolarized resting membrane potential

Given the importance of fusiform cell intrinsic conductances in mediating vulnerability to tinnitus (Li et al., 2013), we blocked excitatory and inhibitory neurotransmission to study the role of its intrinsic properties in tinnitus resilience (Materials and Methods). Because pathogenic intrinsic plasticity underlying vulnerability to tinnitus induction matches the behavioral evidence for tinnitus and appears specifically in fusiform cells that represent high (~≥20 kHz, dorsal part) but not low sound frequencies (<20 kHz, ventral part) (Li et al., 2013), we conducted our recordings on fusiform cells located in the high frequency part of the DCN (Materials and Methods 3.5.6)(Li et al., 2013). Fusiform cells from sham-exposed (control) and non-tinnitus mice showed no differences in their spike parameters (Table 2, Materials and Methods 3.5.6). Although fusiform cells from non-tinnitus mice showed a spontaneous firing rate that is not different from control mice (Materials and Methods)(Li et al., 2013), they revealed more hyperpolarized membrane potential in the early part of the inter-spike interval (Figure 6A, shaded area). To quantify this difference, we measured the membrane potential at the middle time point of the inter-spike interval (medium inter-spike potential, Figure 6A, dotted line). This analysis revealed that fusiform cells from non-tinnitus mice have significantly more hyperpolarized medium inter-spike potential, suggesting changes in subthreshold conductance(s) (Figure 6B, control: -61.1 ± 0.8 mV, n = 8; non-tinnitus: -64.9 ± 0.86 mV, n = 8; p = 0.002). Consistent with this notion, after blocking spontaneous firing activity with tetrodotoxin (TTX, 0.5 μM), we found that fusiform cells from non-tinnitus mice showed more hyperpolarized resting membrane potential (Figure 6C, control: -64.2 ± 1.3 mV, n = 14; non-tinnitus: -67.5 ± 0.7

mV, n = 15, p = 0.04). Moreover, when small current steps were used to evaluate the initial and steady state input resistance, we observed that the initial input resistance was not different among control, tinnitus and non-tinnitus mice, but non-tinnitus mice displayed a significantly increased steady state input resistance, which is measured at a later time point during the hyperpolarizing or depolarizing pulses (Materials and Methods 3.5.6; Figure 6D; Figure 6E, steady state input resistance, control: 58.2 ± 3.6 MΩ, n = 8; tinnitus: 54.8 ± 4.2 MΩ, n = 7; non-tinnitus: 97.7 ± 16.9 MΩ, n = 8; p = 0.01; Figure 6F, initial state input resistance, control: 97.9 ± 8.4 MΩ, n = 8; tinnitus: 90.1 ± 4.8 MΩ, n = 7; non-tinnitus: 105.7 ± 18.5 MΩ, n = 8; p = 0.73). Taken together, these results suggest that non-tinnitus mice exhibit a decrease in a slowly activating and deactivating depolarizing conductance (Figure 6D-F) that is open at subthreshold potentials. The decrease in this conductance hyperpolarizes subthreshold dynamics and reduces resting membrane potential (Figure 6A-C). These results highlight that although control and non-tinnitus mice show similar non-tinnitus behavior, non-tinnitus mice are biophysically distinct from control mice, and suggest the development of resilience mechanisms in non-tinnitus mice.

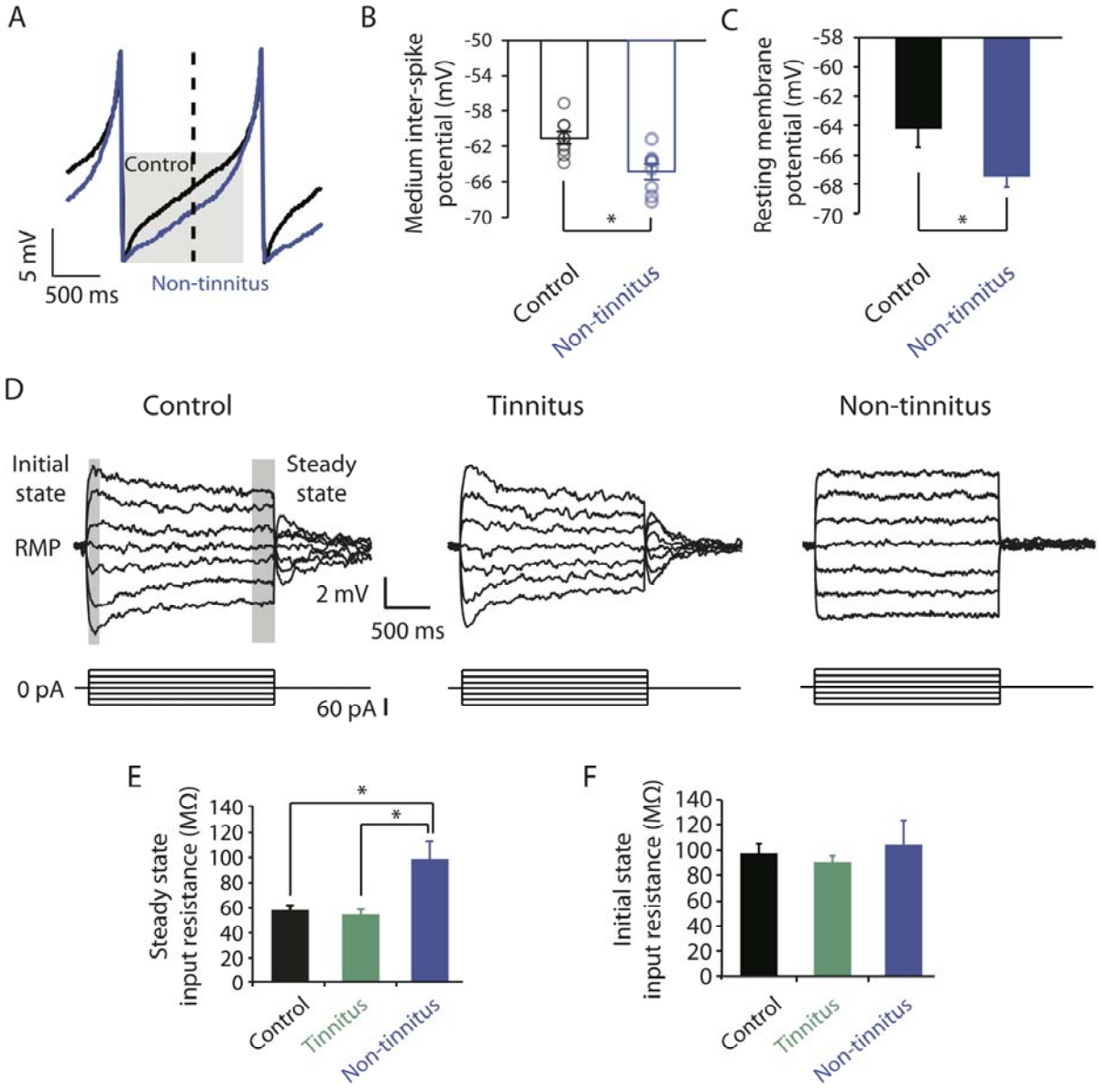

Figure 6. Fusiform cells from non-tinnitus mice show hyperpolarized subthreshold dynamics.

Legends for Figure 6.

A. Representative spontaneous spikes from control (Black) and non-tinnitus (Blue) mice with the same inter-spike interval (ISI) aligned at the negative peak of the spike. Shaded box highlights the region where fusiform cells from non-tinnitus mice display more hyperpolarized subthreshold dynamics. Dotted line indicates the middle time point of ISI where medium inter-spike potential is measured.

B. Summary graph of the medium inter-spike potential from control and non-tinnitus mice (control: n = 8; non-tinnitus: n = 8).

C. Summary graph of resting membrane potential of fusiform cells from control and non-tinnitus mice after blocking spontaneous firing with 0.5 μM TTX (control: n = 14; non-tinnitus: n = 15).

D. Representative voltage traces of fusiform cells from control, tinnitus and non-tinnitus mice (Top) in response to small depolarizing and hyperpolarizing current steps (Bottom) for measuring input resistance. Shaded areas indicate the region for evaluating initial and steady state input resistance (Materials and Methods).

E. Summary graph of steady state input resistance of fusiform cells from control, tinnitus and non-tinnitus mice (control: n = 8; tinnitus: n = 7; non-tinnitus: n = 8).

F. Summary graph of initial state input resistance of fusiform cells from control, tinnitus and non-tinnitus mice (control: n = 8; tinnitus: n = 7; non-tinnitus: n = 7).

Asterisk, $p < 0.05$. Error bars indicate SEM.

Table 2. Spike parameters of fusiform cells from high-frequency region of DCN in control and non-tinnitus mice

	Spike threshold	Spike amplitude	Depolarization slope	Hyperpolarization slope	Half height width	fAHP
Control	-47.1 ± 0.5 mV	40.6 ± 1.2 mV	219.2 ± 7.5 V/s	-165.3 ± 5.5 V/s	0.31 ± 0.01 ms	22.0 ± 1.3 mV
Non-tinnitus	-48.4 ± 0.7 mV	40.5 ± 1.6 mV	206.0 ± 7.6 V/s	-152.0 ± 3.7 V/s	0.33 ± 0.01 ms	22.7 ± 0.8 mV

* fAHP: fast afterhyperpolarization;
* Depolarization slope: maximum depolarizing slope;
* Hyperpolarization slope: minimum hyperpolarizing slope;

Legends for Table 2.

All recordings were performed in fusiform cells in the high-frequency region of the DCN (spike threshold, control: n = 8, non-tinnitus: n = 8, P = 0.16; spike amplitude: control, n = 8, non-tinnitus, n = 8, p = 0.98; depolarization slope, control: n = 8, tinnitus: n = 8, P = 0.97; hyperpolarization slope, control: n = 8, tinnitus, n = 8, P = 0.07; half height width, control: n = 8, tinnitus: n = 8, P = 0.09; fAHP, control: n = 8, tinnitus: n =8, P = 0.68). Depolarization slope: maximum depolarizing slope; hyperpolarization slope: minimum hyperpolarizing slope; fAHP: fast afterhyperpolarization.

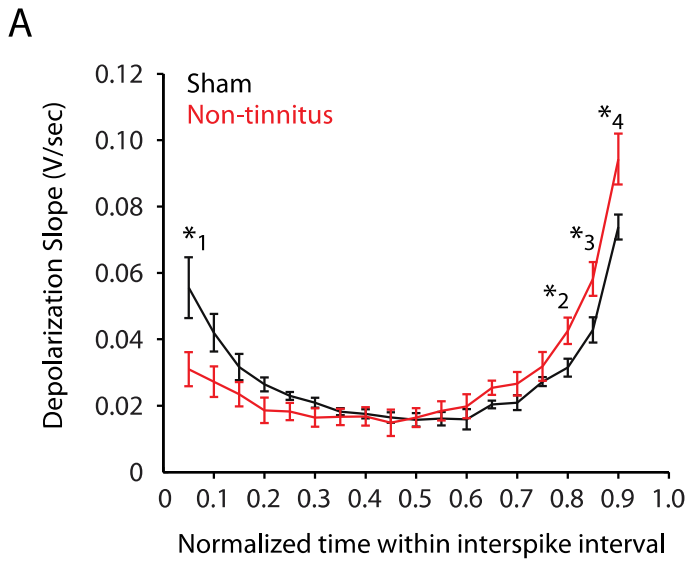

Figure S 10 Fusiform cells from non-tinnitus mice show different subthreshold membrane dynamics comparing with cells from sham-exposed control mice.

Legends for Figure S 10.

A. Spike trace between negative peak of a previous spike and spike threshold of the following spike were down-sampled from 20 kHz to 40Hz. Inter-spike interval is normalized relative to the negative peak of a previous spike and spike threshold of the following spike. Fusiform cells from non-tinnitus mice show significantly smaller depolarization slope immediately after a spike (sham-1: 0.06 ± 0.01, n = 8; non-tinnitus-1: 0.03 ± 0.005, n = 9, p = 0.03). However, cells from non-tinnitus mice show significantly faster depolarization at end of the interspike interval (sham-2: 0.03 ± 0.003, non-tinnitus-2: 0.04 ± 0.004, p = 0.04; sham-3: 0.04 ± 0.004, non-tinnitus-3: 0.06 ± 0.005, p = 0.03; sham-4: 0.07 ± 0.004, non-tinnitus-4: 0.10 ± 0.008, p = 0.04). Error bars indicate SEM.

3.3.3 Reduced HCN channel activity underlies hyperpolarized subthreshold dynamics and hyperpolarized resting membrane potential in non-tinnitus mice

Previous studies have revealed hyperpolarization-activated cyclic nucleotide-gated channels (HCN channels) as important regulators of subthreshold dynamics in fusiform cells (Manis, 1990; Leao et al., 2012). Given the more hyperpolarized medium inter-spike potential, the hyperpolarized resting membrane potential and the increased steady state input resistance in non-tinnitus mice (Figure 6B, C, E), we hypothesized that a decrease in HCN channel activity may lead to the hyperpolarized subthreshold dynamics and increased steady state input resistance in non-tinnitus mice.

To test this hypothesis, we injected hyperpolarizing current (-550 pA, 2s) to activate HCN channels (Materials and Methods 3.5.6). HCN channel activation led to a characteristic rebound in the membrane voltage (voltage sag) that was sensitive to the specific HCN channel blocker ZD7288 (10 μM; Figure 7. A, Red: before ZD7288; Black: after ZD7288). HCN channel activity was evaluated by the ZD7288-sensitive sag ratio, which was calculated as the difference between the peak and steady state voltage normalized to the peak voltage (Sag ratio = $(V_{peak} - V_{ss})/V_{peak}*100\%$, Materials and Methods 3.5.6)(Sheets et al., 2011). Consistent with our hypothesis, fusiform cells from non-tinnitus mice showed significantly reduced HCN channel activity (Figure 7B, control: 15.5 ± 2.2%, n = 8; tinnitus: 14.1 ± 1.1%, n = 6; non-tinnitus: 8.3 ± 1.1%, n = 8, p = 0.004). To confirm whether reduction in HCN channel activity is responsible for the non-tinnitus-specific intrinsic properties, we evaluated the effect of ZD7288 on steady state input resistance, resting membrane potential and subthreshold membrane dynamics. ZD7288 application abolished the voltage deflection in response to small current steps in fusiform cells from control and tinnitus mice (compare Figure 6D vs. Figure 7C), and therefore eliminated the

differences in steady state input resistance (Figure 7D, control: 79.2 ± 22.8 MΩ, n = 4; tinnitus: 54.9 ± 10.9 MΩ, n = 4; non-tinnitus: 70.02 ± 15.1 MΩ, n = 3, p = 0.7). Moreover, ZD7288 application eliminated the difference in resting membrane potential among control, tinnitus and non-tinnitus mice (Figure 7E, control: -67.4 ± 2.6 mV, n = 6; tinnitus: -67.4 ± 0.9 mV, n = 6; non-tinnitus: -65.8 ± 2.1 mV, n = 8, p = 0.6). Finally, ZD7288 application in control mice mimicked the hyperpolarization in the medium inter-spike potential observed in fusiform cells from non-tinnitus mice (Materials and Methods 3.5.6, Figure 7F, G, Before ZD7288: -63.6 ± 1.5 mV, After ZD7288: -66.0 ± 1.2 mV, n = 8, $p < 0.001$). Together, our results suggest that reduced HCN channel activity is responsible for hyperpolarized subthreshold dynamics, hyperpolarized resting membrane potential and increased steady state input resistance in non-tinnitus mice. These results suggest that reduction in HCN channel activity is a biophysical change associated with resilience to tinnitus.

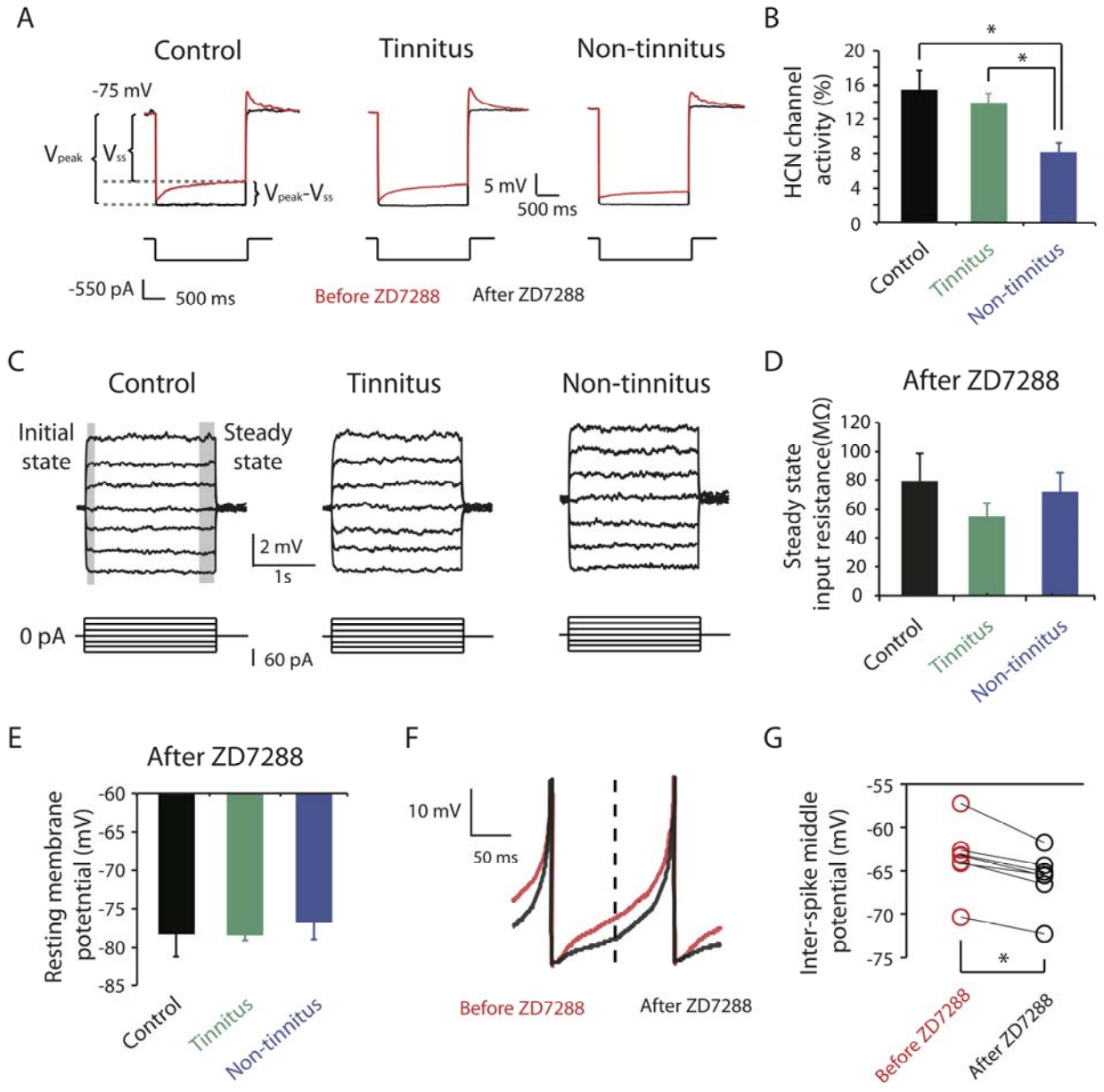

Figure 7. Reduced HCN channel activity underlies hyperpolarized subthreshold dynamics and hyperpolarized resting membrane potential in non-tinnitus mice.

Legends for Figure 7.

A. Representative voltage traces (Top) of fusiform cells from control, tinnitus and non-tinnitus mice in response to a hyperpolarizing current step (Bottom) for measuring HCN channel activity before (Red) and after (Black) 10 μM ZD7288. HCN channel activity is measured by the calculating sag ratio ((V_{peak} - V_{ss})/V_{peak}*100 (%)) that is sensitive

to ZD7288 (Materials and Methods 3.5.6).

B. Summary graph showing HCN channel activity as measured by the protocol described in A (control: n = 8; tinnitus: n = 6; non-tinnitus: n = 8).

C. Representative voltage traces of fusiform cells from control, tinnitus and non-tinnitus mice in response to current steps for measuring input resistance as in Figure 6D but now in the presence of 10 μM ZD7288. D. Summary graph showing steady state input resistance in control, tinnitus and non-tinnitus mice in 10 μM ZD7288 (control, n = 4; tinnitus, n = 4; non-tinnitus, n = 3).

E. Summary graph showing resting membrane potential in control, tinnitus and non-tinnitus mice in 10 μM ZD7288 (control, n = 6; tinnitus, n = 6; non-tinnitus, n = 8).

F. Representative spontaneous spikes of fusiform cells from control mice before (Red) and after ZD7288 (Black). Traces are aligned at the negative peak of the spike. Dotted line indicates the middle point of ISI where medium inter-spike potential is measured.

G. Summary graph of medium inter-spike potential before and after ZD7288 in fusiform cells from control mice (Before ZD7288: n = 8; After ZD7288: n = 8).

Asterisk, $p < 0.05$. Error bars indicate SEM.

3.3.4 Noise-induced KCNQ2/3 plasticity occurs before HCN plasticity

While vulnerability to tinnitus is associated with reduced KCNQ2/3 and control-level HCN channel activity (Figure 7B and Li et al., 2013), resilience to tinnitus is associated with reduced HCN channel activity and control-level KCNQ2/3 channel activity (Figure 7B and Li et al., 2013). Based on these observations, one hypothesis predicts that it is the lack of reduction in KCNQ2/3 channels activity that determines resilience to tinnitus, while another hypothesis points to the reduction in HCN channel activity as a major determinant of resilience. To distinguish between these two hypotheses and to determine the temporal hierarchy in the development of KCNQ2/3 and HCN plasticity after noise-exposure, we measured KCNQ2/3 current amplitude as well as HCN channel activity in fusiform cells from noise-exposed mice 4 days post noise exposure (4 days noise-expose mice; Figure 8A, C). To quantify KCNQ channel activity, we held fusiform cells at −30 mV for 5 s and then stepped the voltage to −50 mV for 1 s to unmask the deactivation of KCNQ channels. Consistent with previous KCNQ currents measurements in fusiform cells (Li et al., 2013), this protocol revealed both a fast and slow deactivating current and that was significantly reduced by XE991 application. Only the slow deactivation current was used for analysis in our study (10 μM, a specific KCNQ channel blocker; Figure 8A shows the slowly deactivating XE991-sensitive current, Materials and Methods). Because KCNQ2/3 heteromers mediate the KCNQ currents in fusiform cells, the XE991-sensitive component of these recordings represents the KCNQ2/3 current amplitude (Li et al., 2013). Four days after exposure, exposed mice showed significantly reduced KCNQ2/3 currents (Figure 8B, 4 days sham-exposed, 73.1 ± 9.8 pA, n = 4; 4 days noise-exposed, 40.2 ± 6.7 pA, n = 15, p = 0.004). However, HCN channel activity, measured as in Figure 7A was not different between 4 days sham-exposed and 4 days noise-exposed mice (Figure 8D, 4 days sham-

exposed, 27.2 ± 2.5%, n = 4; 4 days, 24.4 ± 5.4%, n = 7, p = 0.7). Our data therefore suggest that the decrease in KCNQ2/3 activity happens before the reduction of HCN channel activity.

Four days after noise exposure, noise-exposed mice display homogeneous tinnitus-like biophysics: reduced KCNQ2/3 and control-level HCN channel activity. Therefore, we suggest that it is not the lack of reduction in KCNQ2/3 channels activity that determines resilience to tinnitus. Instead, we propose that it is the recovery of KCNQ2/3 currents, together with the reduced HCN channel activity, both occurring 4 to 7 days after noise-exposure, that contribute to tinnitus resilience. Mice that maintain their tinnitus-like biophysical properties, which are established 4 days post noise exposure, develop tinnitus by 7 days post noise exposure.

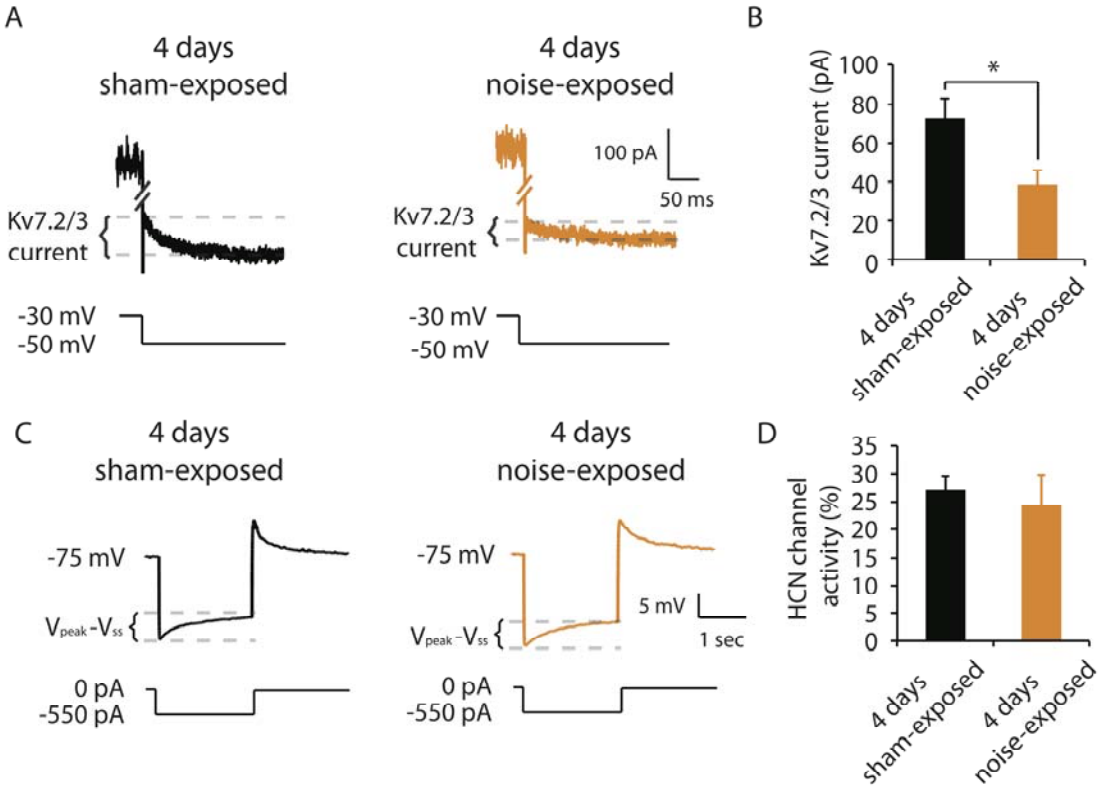

Figure 8. Noise-induced KCNQ2/3 plasticity occurs before HCN plasticity

Legends for Figure 8.

A. Representative traces illustrating XE991 (10 μM)-sensitive KCNQ2/3 current (Top) in fusiform cells from 4 days sham-exposed and 4 days noise-exposed mice in response to a hyperpolarizing voltage step form -50 to -30 mV (Bottom).

B. Summary graph showing KCNQ2/3 current amplitude in fusiform cells from 4 days sham-exposed and 4 days noise-exposed mice (4 days sham-exposed mice, n = 4; 4 days noise-exposed mice, n = 7).

C. Representative traces illustrating ZD7288 (10 μM)-sensitive HCN channel activity (Top) in fusiform cells from 4 days sham-exposed and 4 days noise-exposed mice; HCN activity was measured as in Figure 7A, B.

D. Summary graph showing HCN channel activity in fusiform cells from 4 days sham-exposed and 4 days noise-exposed mice (4 days sham-exposed mice, n = 4; 4 days noise-exposed mice, n = 7).

Asterisk, $p < 0.05$. Error bars indicate SEM.

3.3.5 Pharmacological activation of KCNQ channels prevents the development of tinnitus and promotes a reduction in HCN channel activity

Reduced KCNQ2/3 currents appear in all noise-induced mice 4 days post noise exposure (Figure 8B); however, non-tinnitus mice display control-level KCNQ2/3 currents 7 days post exposure, indicating that fusiform cells in non-tinnitus mice experience a recovery in KCNQ2/3 channel activity between 4 and 7 days post noise exposure. Moreover, previous findings showed that *in vivo* pharmacological activation of KCNQ currents with retigabine (KCNQ channel activator) prevents the development of tinnitus (Li et al., 2013). Therefore, we propose that it is the recovery in KCNQ2/3 activity that drives the resilience to tinnitus. Given the determinant role of KCNQ channel activity in tinnitus resilience, we hypothesized that reduction in HCN channel activity in non-tinnitus mice may represent a homeostatic response that is driven by changes in KCNQ channel activity. To test these hypotheses, we first explored whether *in vivo* pharmacological activation of KCNQ currents prevents the development of tinnitus (positive control), and then we determined whether the same manipulation affects HCN channel activity. Consistent with previous results (Li et al., 2013), pharmacological activation of KCNQ channels with intraperitoneal injection of KCNQ channel activators, such as retigabine or flupirtine (10 mg/kg, 30 mins after noise exposure for 5 days, Methods), prevented the development of tinnitus in noise-exposed mice (Figure 9A, control: 9.5% (2 of 21); noise-exposed mice: 53.4% (11 of 21); noise-exposed mice + KCNQ activator: 25% (5 of 20); noise-exposed mice + saline: 50% (9 of 18)). The effect KCNQ channel activators on eliminating tinnitus was not due to changes in temporal processing or inability of the mice to hear the background sound, for prepulse inhibition, unlike gap detection, was not affected by KCNQ activators (Figure 9B, noise-exposed mice + saline, before noise-exposure: 0.47 ± 0.03, n = 18, after noise-exposure + saline, 0.51 ±

0.03, n = 18, p = 0.07; noise-exposed mice + KCNQ activator, before noise-exposure: 0.56 ± 0.03, n = 20, after noise-exposure + KCNQ activator, 0.49 ± 0.03, n = 20, p = 0.12). Moreover, consistent with the known role of KCNQ channel activators in enhancing KCNQ currents and decreasing spontaneous firing rates, *in vitro* recordings showed that fusiform cells from mice injected with retigabine exhibited significantly increased KCNQ2/3 currents, and reduced spontaneous firing rate (Figure 9C, KCNQ2/3 current, noise-exposed mice + saline: 47.3 ± 8.2 pA, n = 7; noise-exposed mice + retigabine: 86.9 ± 15.2 pA, n = 8, $p < 0.05$; Figure 9D, spontaneous firing rate, noise-exposed mice + saline: 15.0 ± 1.5 Hz, n = 5; noise-exposed mice + retigabine: 7.5 ± 2.2 Hz, n = 7, p = 0.02).

After establishing that pharmacological enhancement of KCNQ channel activity is sufficient for preventing the development of tinnitus, we tested whether reduction in HCN channel activity is driven by changes in KCNQ2/3 channel activity, which we realized through pharmacologically activating KCNQ channels (mice injected with retigabine from Figure 9A were used for these recordings). In agreement with this hypothesis, fusiform cells from retigabine-injected mice displayed significantly reduced HCN channel activity, suggesting that increased KCNQ2/3 channel activity promotes a decrease in HCN channel activity. (Figure 9E, F, noise-exposed mice + saline: 26.1 ± 0.6%, n = 13; noise-exposed mice + retigabine: 17.9 ± 0.5%, n = 14, p = 0.008). Taken together, our results suggest that it is the recovery in KCNQ2/3 channel activity, between 4 to 7 days post noise exposure, that provides resilience to tinnitus and promotes a decrease in HCN currents in non-tinnitus mice.

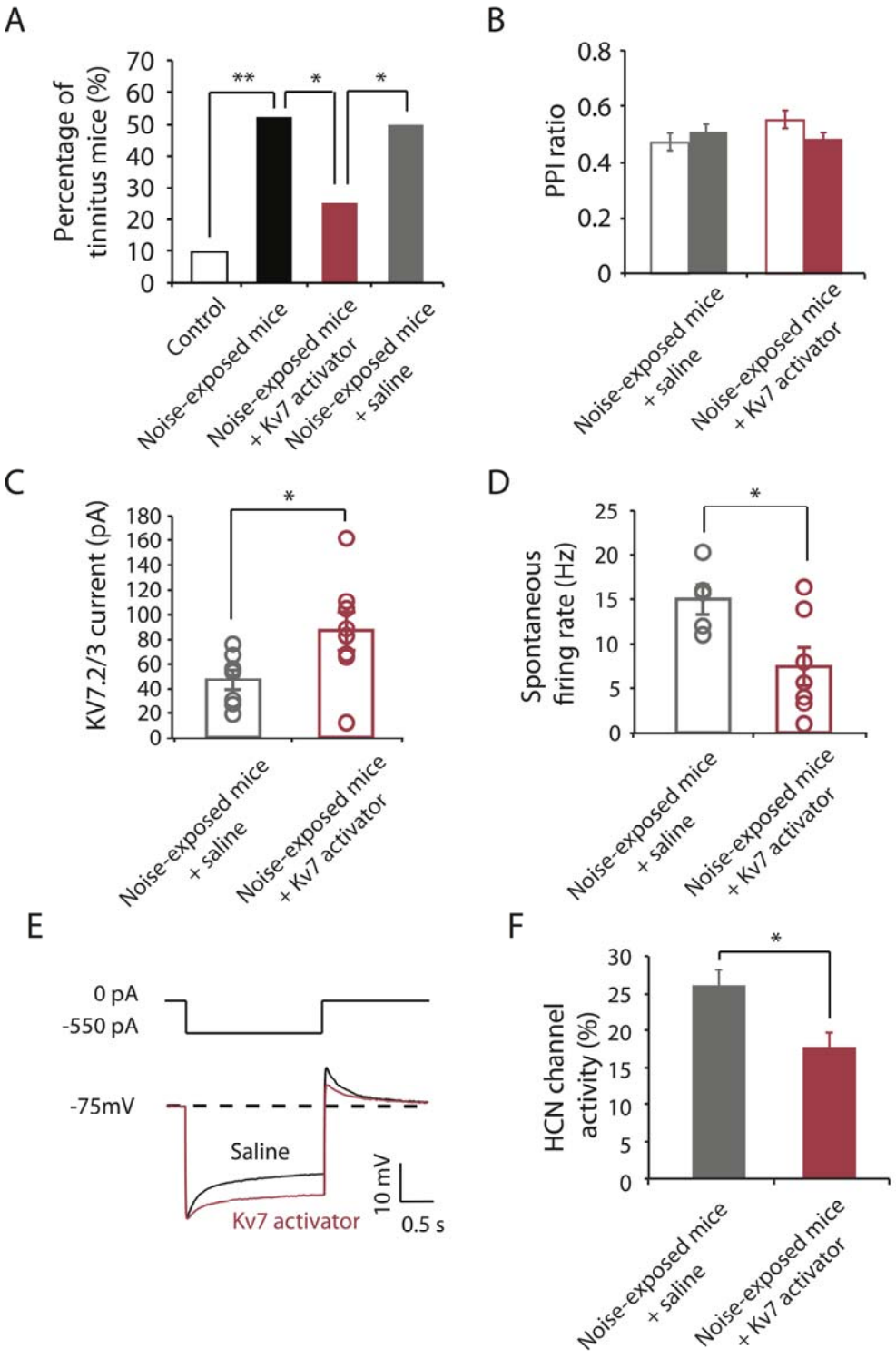

Figure 9. Pharmacological activation of KCNQ channels prevents the development of tinnitus and promotes a reduction in HCN channel activity

Legends for Figure 9.

A. Percentage of mice that develop tinnitus in control mice, noise-exposed mice, noise-exposed mice injected with KCNQ channel activator (retigabine or flupirtine, intraperitoneal injection, 10 mg/kg) and noise-exposed mice injected with saline (control: n = 21, noise-exposed mice: n = 21, noise-exposed mice with KCNQ activator: n = 20, noise-exposed mice with saline: n = 18).

B. PPI ratio in noise-exposed mice injected with saline and noise-exposed mice injected with KCNQ activator injection before (Open bar) and after (Filled bar) noise-exposure (noise-exposed mice with saline: n = 18; noise-exposed mice with KCNQ activator (retigabine): n = 20).

C. Summary graph showing KCNQ2/3 current amplitude in noise-exposed mice with saline injection and noise-exposed mice with KCNQ activator injection (noise-exposed mice with saline: n = 7; noise-exposed mice with KCNQ activator (retigabine): n = 8).

D. Summary graph showing spontaneous firing rate in fusiform cells from noise-exposed mice injected with either saline or KCNQ activator (noise-exposed mice with saline: n = 5; noise-exposed mice with activator: n = 7).

E. Representative voltage traces (Bottom) from fusiform cells in response to hyperpolarizing current step (Top) for measuring HCN channel activity (saline-injected, black; activator-injected, red).

F. Summary graph showing HCN channel activity as measured by the protocol in Figure 7A**.** (noise-exposed mice with saline: n = 13; noise-exposed mice with activator: n = 14).

Asterisk, $p < 0.05$. Error bars indicate SEM.

3.3.6 Four days after noise exposure, mice have reduced KCNQ2/3 currents but do not show tinnitus

Four days post noise exposure, fusiform cells from noise-exposed mice display homogeneous tinnitus-like biophysical properties (reduced KCNQ2/3 and control level HCN activity), suggesting that these mice may have increased fusiform cell spontaneous firing activity and tinnitus behavior. Surprisingly, behavioral testing revealed that 4 days noise-exposed mice did not show behavioral evidence of tinnitus (Figure 10A, 4 days sham-exposure: tinnitus 1/19; 4 days noise-exposure: tinnitus 2/20, $p = 0.28$). Moreover, fusiform cells from 4 days noise-exposed mice did not show increased spontaneous firing activity (Figure 10B, 4 days sham-exposed: 14.3 ± 4.7 Hz, $n = 6$; 4 days noise-exposed: 5.6 ± 2.3 Hz, $n = 6$, $p = 0.13$). Given that 4 days noise-exposed mice show reduced KCNQ2/3 current but do not show either increased spontaneous firing rate or tinnitus behavior, our results suggest the crucial role of fusiform cell hyperactivity underlying the induction of tinnitus. Consistent with decreased spontaneous firing rate, fusiform cells in 4 days noise-exposed mice had more hyperpolarized resting membrane potential, suggesting plasticity of ion channel(s) other than KCNQ2/3 and HCN (Figure 10C, 4 days sham-exposed: -64.4 ± 1.2 mV, $n = 6$; 4 days noise-exposed: -67.7 ± 0.8 mV, $n = 14$, $p = 0.04$). Taken together, our data uncovered that reduction of KCNQ2/3 channel activity happens by 4 days after noise exposure; however, at this time no tinnitus has developed yet, probably due to the absence of fusiform cell hyperactivity. Preservation of reduced KCNQ2/3 channel activity till 7 days post exposure leads to fusiform cell hyperactivity and behavioral evidence of tinnitus. Recovery of KCNQ2/3 channel to control level between 4 to 7 days after noise-exposure determines resilience to tinnitus and drives the reduction of HCN channel activity in non-tinnitus mice.

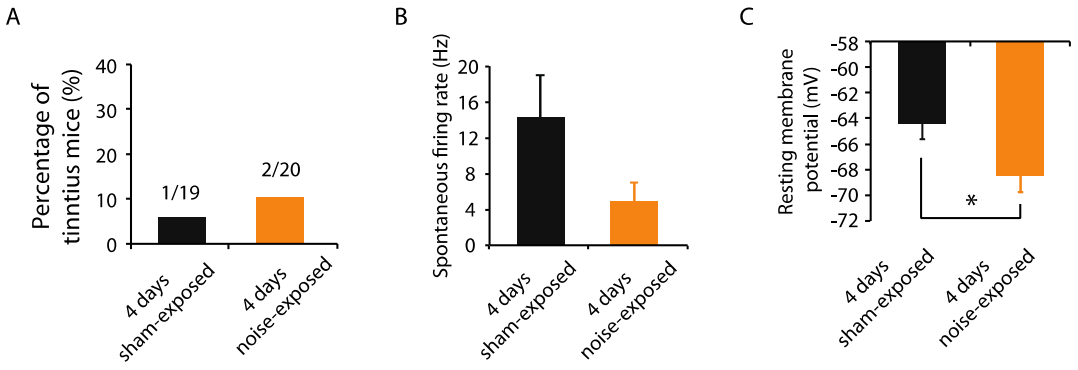

Figure 10. Four days post noise exposure mice have reduced KCNQ2/3 current amplitude but do not show tinnitus.

Legends for Figure 10.

A. Percentage of mice that develop tinnitus in 4 days sham-exposed and 4 days noise-exposed mice (4 days sham-exposed: n = 19; 4 days noise-exposed: n = 20).

B. Summary graph showing spontaneous firing rate in fusiform cells from 4 days sham-exposed and 4 days noise-exposed mice (4 days sham-exposed: n = 6; 4 days noise-exposed: n = 6).

C. Summary graph showing resting membrane potential in 4 days sham-exposed mice and 4 days noise-exposed mice (4 days sham-exposed: n = 6; 4 days noise-exposed: n = 14).

Asterisk, $p < 0.05$. Error bars indicate SEM.

3.4 DISCUSSION

3.4.1 Plasticity of KCNQ2/3 channels and its contribution to vulnerability and resilience to hyperexcitability-related disorders

KCNQ2/3 channels are slowly activating, non-inactivating voltage-dependent potassium channels that are open at hyperpolarized (subthreshold) voltages. As a result, they control subthreshold membrane potential and serve as a powerful brake on neuronal firing activity (Maljevic et al., 2008; Brown and Passmore, 2009). The crucial role of these channels in controlling neuronal excitability is illustrated by the finding that disorders that are characterized by neuronal hyperexcitability, such as epilepsy, neuropathic pain, and tinnitus are linked to genetic or experience-dependent reduction in KCNQ2/3 channel activity (Biervert et al., 1998; Schroeder et al., 1998; Dedek et al., 2001; Kullmann, 2002; Wuttke et al., 2007; Li et al., 2013). Pharmacological activation of KCNQ channels by retigabine, an FDA approved anti-epileptic drug that activates KCNQ2-5 channel activity, prevents seizures, neuropathic pain and the development of tinnitus (Tatulian et al., 2001; Gunthorpe et al., 2012; Li et al., 2013). Because *in vitro* studies have shown that KCNQ2/3 channel activity is plastic and can be enhanced in response to increased neuronal activity (Wu et al., 2008; Brown and Randall, 2009; Misonou, 2010), it is possible that endogenous, non-pharmacologically driven recovery in KCNQ2/3 channel activity may provide resilience to KCNQ2/3-related pathology. However, such KCNQ2/3-mediated resilience mechanisms have not been observed in hyperexcitability-related disorders. Here we report that natural, non-pharmacologically driven recovery in KCNQ2/3 channel activity is linked with resilience to noise-induced tinnitus. This novel finding suggests a temporal window during which endogenous, intrinsic mechanisms can restore

KCNQ2/3 channel activity and lead to tinnitus resilience. Elucidation of these mechanisms will unmask previously unknown plasticity mechanisms of KCNQ2/3 channel activity, and lead to new targets for drug development towards enhancing resilience to noise-induced tinnitus in humans.

Reduction of KCNQ2/3 currents is associated with increased spontaneous firing rate and tinnitus behavior 7 days after noise exposure (Li et al., 2013). However, at 4 days after noise exposure, fusiform cells showed reduced KCNQ2/3 currents (Figure 8A, B) but without hyperactivity (Figure 10). This lack of association between reduced KCNQ2/3 channel activity and neuronal hyperactivity can be explained by the hyperpolarized resting membrane potential of fusiform cells 4 days after noise exposure (Figure 10). Because various levels of inwardly rectifying potassium channels (K_{ir}) set the diverse resting membrane potential of fusiform cells (Leao et al., 2012; Li et al., 2013), we suggest that noise-induced increases in K_{ir}s may mediate this hyperpolarization of resting membrane potential and hence resilience to tinnitus. We conclude that reduction in KCNQ2/3 channel activity is a robust mechanism for triggering tinnitus, but its pathogenic effect is gated by the resting membrane potential of fusiform cells. Therefore, besides targeting KCNQ2/3 channel activators for preventing tinnitus, manipulations that hyperpolarize the resting membrane potential of fusiform cell may also provide additional therapeutic approaches.

KCNQ2/3 channels, mediate the native neuronal M-type current (Wang et al., 1998). In 1980, Brown and Adams discovered a slowly activating voltage-gated potassium current that was blocked by muscarinic acetylcholine (M) receptors, which they named the M-current (Brown and Adams, 1980). The M-current has now been identified throughout the central and the peripheral nervous system. KCNQ2/3 currents are strongly inhibited not only by the

activation of M receptors, but also by the activation of other G protein-coupled receptors that reduce membrane phosphatidylinositol-(4,5)-bisphosphate (PIP_2) levels, which is the major determinant in KCNQ channel gating (Marrion, 1997; Zhang et al., 2003). Our previous studies have revealed the important role of cholinergic activity and M receptors, namely M1 and M3, in fusiform cell synaptic plasticity (Zhao et al., 2011). Importantly, because noise exposure increases basal cholinergic activity in the DCN (Jin et al., 2006; Kaltenbach and Zhang, 2007; Manzoor et al., 2013) we propose that noise-induced increases and decreases (or recovery to baseline levels) in basal (tonic) M receptor signaling may underlie the bidirectional plasticity of KCNQ2/3 channel activity in response to noise exposure.

3.4.2 Plasticity of HCN channels and its contribution to vulnerability and resilience to disorders

HCN channels are non-inactivating cation channels that open at hyperpolarized voltages. Because of their voltage-dependent properties and their reversal potential at -30 mV, HCN channels depolarize the resting membrane potential, but also reduce membrane resistance and therefore stabilize the membrane voltage by opposing its alterations in response to synaptic inputs (Pape, 1996; Robinson and Siegelbaum, 2003; Biel et al., 2009). Therefore, changes in HCN channel activity affect intrinsic and synaptic excitability in opposing directions. Down regulation of HCN channel activity may hyperpolarize neurons and decrease intrinsic excitability (Lupica et al., 2001; Noam et al., 2011), but enhance synaptic excitability due to increased input resistance and enhanced temporal summation (Magee, 1998, 1999) This dual role of HCN channels on synaptic and intrinsic neuronal excitability has implicated the plasticity of HCN channel activity in the vulnerability and resilience to several neurological disorders characterized

by abnormal synaptic or intrinsic excitability, such as epilepsy, neuropathic pain, depression and Parkinson's disease (Chaplan et al., 2003; Biel et al., 2009; Chan et al., 2011; Emery et al., 2011; Shah et al., 2013; Friedman et al., 2014). Here, we show that reduction of HCN channel activity is associated with resilience to tinnitus and with normal levels of fusiform cell spontaneous firing activity (Figure 6, Figure 7). We hypothesize that reduced HCN channel activity in non-tinnitus mice prevents fusiform cell hyperactivity and contributes to tinnitus resilience by hyperpolarizing the resting membrane potential of fusiform cells (Figure 6, Figure 7). Immunohistochemical studies have shown that the HCN2 subunit is expressed in fusiform cells that lack HCN1 subunit expression (Koch et al., 2004), suggesting that HCN2 isoforms may mediate the noise-induced plasticity in fusiform cells. Therefore, we propose that manipulations that reduce HCN2 channel activity may serve as a potential therapeutic path for preventing the development of tinnitus. Our results are consistent with an important role of HCN channels in tinnitus resilience; however, it is still unresolved whether the down regulation of HCN channel activity in DCN fusiform cells is necessary for resilience to tinnitus induction or it is a consequence of resilience to tinnitus. Future studies are needed to test the causal relationship between reduction of HCN channel activity in fusiform cells and the resilience to tinnitus.

Decreased HCN channel activity hyperpolarized fusiform cells and maintained normal levels of spontaneous firing rates of fusiform cells (Figure 6, Figure 7). However, decreased HCN channel activity increased the steady state input resistance of fusiform cells (Figure 6, Figure 7), which is expected to enhance the responsiveness of fusiform cells to synaptic inputs. Therefore, reduction of HCN channel activity in fusiform cells may contribute to enhanced evoked activity and potentially to noise-induced hyperacusis -- the perception of moderate-level sounds as intolerably loud (Anari et al., 1999).

Previous studies have shown that large increases in postsynaptic calcium lead to enhancement in HCN current amplitude via NMDA receptor (NMDAR) activation, CaMKII activation and increased HCN channel expression (Fan et al., 2005), while smaller increases in calcium through L-type calcium channels and/or activation of mGluRs and PKC activation lead to activity-dependent decreases in HCN expression (Brager and Johnston, 2007; Chan et al., 2011). Pharmacological enhancement of KCNQ channels with retigabine reduces the spontaneous firing rate in fusiform cells (Figure 9D) and promotes a decrease in HCN current amplitude (Figure 9). Therefore, we propose that decreases in spontaneous firing that may be caused by the enhancement in KCNQ2/3 channel activity lead to changes in intracellular calcium, which, in turn, may trigger a homeostatic mechanism that decreases HCN currents in an effort to normalize spontaneous spike rates.

3.4.3 DCN spontaneous firing rates and tinnitus induction

Ablation of the dorsal acoustic stria (the output of the DCN) prior to noise-exposure prevents the induction of tinnitus (Brozoski et al., 2012b). However, when the same lesion occurs at a later time point after acoustic trauma, it fails to eliminate pre-existing tinnitus (Brozoski and Bauer, 2005). These results highlight the crucial role of the DCN in the induction of tinnitus and justify studying the DCN for understanding the mechanisms underlying resilience and vulnerability to tinnitus induction.

One of the major neural correlates for tinnitus induction is fusiform cell hyperactivity (Zhang and Kaltenbach, 1998; Brozoski et al., 2002a; Li et al., 2013). While a persistent change in other auditory centers such as the ventral cochlear nucleus (VCN), inferior colliculus (IC), auditory thalamus, or auditory cortex (AC) may be crucial for tinnitus maintenance (Eggermont,

2005; Vogler et al., 2011; Kalappa et al., 2014; Ropp et al., 2014), transient increases in DCN spontaneous firing rates appear necessary for tinnitus induction (Li et al., 2013; Ropp et al., 2014). Our results on the correlation of spontaneous firing rates of fusiform cell with behavioral evidence of tinnitus, which may or may not be associated with decreased KCNQ2/3 channel activity, further confirm that noise-induced fusiform cell hyperactivity is the only consistent biophysical change associated with the induction of tinnitus.

3.5 MATERIALS AND METHODS

3.5.1 Mouse model of tinnitus

ICR (CD-1) male and female mice were noise-exposed at postnatal day P17 - P20. After anesthetizing the mouse with 1 - 1.5% isoflurane, a pipette tip that was connected with the speaker was inserted into left ear canal of the mouse (unilateral noise exposure). Narrow bandpass noise with a 1 kHz bandwidth centered at 16 kHz was presented at 116 dB SPL for 45 minutes. For sham-exposed (control) mice, the procedures were identical with the noise-exposed mice but without noise presentation. For 4 days sham- and noise exposure experiments, P20 - P23 (instead of P17 - P20) mice were used for sham- or noise exposure, so that electrophysiological recordings and behavioral assessments 4 days after noise exposure were performed on mice that had similar age with the mice that were used for experiments 7 days after sham- or noise exposure.

3.5.2 Gap Detection

The gap detection paradigm (Turner et al., 2006b; Middleton and Tzounopoulos, 2012; Li et al., 2013) was used for assessing behavioral evidence of tinnitus. Gap detection of sham- or noise-exposed mice was assessed before exposure, 4 days or one week (6 to 7 days) after sham- or noise exposure. Detailed testing has been described in (Li et al., 2013). Briefly, the gap detection testing consists of two types of trials, gap trials and no-gap trials. In gap trials, a sound gap was embedded in a narrow bandpass background sound (1 kHz bandwidth centered at 10, 12, 16, 20, 24, and 32 kHz presented at 70 dB SPL), which was followed by the startle stimulus (20 ms white noise burst at 104 dB SPL); a 50-ms sound gap was introduced 130 ms before the startle stimulus. No-gap trials were the same as gap trials, but that no gap was introduced in the background sound. Gap trials and no-gap trials were presented as paired stimuli for the same background sound frequency, and were delivered in an alternating manner. The startle response represents the waveform of the downward pressing force that the mouse applies onto the platform in response to the startle stimulus. The ability of a mouse to detect sound gap was quantified by the gap startle ratio, which is the ratio of the peak-to-peak value of the startle waveform in gap trials over the peak-to-peak value of the startle waveform of the paired no-gap trials.

3.5.3 Prepulse Inhibition

Prepulse inhibition (PPI) is the inverse of gap detection and was tested together with gap detection before, 4 days or one week after sham- or noise exposure. PPI testing consists of prepulse trials and startle-only trials, which were delivered in an alternating fashion. In prepulse

trials, a brief non-startling sound (prepulse) of similar intensity as the background sound used in the gap detection test (50-ms, 70-dB SPL bandpass sound with 1-kHz bandwidth centered at 10, 12, 16, 20, 24, and 32 kHz). The prepulse was presented 130 ms before the startle stimulus. Startle-only trials were similar to the prepulse trials, but no prepulse was delivered. PPI was quantified by the PPI ratio, which is the ratio of the peak-to-peak value of the startle waveform in prepulse trials over the peak-to-peak value of the startle waveform in startle-only trials.

3.5.4 Gap detection and PPI analysis

For each sham- or noise-exposed mouse, gap detection and PPI ratios were averaged from three rounds of testing before and after sham or noise exposure. Each round of testing included 72 pairs of gap and no-gap trials for gap detection (6 background sound frequencies, 12 pairs for each frequency) and 30 pairs of prepulse and startle-only trials for PPI (6 prepulse sound frequencies, 5 pairs for each frequency). Gap startle and PPI ratios were analyzed separately. Maximum absolute amplitude of the startle response and root mean square of baseline movement preceding the startle response (RMS baseline) were measured with a Labview-based recording system. Mean and standard deviation of RMS baseline of gap, no-gap, prepulse and startle-only trials were measured to assess the variability of baseline movement. Trials with RMS baseline amplitude above or below the mean ± 2.5 standard deviations were eliminated. When a trial was eliminated, its paired trial was also eliminated. For gap detection trials of the same background frequency, gap startle ratios were sorted in an ascending manner. To control for variability of gap startle ratios within a frequency, ratios that showed an increase of more than 0.5 from the preceding value were excluded; the following values were also excluded. If more than 5 ratios were excluded within a frequency, the gap startle ratio for this frequency was not

used. For background and prepulse sound of the same frequency, individual gap startle and PPI ratios were averaged and generated the average ratio for each frequency for each round of testing. Average gap startle and PPI ratios of each frequency were then averaged across the three rounds of pre-exposure and post-exposure testing to generate the final ratio value. According to previous established criteria, gap startle ratios that were bigger than 0.9 before sham or noise exposure, or bigger than 1.1 after exposure were excluded (Li et al., 2013). Similarly, PPI ratios that were bigger than 1 before or after exposure were excluded (Li et al., 2013). Changes in gap startle ratio before and after exposure (Δ gap startle ratio) were calculated by subtracting the post-exposure ratio from the pre-exposure ratio for each testing frequency. The probability distribution of Δ gap startle ratios from all testing frequencies of sham-exposed mice was fitted with a Gaussian distribution, which permitted the calculation of the mean (μ) and the standard deviation (δ) of the probability distribution, as described previously (Li et al., 2013). For evaluating the behavioral evidence of tinnitus, we calculated the point that is 2 standard deviations above the mean and used this value as the threshold (Li et al., 2013). Mice that presented Δ gap startle ratio higher than threshold value in at least one tested frequency were considered tinnitus mice (Li et al., 2013). To determine whether Δ gap startle ratios from 4 days noise-exposed mice were different from Δ gap startle ratios from 4 days sham-exposed mice, we tested thresholds ranging from 1 to -1 with 0.02 increments

3.5.5 *In vivo* administration of KCNQ channel activators

For these experiments, ICR (CD-1) mice (P17 - P20), both male and female were used. Twenty noise-exposed mice were treated with KCNQ channel activators: 10 mice were injected with retigabine (as its dihydrochloride salt from Santa Cruz Biotechnology, LKT Laboratories)

and 10 mice were injected with flupirtine (flupirtine maleate from Selleck Chemicals), another KCNQ channel activator (Mackie and Byron, 2008). Moreover, 18 noise-exposed mice were treated with vehicle (11 mice with 0.9% saline paired with the retigabine group; and 7 mice with 30% propylene glycol, 5% Tween 80, 65% D5W paired with the flupirtine group). Prior to noise exposure, all mice were assessed for gap detection and PPI. For the KCNQ channel activator group, retigabine or flupirtine were administered 30 minutes after noise exposure via IP injection (10 mg/kg). In the vehicle group, the same volume of vehicle solution was administered 30 minutes after noise exposure via IP injection. All mice were further administered with KCNQ channel activator or vehicle twice a day for 5 days every 12 hrs. Gap detection and PPI were retested 24 - 48 hours after the final injection. Only mice from the retigabine and saline vehicle group were used for electrophysiological recordings.

3.5.6 Electrophysiological recordings

Coronal slices of the left DCN (210 μm) were prepared from control and noise-exposed mice (P24 - P27). Animals were handled and sacrificed according to methods approved by the Institutional Animal Care and Use Committee of the University of Pittsburgh. Immediately after brain slices were prepared, they were incubated in normal artificial cerebral spinal fluid (ACSF) at 36°C for one hour, and then at room temperature. Fusiform cells were visualized using an Olympus upright microscope under oblique illumination condenser equipped with a XC-ST30 CCD camera and analog monitor. Cells were identified based on their morphological and electrophysiological characteristics. The preparation of slices and the identification for fusiform cells have been described in detail previously (Tzounopoulos et al., 2004b). The incubation as well as external recording solution contained (in mM): 130 NaCl, 3 KCl, 1.2 KH_2PO4, 2.4

$CaCl_2.2H_2O$, 1.3 $MgSO_4$, 20 $NaHCO_3$, 3 NaHEPES, and 10 D-glucose, saturated with 95% O_2 / 5% CO_2. DNQX (20 μM, AMPA and Kainate receptor antagonist, Abcam), strychnine (0.5 μM, glycine receptor antagonist, Sigma-Aldrich), SR95531 (20 μM, GABAa receptor antagonist, Abcam) were used to block glutamatergic, glycinergic as well as GABAergic synaptic transmission, respectively. XE991 (10 μM, KCNQ channel blocker, Abcam) was applied for blocking KCNQ currents. Tetrodotoxin (TTX, selective inhibitor for sodium channel, 0.5 μM, Abcam) was used to block spiking activity. ZD7288 (10 μM, blocker for HCN channel, Abcam) was used to block HCN channel activity. Recordings were performed at 34 - 37 °C using an inline heating system (Warner Instruments, Hamden, CT) with perfusion speed maintained (4-6 ml min^{-1}).

Because fusiform cells from DCN regions that represent high, but not low, frequency sounds are involved in tinnitus-related biophysical changes (Li et al., 2013), we recorded from fusiform cells from high-frequency DCN regions (≥20 kHz, dorsal part). For whole-cell voltage and current clamp experiments, pipettes (3 - 5 MΩ) were filled with a K^+-based internal solution containing (in mM): 113 K-gluconate, 4.5 $MgCl_2$, 2.6 H_20, 14 Tris-Phosphocreatine, 9 HEPES, 0.1 EGTA, 4 Na_2ATP, 0.3 Tris-GTP, 10 Sucrose, pH 7.3, and 300 mOsmol. Liquid junction potential of -11 mV was corrected. Access resistance was monitored throughout the experiment from the size and shape of the capacitive transient in response to a 5 mV depolarization step. Recordings with access resistance larger than 15 MΩ were eliminated. Recordings were performed with Clampex 10.2 and Multiclamp 700B amplifier interfaced with Digidata 1440A data acquisition system (Axon Instruments). For whole-cell voltage clamp experiments, fast, slow capacitive currents as well as series resistance (Rs) were compensated (70%, bandwidth 15kHz). All recording protocols, except for the gap-free recording in current clamp, were applied

below 0.1 Hz to eliminate potential short-term plasticity effects. Spike parameters were analyzed from spontaneous firing spikes whole-cell, voltage-follower mode recordings (current clamp, at I = 0; synaptic transmission was pharmacologically blocked). To assess spike properties, 20 consecutive spontaneous spikes were aligned at the negative peak and averaged. Spike threshold is the membrane potential at which the depolarization slope exceeds 10 V/s. Spike amplitude is the voltage difference between the spike threshold and the peak amplitude of the spike. Depolarization and hyperpolarization slope indicate the maximum positive slope during the depolarization and minimum negative slope during hyperpolarization phase of the spike. Half height width is the width of the spike when voltage equals to (spike threshold + half of spike amplitude). Fast afterhyperpolarization (fAHP) is the voltage difference between spike threshold and negative peak of the spike. Resting membrane potential (RMP) was measured with whole-cell, voltage-follower mode recordings (current clamp, at I = 0) 5 minutes after TTX (0.5 μM) application. ZD7288 was applied after TTX for evaluating its effect on resting membrane potential. Input resistance (R_{in}) was measured in current clamp mode through current injection (-60 pA to 60 pA, 20 pA step size, 2 sec). Initial state input resistance is the slope of the current - voltage (I - V) relationship of the average membrane voltage response of the initial 100 ms after current injection. Steady state input resistance was calculated similarly to the initial state input resistance, but the last 250 ms of the voltage response were used. To quantify KCNQ2/3 currents, we measured the XE991-sensitive tail current amplitude in response to a voltage step to -50 mV from a holding potential of -30 mV, described in detail previously (Li et al., 2013). To measure HCN channel activity, we injected bias current to maintain the membrane potential at -75 mV. A hyperpolarizing current step (-550 pA, 2 sec) was then used to activate HCN channels. The biggest membrane potential change from -75 mV (V_{peak}), and the membrane potential

change at the end of hyperpolarizing current (V_{ss}) were used to calculate the sag ratio: Sag ratio = $(V_{peak}-V_{ss})/V_{peak}\times 100\%$. Sag ratio before and after ZD7288 (15 min application) was subtracted and generated the ZD7288-sensitive sag ratio.

3.5.7 Statistics

For data that were normally distributed (based on Liliefors test), we conducted Student's t-test or One-Way Analysis of Variance (ANOVA). Post-hoc analysis for one-way ANOVA was performed with Tukey's least significant test. For non-normally distributed data, we performed non-parametric Wilcoxon ran sum test or Kruskal-Wallis test. F-test was applied for comparing the variance of KCNQ currents amplitudes between 4 days sham-exposed mice and 4 days noise-exposed mice. Binomial test was used for comparing percentages of tinnitus mice in response to different experimental manipulations.

4.0 GENERAL DISCUSSION

4.1.1 Potential mechanisms underlying the heterogeneous development of noise-induced tinnitus

Four days after noise exposure, fusiform cells from all noise-exposed mice show reduced KCNQ2/3 channel activity. Recovery of KCNQ2/3 current that happens between 4 to 7 days after exposure in a fraction of mice prevents the generation of fusiform cell hyperactivity, and gives rise to non-tinnitus behavior. To further understand the mechanism underlying resilience to tinnitus, it is key to understand what leads to the recovery of KCNQ2/3 current, and what differentiates the mice in which KCNQ2/3 current recover from ones that do not.

KCNQ2/3 channels mediate the native neuronal M-type potassium currents (M currents), which are strongly inhibited by activation of muscarinic acetylcholine receptors (mAChRs) (Brown and Adams, 1980; Wang et al., 1998). One of the major neuromodulatory inputs that DCN neurons receive is the cholinergic input (Mellott et al., 2011). Previous experiments revealed that cholinergic input influences the spontaneous firing of fusiform cells and is mediated predominantly by muscarinic receptors (Chen et al., 1994, 1998). Therefore, it is possible that variability of cholinergic innervation in DCN contributes to the differential recovery of KCNQ2/3 channel activity 4 to 7 days after noise exposure. The DCN receives cholinergic projections from medial olivo-cochlear neurons and midbrain pontomesencephalic

tegmentum (PMT) (Mellott et al., 2011; Schofield et al., 2011), which target granule cells (Godfrey et al., 1990; Brown, 1993; Manzoor et al., 2013), cartwheels cells (He et al., 2014b) and fusiform cells (Chen et al., 1998; Zhao and Tzounopoulos, 2011). Therefore, influence of cholinergic modulation on the intrinsic plasticity of fusiform cells may happen at cholinergic-fusiform cell terminals (Chang et al., 2002) through muscarinic acetylcholine receptors (Jin and Godfrey, 2006). Alternatively, it may exert indirectly through cholinergic modulation on granule cells and/or cartwheel cells (He et al., 2014b).

Previous research has shown the existence of homeostasis -- a biological 'setpoint' of activity that neurons and networks return to after perturbations (LeMasson et al., 1993; Liu et al., 1998; Turrigiano, 2007). Therefore, recovery of KCNQ2/3 channel after initial reduction may result from compensatory changes of sub-cellular signaling molecules that maintain the previously established homeostatic 'setpoint' (Delmas and Brown, 2005; Brown and Passmore, 2009). The persistence of reduced KCNQ2/3 channel activity that leads to tinnitus may represent the establishment of a new homeostatic point. It has been shown that ability of a neuron to retain its original homeostatic setpoint after perturbation is influenced by the biophysical profile of the neuron, the synaptic inputs that it receives, the current network connectivity, and the type and strength of the perturbation (O'Leary et al., 2014). Accordingly, a detailed investigation of ion channel expression profiles, transcriptional/translational molecules that modulate expression of ion channels, synaptic and neural network activity, as well as the impact of noise-exposure in these parameters is needed for understanding the differentiating factors leading to KCNQ2/3 recovery in only a portion of the mice.

Induction and development of tinnitus could also be influenced by the psychological and emotional state of the subjects, especially stress level (Mazurek et al., 2012). Stress excites

neuroendocrine pathways, among which the hypothalamus-pituitary-adrenal axis (HPA axis) influences both the function of auditory system and neural plasticity. Mineralcorticoid and glucocorticoid receptors have been identified in rat cochlea (Zachos et al., 1995; Yao and Rarey, 1996). Hyperactivity of mineralcorticoid receptors has been shown influencing the potassium-sodium balance of the inner ear and affects the development of tinnitus in Ménière's disease (Mazurek et al., 2012). Given that otologists and audiologists frequently observe tinnitus patients complain of psycho-social distress before or during the onset of tinnitus, it is possible that stress-related factors and variability of HPA axis also contribute to heterogeneous development of noise-induced tinnitus.

4.1.2 A latent period exists before the development of noise-induced tinnitus

Previous *in vivo* longitudinal studies revealed that the onset of noise-induced DCN hyperactivity is not immediate. Instead, it develops 2 to 5 days after noise exposure (Kaltenbach et al., 2000). By showing that 4 days post noise-exposed mice display no fusiform cell hyperactivity (Figure 10), our result confirmed previous findings. Importantly, our data also revealed the lack of tinnitus behavior in 4 days noise-exposed mice, indicating a delayed onset of tinnitus after noise exposure. Similarly, delayed onsets have also been observed in kainite model of seizures as well as in animal model of neuropathic pain, implying that a latent period is needed for the initial damage to trigger pathogenic plasticity at physiological and behavioral level (Shah et al., 2004; Xie et al., 2005). Increased firing rate in the primary auditory cortex (A1) has been detected several hours post noise exposure (Norena and Eggermont, 2003). The fact that fusiform cell hyperactivity happens after the hyperactivity of cortical neurons indicates that cortical modulation from top-down projection neurons, e.g. layer 5B neurons, may

contribute to the pathogenic plasticity in the brainstem (Eggermont and Roberts, 2004; Eggermont, 2005).

4.1.3 Potential modulators contributing to the noise-induced plasticity of KCNQ channel

Reduction of KCNQ2/3 currents 7 days after noise exposure leads to hyperactivity of DCN fusiform cell and the development of tinnitus (Figure 2b). To understand the mechanism behind this, it is important to look into the determinants of KCNQ2/3 channel conductance, as well as how it has changed in other hyperactivity-related neuronal disorders. Members of the KCNQ channel family are composed of six trans-membrane segments, with a voltage sensing domain (S1 - S4) and a pore domain (S5 - S6) (Haitin and Attali, 2008). Uniquely, subunits of KCNQ channels contain a large carboxy terminal tail (C terminus), which is important for binding modulatory molecules and influencing the channel gating, trafficking and expression (Maljevic et al., 2003; Shamgar et al., 2006; Haitin and Attali, 2008). Benign familial neonatal convulsion (BFNC) in humans has been associated with mutations in the pore and voltage sensing regions of the KCNQ2 and KCNQ3 channel as well as the C terminus of KCNQ2 that leads to a reduction in K^+ current (Schwake et al., 2000; Schwake et al., 2003; Singh et al., 2003; Richards et al., 2004; Schwake et al., 2006). Therefore, a direct change at the voltage sensing/gating domain and a modulatory effect through the C terminus are possible paths that lead to the reduction of KCNQ2/3 channel activity in tinnitus.

In KCNQ channels, tetrametic assembly of KCNQ subunits gives rise to four voltage-sensing domains (VSD) and one central pore-gate domain (PGD) (Zaydman and Cui, 2014). Through VSD-PGD coupling, VSD activation promotes PGD opening and yields a voltage-dependent conductance (Seoh et al., 1996). Previous studies have shown that all five members of

KCNQ channel family require membrane expression of phosphatidylinositol 4,5-bisphosphate (PIP_2) to conduct KCNQ currents (Gamper and Shapiro, 2003; Delmas and Brown, 2005). Reduction of PIP_2 expression in the membrane effectively reduced the KCNQ currents (Zaydman and Cui, 2014). Availability of PIP_2 on the membrane influence neither the number of KCNQ channel expressed (Zaydman et al., 2012), nor the single channel conductance (Li et al., 2005). Therefore, it is plausible that reduced membrane PIP_2 level inhibit KCNQ channel activity in tinnitus animal through interfering with the voltage dependent gating (Zaydman and Cui, 2014).

Calmodulin (CaM) is a ubiquitous intracellular Ca^{2+} binding protein (Hoeflich and Ikura, 2002). Changes in intracellular Ca^{2+} levels, which is frequently a result of changes in neuronal activity, influences the CaM biniding on voltage-gated ion channels (Hoeflich and Ikura, 2002). Mutations in the C terminus of KCNQ2 that yield weaker CaM binding cause reduction in KCNQ currents (Wen and Levitan, 2002; Richards et al., 2004), suggesting that functional expression of KCNQ2/3 channel requires constitutive interaction with CaM. Rise in the intracellular Ca^{2+} level, by forming CaM/Ca^{2+}, also suppresses KCNQ2/3 channel activity in heterologous system and in sympathetic neurons (Gamper et al., 2005; Zaika et al., 2007). Therefore, it is possible that change in Ca^{2+} signaling and/or CaM binding may lead to the changes in the KCNQ2/3 channels in fusiform cells. Besides being modulated by CaM, KCNQ channel also display phosphorylation-dependent regulation. Increase of protein kinase C (PKC) in Xenopus oocytes facilitates KCNQ channel activity by leftward shifting of the KCNQ channel in a subunit specific manner (Nakajo and Kubo, 2005). Src tyrosine kinase also diminished the probability of the opening of KCNQ2/3 channels in heterologous cells, and decreased KCNQ2/3 currents amplitude in sympathetic neurons (Gamper et al., 2003). Therefore, plasticity of the

KCNQ channel in noise-induced tinnitus may be a synergistic effect of multiple signaling molecules.

4.1.4 Potential modulators contributing to the noise-induced plasticity of HCN channel

Seven days after noise exposure, mice without behavioral evidence of tinnitus show reduced HCN channel activity in DCN fusiform cells (Figure 7B). The reduction in HCN channel activity happens after 4 days post noise exposure and could be triggered by the increase in KCNQ channel activity (Figure 9). Therefore, signaling molecules that potentially influence KCNQ channel activity are important candidates leading to plasticity of HCN channel in DCN fusiform cell.

Various intracellular molecules regulate HCN channel gating, kinetics and membrane expression, including small molecules (cAMP, PIP_2, protons), protein kinases (SrC, p38-MAPK, PKC, cGKII, CaMKII) and associated proteins (Wahl-Schott and Biel, 2009; Lewis et al., 2010). Cyclic adenosine monophosphate (cAMP) positively shifts the voltage dependent property of the HCN channel and facilitates channel activation in a subunit specific manner (Chen et al., 2001). Similar to KCNQ channels, HCN channels are also subjective to modulation of membrane PIP_2. PIP_2 facilitates activation of HCN channels by shifting the voltage dependence of HCN channels in a positive direction (Pian et al., 2006; Zolles et al., 2006). Previous study revealed that the PIP_2-mediated up-regulation of HCN3 channel activity gave rise to burst firing and spontaneous oscillation in neurons from the thalamic intergenuculate leaflet (IGL). Depletion of PIP_2 also reduced the excitability of IGL neurons (Ying et al., 2011). Therefore, PIP_2 mediated modulation of HCN channel activity plays a critical role controlling neuronal excitability (Biel et al., 2009). Besides small molecules, protein kinases also play a key role modulating HCN channel activity

(He et al., 2014a). Different from the facilitating effect of PKC on KCNQ channels, activation of PKC induces a down-regulation of HCN channel activity in dopaminergic neurons of the ventral tegmental area, and in non-neuronal as well as neuronal cells transfected with HCN1 channel (Liu et al., 2003; Inyushin et al., 2010; Reetz and Strauss, 2013). HCN channels have also been shown to be subjective to modulation of Ca^{2+} through the CaM-dependent protein kinase II (II). Ca^{2+}/CaMKII plays a key role in the rapid regulation of the HCN channel current through altering the channel trafficking and expression (Shin and Chetkovich, 2007; Noam et al., 2010). Increase of postsynaptic HCN channel activity following enhancement of presynaptic activity has also been shown to require Ca^{2+} influx and activation of CaMKII (van Welie et al., 2004; Fan et al., 2005). Moreover, in an *in vitro* seizure model, increase in glutamate leads to reduce of HCN1 expression that requires Ca^{2+} influx via Ca^{2+} permeable AMPA-receptors and activation of Ca^{2+}/CaMKII (Bender and Baram, 2008; Richichi et al., 2008). Computational simulation derived a potential calcium-dependent plasticity rule for HCN channels where firing rate homeostasis could be maintained in the face of synaptic plasticity. As the model revealed, reduced increase of cytosolic calcium due to reduced firing activity, which in a Bienenstock-Cooper-Munro (BCM)-like rule underlies synaptic depression, leads to reduction in HCN channel activity. Increased levels of cytosolic calcium, which underlies synaptic potentiation, leads to increased HCN channel activity (Honnuraiah and Narayanan, 2013). It is therefore possible that *in vivo* pharmacological activation of KCNQ2/3 channels (Figure 9C) reduces the firing rate of fusiform cells (Figure 9D), which causes the reduced cytosolic calcium via voltage-gated Ca^{2+} channels (van Welie et al., 2004) and gives rise to the decreased HCN channel activity in non-tinnitus mice through a Ca^{2+}/CaMKII dependent pathway.

4.1.5 Reduction in HCN channel activity in DCN fusiform cell serves as a protection mechanism against noise-induced tinnitus

Previous study has revealed the contribution of HCN channels to the intrinsic excitability of DCN fusiform cells (Pal et al., 2003; Leao et al., 2012). Our study for the first time uncovered that HCN channel in DCN fusiform cells may contribute to the resilience to tinnitus induction. Immunohistochemical studies in the DCN have shown consistent and strong HCN2 subunit expression in fusiform cells (Pal et al., 2003; Koch et al., 2004; Notomi and Shigemoto, 2004), suggesting that HCN2 isoforms may mediate the noise-induced plasticity in fusiform cells.

Plasticity of HCN channels has shown both a pathogenic effect leading to development of diseases states and a neural protective effect that compensates the insult-induced disturbances. Down-regulation of HCN channels has been linked to the generation of epilepsy in the entorhinal cortex (EC) (Shah et al., 2004). As spontaneous activity in EC neurons depends on synaptic inputs, decreased HCN channel activity in EC neurons plays a pathogenic role in inducing epilepsy due to its effect in increasing dendritic excitability and in increasing spontaneous activity of EC neurons (Shah et al., 2004). Our results, however, revealed that reduction in HCN channel activity in DCN fusiform cells contributes to the resilience to tinnitus. Decreased HCN channel activity hyperpolarizes the resting membrane potential of fusiform cells and prevents them from generating increased spontaneous firing activity. Therefore, plasticity of HCN channels could play either a pathogenic or a neural protective role underlying the development of neuronal disorders depending on how it influences neuronal as well as network activity.

4.1.6 Plasticity of KCNQ and HCN channels underlying the development of neuropathic pain

Our study revealed that 7 days following noise exposure, DCN fusiform cell display divergent plasticity of ion channels that leads to vulnerability and resilience to tinnitus. Fusiform cells in tinnitus mice show increased spontaneous firing rate that is independent of synaptic transmission (Figure 1). This hyperactivity is mediated by a reduction of KCNQ2/3 channel activity and is due to a depolarizing shift of the voltage dependence of the channel activation (Figure 3). Fusiform cells in non-tinnitus mice experience an initial decrease of KCNQ channel activity 4 days after noise exposure (Figure 7). This reduction is followed by a recovery of KCNQ currents 7 days after noise exposure as well as a reduced HCN channel activity (Figure 8), which gives rise to an unchanged spontaneous firing rate of fusiform cells.

Hyperactivity of DCN fusiform cells is an important neural correlate for the development of tinnitus (Kaltenbach and McCaslin, 1996; Kaltenbach and Afman, 2000; Brozoski et al., 2002a; Kaltenbach et al., 2002). Similarly, hyperactivity of nociceptive sensory neurons in the dorsal root ganglion (DRG) following damage of the peripheral sensory nerve is key to the induction of neuropathic pain (von Hehn et al., 2012). Plasticity of both KCNQ and HCN channel has also been revealed in DRG neurons contributing to the induction of chronic inflammatory and neuropathic pain. However, a direct link is lacking as for the relationship between a change in KCNQ and a change in HCN channel activity.

KCNQ channels are present in the DRG neurons and play an important role regulating the excitability of nociceptors (Passmore et al., 2003). Reduced KCNQ channel activity in DRG neurons contributes to the generation of neuronal hyperactivity and induction of inflammatory neuropathic pain (Linley et al., 2008; Liu et al., 2010). Repression of the KCNQ2 channel in

DRG neurons has also been identified at the transcription level following partial sciatic nerve ligation, indicating a long lasting change of the KCNQ channel underlying the induction of neuropathic pain (Rose et al., 2011). In a proteases-induced inflammatory pain model, depletion of membrane PIP_2 and rise in cytosolic Ca^{2+} concentration (through CaM) mediated the reduction of KCNQ channel activity (Linley et al., 2008). Rise in cytosolic Ca^{2+} also underlies the suppression of KCNQ channel activity during bradykinin induced spontaneous pain (Liu et al., 2010). Therefore, Ca^{2+} and PIP_2 mediated reduction of KCNQ channel activity could be shared mechanisms for the induction of tinnitus and neuropathic pain. KCNQ channel activators, including retigabine, have also shown a stabilizing effect on nociceptive pathway following nerve lesion, and reduce signs of neuropathic pain (Blackburn-Munro and Jensen, 2003; Dost et al., 2004). Importantly from our study, we revealed for the first time that a KCNQ channel opener could also prevent the induction of noise-induced tinnitus in animal models, and potentially be used as a preventive and therapeutic drug for treating tinnitus in humans.

HCN channels are abundantly expressed in DRG neurons and play a key role regulating neuronal excitability (Dunlop et al., 2009). HCN1 isoforms are the majority HCN channels subunits expressed in DRG neurons, mainly in large and medium size neurons. However, knockout study revealed that HCN1 subunits in DRG neurons contribute little to the induction of inflammatory and neuropathic pain (Jiang et al., 2008; Momin et al., 2008). HCN2 isoforms are expressed in large and medium size DRG neurons, as well as in small size DRG neurons co-localized with peptidergic nociceptive neuron marker (Jiang et al., 2008). Previous study has shown that HCN channel activity is significantly increased 1 - 3 weeks after spinal nerve ligation (SNL) (Chaplan et al., 2003). The same change were observed within 1 week after DRG chronic compression (Yao et al., 2003) and within 3 days after chronic constriction injury (Kitagawa et

al., 2006), indicating a contribution of increase of HCN channel activity underlying the generation of spontaneous activity of DRG neurons (Jiang et al., 2008). However, reduction of HCN2 mRNA expression has been identified in DRG neurons 1 - 3 weeks after SNL (Dunlop et al., 2009). Sciatic nerve section also revealed reduction of HCN channel activity 2 - 7 weeks later (Abdulla and Smith, 2001b, a). According to our results, decrease of HCN channel in fusiform cell didn't happen until 4 - 7 days after noise exposure. We also observed an initial increase of HCN channel activity 2 hours - 2 days after noise exposure (data not shown). Therefore, it is possible that the increase and decrease of HCN channel activity in DRG neurons play different roles underlying the development of neuropathic pain. Given that reduction of HCN channel activity either through pharmacological blocking (Chaplan et al., 2003; Lee et al., 2005; Sun et al., 2005; Jiang et al., 2008) or conditional knockout (Emery et al., 2011) significantly reduced the spontaneously generated firing in DRG neurons and eliminated symptoms of neuropathic pain, it is possible that the reduction in HCN channel activity in DRG neurons following nerve injury serves as a protective role against the development of neuropathic pain.

4.1.7 Resting membrane potential of fusiform cells controls the outcome of pathogenic plasticity of KCNQ2/3 channels

Fusiform cell hyperactivity and development of tinnitus is associated with reduced KCNQ2/3 channel activity 7 days after noise exposure. Differently, normal firing of fusiform cells and non-tinnitus behavior is associated with a reduced resting membrane potential through either reduced HCN channel activity 7 days after noise exposure, or other unidentified mechanisms 4 days after noise exposure. Therefore, pathogenic effect of reduction in KCNQ2/3

channel activity could be gated by the resting membrane potential of fusiform cells. This is an interesting finding and revealed the dominant regulation of resting membrane potential on KCNQ2/3 channel activity with little contribution vice versa (Li et al., 2013), unless the voltage dependence of KCNQ2/3 is pharmacologically shifted towards hyperpolarized potential (Brown and Passmore, 2009). Previous treatments of KCNQ2/3 channel-mediated channelopathy focused on KCNQ2/3 activators, which activate KCNQ2/3 channel majorly through rightward shifting the voltage dependence of KCNQ2/3 channel activity. Here, our results indicate that reducing resting membrane potential of fusiform cells will be another potential method for treating KCNQ2/3 channelopathy.

4.1.8 Retigabine may have long lasting influence on KCNQ channel activity

To prevent the reduction of KCNQ channel activity after noise exposure, we administrated retigabine through IP Injection twice a day for 5 days. We performed electrophysiology recording on retigabine-injected mice 12 - 24 hours after the final injection, ensuring that retigabine is out of the physiological system (Luszczki et al., 2009). However, our result revealed that noise-induced mice with retigabine injection has significantly increased KCNQ currents comparing with noise-induced mice with saline injection, and is not different from the KCNQ currents amplitude in sham-exposed control mice (Figure 9C). Previous study revealed that retigabine opens Kv2 - Kv5 channels through binding to the hydrophobic pocket near the channel gate and stabilizing the open form of the channels (Gunthorpe et al., 2012). Our finding indicates that binding of retigabine on KCNQ channel may exerts long lasting effect on KCNQ channel activity.

4.1.9 Fusiform cell hyperactivity is an important neural correlate for noise-induced tinnitus

Reduced KCNQ2/3 channel activity in fusiform cells is associated with no fusiform cell hyperactivity and no behavioral evidence of tinnitus 4 days after noise-exposure, indicating an indispensible role of fusiform cell hyperactivity underlying the induction of tinnitus (Kaltenbach and McCaslin, 1996; Kaltenbach and Afman, 2000; Brozoski et al., 2002a). Our previous finding revealed the essential role of KCNQ2/3 channel on induction of tinnitus and implicated KCNQ2/3 activators as potential therapeutic drugs for preventing the induction of tinnitus (Li et al., 2013). Here, our data expanded upon the previous finding and showed that eliminating the hyperactivity of fusiform cell during the induction phase of tinnitus could potentially prevent the development of tinnitus. Therapeutic methods aiming at occluding tinnitus-related neuronal hyperactivity have been implemented through reducing central excitation and/or increasing inhibition and showed limited effect (Simpson and Davies, 1999; Simpson et al., 1999; Bauer and Brozoski, 2001; Guitton et al., 2004; Brozoski et al., 2007). Given that spontaneous firing of fusiform cells is not dependent on synaptic input (Leao et al., 2012), eliminating fusiform cell hyperactivity through manipulating intrinsic ionic conductances may be more efficient. Our data revealed that resilience of noise-exposed fusiform cell hyperactivity and behavioral evidence of tinnitus can be achieved with control level KCNQ2/3 current amplitude together with decreased HCN channel activity. Therefore, besides activation of KCNQ2/3 channels as previously proposed, blocking of HCN channels during the induction phase of tinnitus may be useful a method for preventing the development of tinnitus.

4.1.10 Homeostatic plasticity and tinnitus

Fusiform cells from control, 4 days noise-exposed and 7 days non-tinnitus mice show similar spontaneous firing rates but with different combinations of ionic conductances (Figure 1, Figure 10). These findings complement and extend previous experimental and theoretical work showing that similar neuronal output can result from multiple combinations of intrinsic and synaptic properties (Edelman and Gally, 2001; Prinz et al., 2004; Marder and Goaillard, 2006; Goaillard and Dufour, 2014; Ratte et al., 2014).

In accordance with this view, activity-dependent changes in conductances that affect neuronal excitability frequently trigger homeostatic, compensatory changes in different conductances, which result in constant neuronal output (LeMasson et al., 1993; Desai et al., 1999; Turrigiano, 2008; O'Leary et al., 2010; O'Leary et al., 2013; O'Leary et al., 2014). Our results are consistent with such homeostatic mechanisms and highlight that recovery of KCNQ channel activity is associated with a reduction in HCN channel activity and the maintenance of normal spontaneous firing rates in non-tinnitus mice (Figure 9). Because homeostatic and coordinated regulation of potassium and HCN currents occurs in different species and neuronal circuits, such as dopaminergic neurons in rat susbstantia nigra pars compact and neurons of the lobster stomatogastric ganglion (MacLean et al., 2003; Amendola et al., 2012), we propose that coordinated plasticity of potassium and HCN channels may represent a general biophysical strategy for achieving neuronal homeostasis.

The fact that multiple molecular pathologies underlie hyperexcitability-related disorders, such as neuropathic pain and epilepsy, has led to the suggestion that drugs that simultaneously target more than one type of ion channels could treat these disorders more effectively (Klassen et al., 2011; Goaillard and Dufour, 2014; Ratte et al., 2014). Similarly, because plasticity of

multiple conductances is involved in tinnitus, we propose that a combination of drugs that enhance KCNQ2/3 and reduce HCN channel activity represents a potent therapeutic approach that will enhance resilience and reduce vulnerability to tinnitus.

APPENDIX A: VALUES FOR MAIN FIGURES OF CHAPTER 1

Figure 1**b,** control, before sham-exposure: 0.71 ± 0.02, after sham-exposure: 0.69 ± 0.02, n = 16, p = 0.55; tinnitus, before noise-exposure: 0.65 ± 0.02, after noise-exposure: 0.88 ± 0.02, n = 18, p < 0.001; non-tinnitus, before noise-exposure: 0.69 ± 0.03, after noise-exposure: 0.63 ± 0.03, n = 17, p = 0.20.

Figure 1**c,** control, before: 0.69 ± 0.02, after: 0.66 ± 0.04, n = 16, p = 0.47; tinnitus, before: 0.75 ± 0.03, after: 0.79 ± 0.03, n = 18, p = 0.17; non-tinnitus, before: 0.73 ± 0.04, after: 0.66 ± 0.04, n=17, p = 0.14.

Figure 1**e,** control, before: 0.51 ± 0.05, after: 0.53 ± 0.06, n = 18, p = 0.72; tinnitus, before: 0.60 ± 0.06, after: 0.56 ± 0.04, n = 16, p = 0.61; non-tinnitus, before: 0.46 ± 0.05, after: 0.52 ± 0.04, n = 17, p = 0.32.

Figure 1**f,** control, before: 0.47 ± 0.04, after: 0.50 ± 0.04, n = 18, p = 0.62; tinnitus, before: 0.52 ± 0.03, after: 0.48 ± 0.03, n = 18, p = 0.26; non-tinnitus, before: 0.54 ± 0.04, after: 0.52 ± 0.03, n = 17, p = 0.83.

Figure 3**a,** RMP, control: -62.7 ± 0.7 mV, n = 6, tinnitus: -62.9 ± 0.7 mV, n = 11, p = 0.87; control: -61.8 ±1.4 mV, n = 6, after XE991: -62.0 ± 1.4 mV, n = 6, p = 0.74.

Figure 3**b,** spike threshold, control: -48.1 ± 1.0 mV, n = 11, tinnitus: -46.8 ± 0.5 mV, n = 11, p = 0.26; control: -48.4 ± 1.8 mV, n = 6; after XE991: -48.5 ± 1.7 mV, n = 6, p = 0.85.

Figure 3**h,** 0.1 mM, 11.5 ± 3.5%, n = 5; 1 mM, 39.9 ± 3.7%, n = 6; 10 mM, 75.4 ± 6.8%, n = 6; 30 mM, 82.3 ± 4.3%, n=4.

Figure 4**b,** PPI startle ratio, control: 0.47 ± 0.06, n = 16, noise-exposed: 0.53 ± 0.04, n = 33, noise-exposed + retigabine: 0.54 ± 0.06, n = 16, noise-exposed + saline: 0.65 ± 0.04, n = 16, p = 0.55.

Figure 4**c,** ABR threshold, control: 46.7 ± 2.7 dB, n = 7, noise-exposed: 51.6 ± 2.0 dB, n = 18, noise-exposed + retigabine: 50.2 ± 2.7 dB, n = 7, noise-exposed + saline: 46.7 ± 2.2 dB, n = 7, p = 0.35.

APPENDIX B: VALUES FOR MAIN FIGURES OF CHAPTER 2

Figure 5**A**, control, high frequency: before exposure, 0.70 ± 0.01, after exposure: 0.68 ± 0.02, n = 21, p = 0.6; low frequency, before exposure, 0.67 ± 0.02, after exposure, 0.71 ± 0.02, n = 21, p = 0.2; tinnitus, high frequency: before exposure, 0.64 ± 0.02, after exposure: 0.82 ± 0.03, n = 11, p < 0.001; low frequency, before exposure, 0.66 ± 0.03, after exposure, 0.74 ± 0.03, p = 0.06, n = 11; non-tinnitus, high frequency: before exposure, 0.69 ± 0.03, after exposure: 0.71 ± 0.04, n = 10, p =0.6; low frequency, before exposure, 0.72 ± 0.02, after exposure, 0.64 ± 0.03, p = 0.07, n = 10

Figure 5**B**, control, high frequency, 0.56 ± 0.03, after exposure, 0.60 ± 0.02, n = 22, p = 0.25; low frequency, before exposure: 0.59 ± 0.02; after exposure: 0.60 ± 0.01, n = 22, p = 0.56; tinnitus, high frequency, before exposure, 0.52 ± 0.03, after exposure, 0.57 ± 0.02, n = 11, p = 0.18; low frequency, before exposure, 0.52 ± 0.04, after exposure, 0.59 ± 0.03, n = 11, p = 0.17; non-tinnitus, high frequency, before exposure, 0.54 ± 0.03, after exposure, 0.60 ± 0.03, n = 10, p = 0.36; low frequency, before exposure, 0.56 ± 0.04, after exposure, 0.54 ± 0.02, n = 10, p = 0.56

BIBLIOGRAPHY

Abdulla FA, Smith PA (2001a) Axotomy- and autotomy-induced changes in the excitability of rat dorsal root ganglion neurons. Journal of neurophysiology 85:630-643.

Abdulla FA, Smith PA (2001b) Axotomy- and autotomy-induced changes in Ca2+ and K+ channel currents of rat dorsal root ganglion neurons. Journal of neurophysiology 85:644-658.

Amendola J, Woodhouse A, Martin-Eauclaire MF, Goaillard JM (2012) Ca(2)(+)/cAMP-sensitive covariation of I(A) and I(H) voltage dependences tunes rebound firing in dopaminergic neurons. The Journal of neuroscience : the official journal of the Society for Neuroscience 32:2166-2181.

Anari M, Axelsson A, Eliasson A, Magnusson L (1999) Hypersensitivity to sound--questionnaire data, audiometry and classification. Scandinavian audiology 28:219-230.

Axelsson A, Ringdahl A (1989) Tinnitus--a study of its prevalence and characteristics. Br J Audiol 23:53-62.

Baron R (2000) Peripheral neuropathic pain: from mechanisms to symptoms. The Clinical journal of pain 16:S12-20.

Basbaum AI, Bautista DM, Scherrer G, Julius D (2009) Cellular and molecular mechanisms of pain. Cell 139:267-284.

Bauer CA, Brozoski TJ (2001) Assessing tinnitus and prospective tinnitus therapeutics using a psychophysical animal model. Journal of the Association for Research in Otolaryngology : JARO 2:54-64.

Bell JT et al. (2014a) Differential methylation of the TRPA1 promoter in pain sensitivity. Nature communications 5:2978.

Bell JT et al. (2014b) Differential methylation of the TRPA1 promoter in pain sensitivity. Nature communications 5:2978.

Bender RA, Baram TZ (2008) Hyperpolarization activated cyclic-nucleotide gated (HCN) channels in developing neuronal networks. Progress in neurobiology 86:129-140.

Berliner KI, Shelton C, Hitselberger WE, Luxford WM (1992) Acoustic tumors: effect of surgical removal on tinnitus. The American journal of otology 13:13-17.

Biel M, Wahl-Schott C, Michalakis S, Zong X (2009) Hyperpolarization-activated cation channels: from genes to function. Physiological reviews 89:847-885.

Biervert C, Schroeder BC, Kubisch C, Berkovic SF, Propping P, Jentsch TJ, Steinlein OK (1998) A potassium channel mutation in neonatal human epilepsy. Science 279:403-406.

Blackburn-Munro G, Jensen BS (2003) The anticonvulsant retigabine attenuates nociceptive behaviours in rat models of persistent and neuropathic pain. European journal of pharmacology 460:109-116.

Blumenthal TD, Noto JV, Fox MA, Franklin JC (2006) Background noise decreases both prepulse elicitation and inhibition of acoustic startle blink responding. Biological psychology 72:173-179.

Brager DH, Johnston D (2007) Plasticity of intrinsic excitability during long-term depression is mediated through mGluR-dependent changes in I(h) in hippocampal CA1 pyramidal neurons. The Journal of neuroscience : the official journal of the Society for Neuroscience 27:13926-13937.

Brown DA, Adams PR (1980) Muscarinic suppression of a novel voltage-sensitive K+ current in a vertebrate neurone. Nature 283:673-676.

Brown DA, Passmore GM (2009) Neural KCNQ (Kv7) channels. British journal of pharmacology 156:1185-1195.

Brown JT, Randall AD (2009) Activity-dependent depression of the spike after-depolarization generates long-lasting intrinsic plasticity in hippocampal CA3 pyramidal neurons. The Journal of physiology 587:1265-1281.

Brown MC (1993) Fiber pathways and branching patterns of biocytin-labeled olivocochlear neurons in the mouse brainstem. The Journal of comparative neurology 337:600-613.

Brozoski T, Odintsov B, Bauer C (2012a) Gamma-aminobutyric acid and glutamic acid levels in the auditory pathway of rats with chronic tinnitus: a direct determination using high resolution point-resolved proton magnetic resonance spectroscopy (H-MRS). Frontiers in systems neuroscience 6:9.

Brozoski TJ, Bauer CA (2005) The effect of dorsal cochlear nucleus ablation on tinnitus in rats. Hear Res 206:227-236.

Brozoski TJ, Bauer CA, Caspary DM (2002a) Elevated fusiform cell activity in the dorsal cochlear nucleus of chinchillas with psychophysical evidence of tinnitus. The Journal of neuroscience : the official journal of the Society for Neuroscience 22:2383-2390.

Brozoski TJ, Bauer CA, Caspary DM (2002b) Elevated fusiform cell activity in the dorsal cochlear nucleus of chinchillas with psychophysical evidence of tinnitus. Journal of Neuroscience 22:2383-2390.

Brozoski TJ, Ciobanu L, Bauer CA (2007) Central neural activity in rats with tinnitus evaluated with manganese-enhanced magnetic resonance imaging (MEMRI). Hear Res 228:168-179.

Brozoski TJ, Wisner KW, Sybert LT, Bauer CA (2012b) Bilateral dorsal cochlear nucleus lesions prevent acoustic-trauma induced tinnitus in an animal model. Journal of the Association for Research in Otolaryngology : JARO 13:55-66.

Cavaliere S, Hodge JJ (2011) Drosophila KCNQ channel displays evolutionarily conserved electrophysiology and pharmacology with mammalian KCNQ channels. PLoS One 6:e23898.

Chan CS, Glajch KE, Gertler TS, Guzman JN, Mercer JN, Lewis AS, Goldberg AB, Tkatch T, Shigemoto R, Fleming SM, Chetkovich DM, Osten P, Kita H, Surmeier DJ (2011) HCN channelopathy in external globus pallidus neurons in models of Parkinson's disease. Nature neuroscience 14:85-92.

Chang H, Chen K, Kaltenbach JA, Zhang J, Godfrey DA (2002) Effects of acoustic trauma on dorsal cochlear nucleus neuron activity in slices. Hear Res 164:59-68.

Chaplan SR, Guo HQ, Lee DH, Luo L, Liu C, Kuei C, Velumian AA, Butler MP, Brown SM, Dubin AE (2003) Neuronal hyperpolarization-activated pacemaker channels drive neuropathic pain. The Journal of neuroscience : the official journal of the Society for Neuroscience 23:1169-1178.

Chen K, Waller HJ, Godfrey DA (1994) Cholinergic modulation of spontaneous activity in rat dorsal cochlear nucleus. Hear Res 77:168-176.

Chen K, Waller HJ, Godfrey DA (1998) Effects of endogenous acetylcholine on spontaneous activity in rat dorsal cochlear nucleus slices. Brain Res 783:219-226.
Chen S, Wang J, Siegelbaum SA (2001) Properties of hyperpolarization-activated pacemaker current defined by coassembly of HCN1 and HCN2 subunits and basal modulation by cyclic nucleotide. The Journal of general physiology 117:491-504.
Cooper EC, Harrington E, Jan YN, Jan LY (2001) M channel KCNQ2 subunits are localized to key sites for control of neuronal network oscillations and synchronization in mouse brain. J Neurosci 21:9529-9540.
Costigan M, Scholz J, Woolf CJ (2009) Neuropathic pain: a maladaptive response of the nervous system to damage. Annual review of neuroscience 32:1-32.
De Ridder D, Elgoyhen AB, Romo R, Langguth B (2011) Phantom percepts: tinnitus and pain as persisting aversive memory networks. Proc Natl Acad Sci U S A 108:8075-8080.
Dedek K, Kunath B, Kananura C, Reuner U, Jentsch TJ, Steinlein OK (2001) Myokymia and neonatal epilepsy caused by a mutation in the voltage sensor of the KCNQ2 K+ channel. Proc Natl Acad Sci U S A 98:12272-12277.
Delmas P, Brown DA (2005) Pathways modulating neural KCNQ/M (Kv7) potassium channels. Nature reviews Neuroscience 6:850-862.
Denk F, McMahon SB, Tracey I (2014) Pain vulnerability: a neurobiological perspective. Nature neuroscience 17:192-200.
Desai NS, Rutherford LC, Turrigiano GG (1999) Plasticity in the intrinsic excitability of cortical pyramidal neurons. Nature neuroscience 2:515-520.
Dost R, Rostock A, Rundfeldt C (2004) The anti-hyperalgesic activity of retigabine is mediated by KCNQ potassium channel activation. Naunyn-Schmiedeberg's archives of pharmacology 369:382-390.
Dunlop J, Vasilyev D, Lu P, Cummons T, Bowlby MR (2009) Hyperpolarization-activated cyclic nucleotide-gated (HCN) channels and pain. Current pharmaceutical design 15:1767-1772.
Edelman GM, Gally JA (2001) Degeneracy and complexity in biological systems. Proc Natl Acad Sci U S A 98:13763-13768.
Eggermont JJ (2005) Tinnitus: neurobiological substrates. Drug discovery today 10:1283-1290.
Eggermont JJ, Roberts LE (2004) The neuroscience of tinnitus. Trends in neurosciences 27:676-682.
Emery EC, Young GT, Berrocoso EM, Chen L, McNaughton PA (2011) HCN2 ion channels play a central role in inflammatory and neuropathic pain. Science 333:1462-1466.
Engineer ND, Riley JR, Seale JD, Vrana WA, Shetake JA, Sudanagunta SP, Borland MS, Kilgard MP (2011a) Reversing pathological neural activity using targeted plasticity. Nature.
Engineer ND, Riley JR, Seale JD, Vrana WA, Shetake JA, Sudanagunta SP, Borland MS, Kilgard MP (2011b) Reversing pathological neural activity using targeted plasticity. Nature 470:101-104.
Fan Y, Fricker D, Brager DH, Chen X, Lu HC, Chitwood RA, Johnston D (2005) Activity-dependent decrease of excitability in rat hippocampal neurons through increases in I(h). Nature neuroscience 8:1542-1551.
Finlayson PG, Kaltenbach JA (2009) Alterations in the spontaneous discharge patterns of single units in the dorsal cochlear nucleus following intense sound exposure. Hear Res 256:104-117.

Fitch RH, Threlkeld SW, McClure MM, Peiffer AM (2008) Use of a modified prepulse inhibition paradigm to assess complex auditory discrimination in rodents. Brain research bulletin 76:1-7.
Fournier P, Hebert S (2013) Gap detection deficits in humans with tinnitus as assessed with the acoustic startle paradigm: does tinnitus fill in the gap? Hear Res 295:16-23.
Friedman AK, Walsh JJ, Juarez B, Ku SM, Chaudhury D, Wang J, Li X, Dietz DM, Pan N, Vialou VF, Neve RL, Yue Z, Han MH (2014) Enhancing depression mechanisms in midbrain dopamine neurons achieves homeostatic resilience. Science 344:313-319.
Gamper N, Shapiro MS (2003) Calmodulin mediates Ca2+-dependent modulation of M-type K+ channels. The Journal of general physiology 122:17-31.
Gamper N, Stockand JD, Shapiro MS (2003) Subunit-specific modulation of KCNQ potassium channels by Src tyrosine kinase. The Journal of neuroscience : the official journal of the Society for Neuroscience 23:84-95.
Gamper N, Li Y, Shapiro MS (2005) Structural requirements for differential sensitivity of KCNQ K+ channels to modulation by Ca2+/calmodulin. Molecular biology of the cell 16:3538-3551.
Goaillard JM, Dufour MA (2014) The pros and cons of degeneracy. eLife 3:e02615.
Godfrey DA, Beranek KL, Carlson L, Parli JA, Dunn JD, Ross CD (1990) Contribution of centrifugal innervation to choline acetyltransferase activity in the cat cochlear nucleus. Hear Res 49:259-279.
Goldman AM, Glasscock E, Yoo J, Chen TT, Klassen TL, Noebels JL (2009) Arrhythmia in heart and brain: KCNQ1 mutations link epilepsy and sudden unexplained death. Sci Transl Med 1:2ra6.
Guitton MJ, Wang J, Puel JL (2004) New pharmacological strategies to restore hearing and treat tinnitus. Acta oto-laryngologica 124:411-415.
Gunthorpe MJ, Large CH, Sankar R (2012) The mechanism of action of retigabine (ezogabine), a first-in-class K+ channel opener for the treatment of epilepsy. Epilepsia 53:412-424.
Haitin Y, Attali B (2008) The C-terminus of Kv7 channels: a multifunctional module. The Journal of physiology 586:1803-1810.
He C, Chen F, Li B, Hu Z (2014a) Neurophysiology of HCN channels: from cellular functions to multiple regulations. Progress in neurobiology 112:1-23.
He S, Wang YX, Petralia RS, Brenowitz SD (2014b) Cholinergic modulation of large-conductance calcium-activated potassium channels regulates synaptic strength and spine calcium in cartwheel cells of the dorsal cochlear nucleus. The Journal of neuroscience : the official journal of the Society for Neuroscience 34:5261-5272.
Heffner HE, Harrington IA (2002) Tinnitus in hamsters following exposure to intense sound. Hear Res 170:83-95.
Heller AJ (2003) Classification and epidemiology of tinnitus. Otolaryngologic clinics of North America 36:239-248.
Henderson D, Hamernik RP (1995) Biologic bases of noise-induced hearing loss. Occupational medicine 10:513-534.
Hoeflich KP, Ikura M (2002) Calmodulin in action: diversity in target recognition and activation mechanisms. Cell 108:739-742.
Honnuraiah S, Narayanan R (2013) A calcium-dependent plasticity rule for HCN channels maintains activity homeostasis and stable synaptic learning. PLoS One 8:e55590.

House JW, Brackmann DE (1981) Tinnitus: surgical treatment. Ciba Foundation symposium 85:204-216.
Hu H, Vervaeke K, Storm JF (2007) M-channels (Kv7/KCNQ channels) that regulate synaptic integration, excitability, and spike pattern of CA1 pyramidal cells are located in the perisomatic region. The Journal of neuroscience : the official journal of the Society for Neuroscience 27:1853-1867.
Huang H, Trussell LO (2011) KCNQ5 channels control resting properties and release probability of a synapse. Nat Neurosci 14:840-847.
Imig TJ, Bibikov NG, Poirier P, Samson FK (2000) Directionality derived from pinna-cue spectral notches in cat dorsal cochlear nucleus. Journal of neurophysiology 83:907-925.
Inyushin MU, Arencibia-Albite F, Vazquez-Torres R, Velez-Hernandez ME, Jimenez-Rivera CA (2010) Alpha-2 noradrenergic receptor activation inhibits the hyperpolarization-activated cation current (Ih) in neurons of the ventral tegmental area. Neuroscience 167:287-297.
Ison JR, Bowen GP, Kellogg C (1991) Potentiation of acoustic startle behavior in the rat (Rattus norvegicus) at the onset of darkness. Journal of comparative psychology 105:3-9.
Jastreboff PJ (1990) Phantom auditory perception (tinnitus): mechanisms of generation and perception. Neuroscience research 8:221-254.
Jastreboff PJ, Brennan JF, Sasaki CT (1988a) An animal model for tinnitus. The Laryngoscope 98:280-286.
Jastreboff PJ, Brennan JF, Coleman JK, Sasaki CT (1988b) Phantom auditory sensation in rats: an animal model for tinnitus. Behav Neurosci 102:811-822.
Jentsch TJ (2000) Neuronal KCNQ potassium channels: physiology and role in disease. Nat Rev Neurosci 1:21-30.
Jiang YQ, Sun Q, Tu HY, Wan Y (2008) Characteristics of HCN channels and their participation in neuropathic pain. Neurochemical research 33:1979-1989.
Jin YM, Godfrey DA (2006) Effects of cochlear ablation on muscarinic acetylcholine receptor binding in the rat cochlear nucleus. J Neurosci Res 83:157-166.
Jin YM, Godfrey DA, Wang J, Kaltenbach JA (2006) Effects of intense tone exposure on choline acetyltransferase activity in the hamster cochlear nucleus. Hear Res 216-217:168-175.
Kajander KC, Wakisaka S, Bennett GJ (1992) Spontaneous discharge originates in the dorsal root ganglion at the onset of a painful peripheral neuropathy in the rat. Neurosci Lett 138:225-228.
Kalappa BI, Brozoski TJ, Turner JG, Caspary DM (2014) Single unit hyperactivity and bursting in the auditory thalamus of awake rats directly correlates with behavioural evidence of tinnitus. The Journal of physiology 592:5065-5078.
Kaltenbach JA, McCaslin DL (1996) Increases in Spontaneous Activity in the Dorsal Cochlear Nucleus Following Exposure to High Intensity Sound: A Possible Neural Correlate of Tinnitus. 3:57-78.
Kaltenbach JA, Afman CE (2000) Hyperactivity in the dorsal cochlear nucleus after intense sound exposure and its resemblance to tone-evoked activity: a physiological model for tinnitus. Hear Res 140:165-172.
Kaltenbach JA, Zhang J (2007) Intense sound-induced plasticity in the dorsal cochlear nucleus of rats: evidence for cholinergic receptor upregulation. Hear Res 226:232-243.
Kaltenbach JA, Zhang J, Afman CE (2000) Plasticity of spontaneous neural activity in the dorsal cochlear nucleus after intense sound exposure. Hear Res 147:282-292.

Kaltenbach JA, Zhang J, Finlayson P (2005) Tinnitus as a plastic phenomenon and its possible neural underpinnings in the dorsal cochlear nucleus. Hear Res 206:200-226.
Kaltenbach JA, Zacharek MA, Zhang J, Frederick S (2004) Activity in the dorsal cochlear nucleus of hamsters previously tested for tinnitus following intense tone exposure. Neurosci Lett 355:121-125.
Kaltenbach JA, Rachel JD, Mathog TA, Zhang J, Falzarano PR, Lewandowski M (2002) Cisplatin-induced hyperactivity in the dorsal cochlear nucleus and its relation to outer hair cell loss: relevance to tinnitus. Journal of neurophysiology 88:699-714.
Kanold PO, Manis PB (1999) Transient potassium currents regulate the discharge patterns of dorsal cochlear nucleus pyramidal cells. The Journal of neuroscience : the official journal of the Society for Neuroscience 19:2195-2208.
Kehne JH, Davis M (1984) Strychnine increases acoustic startle amplitude but does not alter short-term or long-term habituation. Behav Neurosci 98:955-968.
Kharkovets T, Hardelin JP, Safieddine S, Schweizer M, El-Amraoui A, Petit C, Jentsch TJ (2000) KCNQ4, a K+ channel mutated in a form of dominant deafness, is expressed in the inner ear and the central auditory pathway. Proc Natl Acad Sci U S A 97:4333-4338.
Kitagawa J, Takeda M, Suzuki I, Kadoi J, Tsuboi Y, Honda K, Matsumoto S, Nakagawa H, Tanabe A, Iwata K (2006) Mechanisms involved in modulation of trigeminal primary afferent activity in rats with peripheral mononeuropathy. The European journal of neuroscience 24:1976-1986.
Klassen T, Davis C, Goldman A, Burgess D, Chen T, Wheeler D, McPherson J, Bourquin T, Lewis L, Villasana D, Morgan M, Muzny D, Gibbs R, Noebels J (2011) Exome sequencing of ion channel genes reveals complex profiles confounding personal risk assessment in epilepsy. Cell 145:1036-1048.
Koch U, Braun M, Kapfer C, Grothe B (2004) Distribution of HCN1 and HCN2 in rat auditory brainstem nuclei. The European journal of neuroscience 20:79-91.
Koehler SD, Shore SE (2013) Stimulus timing-dependent plasticity in dorsal cochlear nucleus is altered in tinnitus. The Journal of neuroscience : the official journal of the Society for Neuroscience 33:19647-19656.
Koyama S, Appel SB (2006) Characterization of M-current in ventral tegmental area dopamine neurons. Journal of neurophysiology 96:535-543.
Kujawa SG, Liberman MC (2006) Acceleration of age-related hearing loss by early noise exposure: evidence of a misspent youth. The Journal of neuroscience : the official journal of the Society for Neuroscience 26:2115-2123.
Kullmann DM (2002) The neuronal channelopathies. Brain : a journal of neurology 125:1177-1195.
Kvestad E, Czajkowski N, Engdahl B, Hoffman HJ, Tambs K (2010) Low heritability of tinnitus: results from the second Nord-Trondelag health study. Archives of otolaryngology--head & neck surgery 136:178-182.
Leao RM, Li S, Doiron B, Tzounopoulos T (2012) Diverse levels of an inwardly rectifying potassium conductance generate heterogeneous neuronal behavior in a population of dorsal cochlear nucleus pyramidal neurons. J Neurophysiol 107:3008-3019.
Leaver AM, Renier L, Chevillet MA, Morgan S, Kim HJ, Rauschecker JP (2011) Dysregulation of limbic and auditory networks in tinnitus. Neuron 69:33-43.
Lee DH, Chang L, Sorkin LS, Chaplan SR (2005) Hyperpolarization-activated, cation-nonselective, cyclic nucleotide-modulated channel blockade alleviates mechanical

allodynia and suppresses ectopic discharge in spinal nerve ligated rats. The journal of pain : official journal of the American Pain Society 6:417-424.
Lee Y, Lopez DE, Meloni EG, Davis M (1996) A primary acoustic startle pathway: obligatory role of cochlear root neurons and the nucleus reticularis pontis caudalis. The Journal of neuroscience : the official journal of the Society for Neuroscience 16:3775-3789.
Leitner DS, Hammond GR, Springer CP, Ingham KM, Mekilo AM, Bodison PR, Aranda MT, Shawaryn MA (1993) Parameters affecting gap detection in the rat. Perception & psychophysics 54:395-405.
LeMasson G, Marder E, Abbott LF (1993) Activity-dependent regulation of conductances in model neurons. Science 259:1915-1917.
Lewis AS, Estep CM, Chetkovich DM (2010) The fast and slow ups and downs of HCN channel regulation. Channels 4:215-231.
Li S, Choi V, Tzounopoulos T (2013) Pathogenic plasticity of Kv7.2/3 channel activity is essential for the induction of tinnitus. Proc Natl Acad Sci U S A 110:9980-9985.
Li Y, Gamper N, Hilgemann DW, Shapiro MS (2005) Regulation of Kv7 (KCNQ) K+ channel open probability by phosphatidylinositol 4,5-bisphosphate. The Journal of neuroscience : the official journal of the Society for Neuroscience 25:9825-9835.
Liberman MC (1990) Quantitative assessment of inner ear pathology following ototoxic drugs or acoustic trauma. Toxicologic pathology 18:138-148.
Liberman MC, Kiang NY (1978) Acoustic trauma in cats. Cochlear pathology and auditory-nerve activity. Acta oto-laryngologica Supplementum 358:1-63.
Linley JE, Rose K, Patil M, Robertson B, Akopian AN, Gamper N (2008) Inhibition of M current in sensory neurons by exogenous proteases: a signaling pathway mediating inflammatory nociception. The Journal of neuroscience : the official journal of the Society for Neuroscience 28:11240-11249.
Liu B, Linley JE, Du X, Zhang X, Ooi L, Zhang H, Gamper N (2010) The acute nociceptive signals induced by bradykinin in rat sensory neurons are mediated by inhibition of M-type K+ channels and activation of Ca2+-activated Cl- channels. The Journal of clinical investigation 120:1240-1252.
Liu Z, Golowasch J, Marder E, Abbott LF (1998) A model neuron with activity-dependent conductances regulated by multiple calcium sensors. The Journal of neuroscience : the official journal of the Society for Neuroscience 18:2309-2320.
Liu Z, Bunney EB, Appel SB, Brodie MS (2003) Serotonin reduces the hyperpolarization-activated current (Ih) in ventral tegmental area dopamine neurons: involvement of 5-HT2 receptors and protein kinase C. Journal of neurophysiology 90:3201-3212.
Llinas R, Urbano FJ, Leznik E, Ramirez RR, van Marle HJ (2005) Rhythmic and dysrhythmic thalamocortical dynamics: GABA systems and the edge effect. Trends Neurosci 28:325-333.
Lobarinas E, Hayes SH, Allman BL (2013) The gap-startle paradigm for tinnitus screening in animal models: limitations and optimization. Hear Res 295:150-160.
Longenecker RJ, Galazyuk AV (2011) Development of tinnitus in CBA/CaJ mice following sound exposure. Journal of the Association for Research in Otolaryngology : JARO 12:647-658.
Longenecker RJ, Chonko KT, Maricich SM, Galazyuk AV (2014) Age effects on tinnitus and hearing loss in CBA/CaJ mice following sound exposure. SpringerPlus 3:542.

Lupica CR, Bell JA, Hoffman AF, Watson PL (2001) Contribution of the hyperpolarization-activated current (I(h)) to membrane potential and GABA release in hippocampal interneurons. Journal of neurophysiology 86:261-268.

Luszczki JJ (2009) Third-generation antiepileptic drugs: mechanisms of action, pharmacokinetics and interactions. Pharmacol Rep 61:197-216.

Luszczki JJ, Wu JZ, Raszewski G, Czuczwar SJ (2009) Isobolographic characterization of interactions of retigabine with carbamazepine, lamotrigine, and valproate in the mouse maximal electroshock-induced seizure model. Naunyn-Schmiedeberg's archives of pharmacology 379:163-179.

Ma WL, Hidaka H, May BJ (2006) Spontaneous activity in the inferior colliculus of CBA/J mice after manipulations that induce tinnitus. Hear Res 212:9-21.

Mackie AR, Byron KL (2008) Cardiovascular KCNQ (Kv7) potassium channels: physiological regulators and new targets for therapeutic intervention. Molecular pharmacology 74:1171-1179.

MacLean JN, Zhang Y, Johnson BR, Harris-Warrick RM (2003) Activity-independent homeostasis in rhythmically active neurons. Neuron 37:109-120.

Magee JC (1998) Dendritic hyperpolarization-activated currents modify the integrative properties of hippocampal CA1 pyramidal neurons. The Journal of neuroscience : the official journal of the Society for Neuroscience 18:7613-7624.

Magee JC (1999) Dendritic Ih normalizes temporal summation in hippocampal CA1 neurons. Nature neuroscience 2:848.

Maljevic S, Wuttke TV, Lerche H (2008) Nervous system KV7 disorders: breakdown of a subthreshold brake. The Journal of physiology 586:1791-1801.

Maljevic S, Wuttke TV, Seebohm G, Lerche H (2010) KV7 channelopathies. Pflugers Arch 460:277-288.

Maljevic S, Lerche C, Seebohm G, Alekov AK, Busch AE, Lerche H (2003) C-terminal interaction of KCNQ2 and KCNQ3 K+ channels. The Journal of physiology 548:353-360.

Manis PB (1990) Membrane properties and discharge characteristics of guinea pig dorsal cochlear nucleus neurons studied in vitro. The Journal of neuroscience : the official journal of the Society for Neuroscience 10:2338-2351.

Manzoor NF, Chen G, Kaltenbach JA (2013) Suppression of noise-induced hyperactivity in the dorsal cochlear nucleus following application of the cholinergic agonist, carbachol. Brain Res 1523:28-36.

Marder E, Goaillard JM (2006) Variability, compensation and homeostasis in neuron and network function. Nature reviews Neuroscience 7:563-574.

Marrion NV (1997) Control of M-current. Annual review of physiology 59:483-504.

Masterton RB, Granger EM, Glendenning KK (1994) Role of acoustic striae in hearing: mechanism for enhancement of sound detection in cats. Hear Res 73:209-222.

Mazurek B, Haupt H, Olze H, Szczepek AJ (2012) Stress and tinnitus-from bedside to bench and back. Frontiers in systems neuroscience 6:47.

Melcher JR, Sigalovsky IS, Guinan JJ, Jr., Levine RA (2000) Lateralized tinnitus studied with functional magnetic resonance imaging: abnormal inferior colliculus activation. J Neurophysiol 83:1058-1072.

Mellott JG, Motts SD, Schofield BR (2011) Multiple origins of cholinergic innervation of the cochlear nucleus. Neuroscience 180:138-147.

Middleton JW, Tzounopoulos T (2012) Imaging the neural correlates of tinnitus: a comparison between animal models and human studies. Frontiers in systems neuroscience 6:35.
Middleton JW, Kiritani T, Pedersen C, Turner JG, Shepherd GM, Tzounopoulos T (2011) Mice with behavioral evidence of tinnitus exhibit dorsal cochlear nucleus hyperactivity because of decreased GABAergic inhibition. Proc Natl Acad Sci U S A 108:7601-7606.
Misonou H (2010) Homeostatic regulation of neuronal excitability by K(+) channels in normal and diseased brains. The Neuroscientist : a review journal bringing neurobiology, neurology and psychiatry 16:51-64.
Moller AR (2007) Tinnitus and pain. Prog Brain Res 166:47-53.
Momin A, Cadiou H, Mason A, McNaughton PA (2008) Role of the hyperpolarization-activated current Ih in somatosensory neurons. The Journal of physiology 586:5911-5929.
Muhlnickel W, Elbert T, Taub E, Flor H (1998) Reorganization of auditory cortex in tinnitus. Proc Natl Acad Sci U S A 95:10340-10343.
Nakajo K, Kubo Y (2005) Protein kinase C shifts the voltage dependence of KCNQ/M channels expressed in Xenopus oocytes. The Journal of physiology 569:59-74.
Noam Y, Bernard C, Baram TZ (2011) Towards an integrated view of HCN channel role in epilepsy. Current opinion in neurobiology 21:873-879.
Noam Y, Zha Q, Phan L, Wu RL, Chetkovich DM, Wadman WJ, Baram TZ (2010) Trafficking and surface expression of hyperpolarization-activated cyclic nucleotide-gated channels in hippocampal neurons. The Journal of biological chemistry 285:14724-14736.
Norena AJ, Eggermont JJ (2003) Changes in spontaneous neural activity immediately after an acoustic trauma: implications for neural correlates of tinnitus. Hear Res 183:137-153.
Notomi T, Shigemoto R (2004) Immunohistochemical localization of Ih channel subunits, HCN1-4, in the rat brain. The Journal of comparative neurology 471:241-276.
O'Leary T, van Rossum MC, Wyllie DJ (2010) Homeostasis of intrinsic excitability in hippocampal neurones: dynamics and mechanism of the response to chronic depolarization. The Journal of physiology 588:157-170.
O'Leary T, Williams AH, Caplan JS, Marder E (2013) Correlations in ion channel expression emerge from homeostatic tuning rules. Proc Natl Acad Sci U S A 110:E2645-2654.
O'Leary T, Williams AH, Franci A, Marder E (2014) Cell types, network homeostasis, and pathological compensation from a biologically plausible ion channel expression model. Neuron 82:809-821.
Oertel D, Young ED (2004) What's a cerebellar circuit doing in the auditory system? Trends in neurosciences 27:104-110.
Pal B, Por A, Szucs G, Kovacs I, Rusznak Z (2003) HCN channels contribute to the intrinsic activity of cochlear pyramidal cells. Cellular and molecular life sciences : CMLS 60:2189-2199.
Pape HC (1996) Queer current and pacemaker: the hyperpolarization-activated cation current in neurons. Annual review of physiology 58:299-327.
Parham K, Bonaiuto G, Carlson S, Turner JG, D'Angelo WR, Bross LS, Fox A, Willott JF, Kim DO (2000) Purkinje cell degeneration and control mice: responses of single units in the dorsal cochlear nucleus and the acoustic startle response. Hearing Research 148:137-152.
Passmore GM, Selyanko AA, Mistry M, Al-Qatari M, Marsh SJ, Matthews EA, Dickenson AH, Brown TA, Burbidge SA, Main M, Brown DA (2003) KCNQ/M currents in sensory neurons: significance for pain therapy. The Journal of neuroscience : the official journal of the Society for Neuroscience 23:7227-7236.

Peters HC, Hu H, Pongs O, Storm JF, Isbrandt D (2005) Conditional transgenic suppression of M channels in mouse brain reveals functions in neuronal excitability, resonance and behavior. Nature neuroscience 8:51-60.

Pian P, Bucchi A, Robinson RB, Siegelbaum SA (2006) Regulation of gating and rundown of HCN hyperpolarization-activated channels by exogenous and endogenous PIP2. The Journal of general physiology 128:593-604.

Pilati N, Ison MJ, Barker M, Mulheran M, Large CH, Forsythe ID, Matthias J, Hamann M (2012) Mechanisms contributing to central excitability changes during hearing loss. Proc Natl Acad Sci U S A 109:8292-8297.

Pilz PK, Schnitzler HU, Menne D (1987) Acoustic startle threshold of the albino rat (Rattus norvegicus). Journal of comparative psychology 101:67-72.

Prinz AA, Bucher D, Marder E (2004) Similar network activity from disparate circuit parameters. Nature neuroscience 7:1345-1352.

Ratte S, Zhu Y, Lee KY, Prescott SA (2014) Criticality and degeneracy in injury-induced changes in primary afferent excitability and the implications for neuropathic pain. eLife 3:e02370.

Rauschecker JP, Leaver AM, Muhlau M (2010) Tuning out the noise: limbic-auditory interactions in tinnitus. Neuron 66:819-826.

Reetz O, Strauss U (2013) Protein kinase C activation inhibits rat and human hyperpolarization activated cyclic nucleotide gated channel (HCN)1--mediated current in mammalian cells. Cellular physiology and biochemistry : international journal of experimental cellular physiology, biochemistry, and pharmacology 31:532-541.

Richards MC, Heron SE, Spendlove HE, Scheffer IE, Grinton B, Berkovic SF, Mulley JC, Davy A (2004) Novel mutations in the KCNQ2 gene link epilepsy to a dysfunction of the KCNQ2-calmodulin interaction. Journal of medical genetics 41:e35.

Richichi C, Brewster AL, Bender RA, Simeone TA, Zha Q, Yin HZ, Weiss JH, Baram TZ (2008) Mechanisms of seizure-induced 'transcriptional channelopathy' of hyperpolarization-activated cyclic nucleotide gated (HCN) channels. Neurobiology of disease 29:297-305.

Roberts LE, Moffat G, Baumann M, Ward LM, Bosnyak DJ (2008) Residual inhibition functions overlap tinnitus spectra and the region of auditory threshold shift. Journal of the Association for Research in Otolaryngology : JARO 9:417-435.

Roberts LE, Eggermont JJ, Caspary DM, Shore SE, Melcher JR, Kaltenbach JA (2010) Ringing ears: the neuroscience of tinnitus. The Journal of neuroscience : the official journal of the Society for Neuroscience 30:14972-14979.

Robinson RB, Siegelbaum SA (2003) Hyperpolarization-activated cation currents: from molecules to physiological function. Annual review of physiology 65:453-480.

Ropp TJ, Tiedemann KL, Young ED, May BJ (2014) Effects of unilateral acoustic trauma on tinnitus-related spontaneous activity in the inferior colliculus. Journal of the Association for Research in Otolaryngology : JARO 15:1007-1022.

Rose K, Ooi L, Dalle C, Robertson B, Wood IC, Gamper N (2011) Transcriptional repression of the M channel subunit Kv7.2 in chronic nerve injury. Pain 152:742-754.

Saganich MJ, Machado E, Rudy B (2001) Differential expression of genes encoding subthreshold-operating voltage-gated K+ channels in brain. J Neurosci 21:4609-4624.

Salvi RJ, Wang J, Ding D (2000) Auditory plasticity and hyperactivity following cochlear damage. Hear Res 147:261-274.

Schaette R, McAlpine D (2011) Tinnitus with a normal audiogram: physiological evidence for hidden hearing loss and computational model. The Journal of neuroscience : the official journal of the Society for Neuroscience 31:13452-13457.
Schofield BR, Motts SD, Mellott JG (2011) Cholinergic cells of the pontomesencephalic tegmentum: connections with auditory structures from cochlear nucleus to cortex. Hear Res 279:85-95.
Scholz J, Woolf CJ (2007) The neuropathic pain triad: neurons, immune cells and glia. Nature neuroscience 10:1361-1368.
Schroeder BC, Kubisch C, Stein V, Jentsch TJ (1998) Moderate loss of function of cyclic-AMP-modulated KCNQ2/KCNQ3 K+ channels causes epilepsy. Nature 396:687-690.
Schwake M, Jentsch TJ, Friedrich T (2003) A carboxy-terminal domain determines the subunit specificity of KCNQ K+ channel assembly. EMBO reports 4:76-81.
Schwake M, Pusch M, Kharkovets T, Jentsch TJ (2000) Surface expression and single channel properties of KCNQ2/KCNQ3, M-type K+ channels involved in epilepsy. The Journal of biological chemistry 275:13343-13348.
Schwake M, Athanasiadu D, Beimgraben C, Blanz J, Beck C, Jentsch TJ, Saftig P, Friedrich T (2006) Structural determinants of M-type KCNQ (Kv7) K+ channel assembly. The Journal of neuroscience : the official journal of the Society for Neuroscience 26:3757-3766.
Seoh SA, Sigg D, Papazian DM, Bezanilla F (1996) Voltage-sensing residues in the S2 and S4 segments of the Shaker K+ channel. Neuron 16:1159-1167.
Shah MM, Huang Z, Martinello K (2013) HCN and KV7 (M-) channels as targets for epilepsy treatment. Neuropharmacology 69:75-81.
Shah MM, Anderson AE, Leung V, Lin X, Johnston D (2004) Seizure-induced plasticity of h channels in entorhinal cortical layer III pyramidal neurons. Neuron 44:495-508.
Shamgar L, Ma L, Schmitt N, Haitin Y, Peretz A, Wiener R, Hirsch J, Pongs O, Attali B (2006) Calmodulin is essential for cardiac IKS channel gating and assembly: impaired function in long-QT mutations. Circulation research 98:1055-1063.
Shargorodsky J, Curhan GC, Farwell WR (2010) Prevalence and characteristics of tinnitus among US adults. The American journal of medicine 123:711-718.
Sheen K, Chung JM (1993) Signs of neuropathic pain depend on signals from injured nerve fibers in a rat model. Brain Res 610:62-68.
Sheets PL, Suter BA, Kiritani T, Chan CS, Surmeier DJ, Shepherd GM (2011) Corticospinal-specific HCN expression in mouse motor cortex: I(h)-dependent synaptic integration as a candidate microcircuit mechanism involved in motor control. Journal of neurophysiology 106:2216-2231.
Shetake JA, Engineer ND, Vrana WA, Wolf JT, Kilgard MP (2012) Pairing tone trains with vagus nerve stimulation induces temporal plasticity in auditory cortex. Experimental neurology 233:342-349.
Shin M, Chetkovich DM (2007) Activity-dependent regulation of h channel distribution in hippocampal CA1 pyramidal neurons. The Journal of biological chemistry 282:33168-33180.
Simpson JJ, Davies WE (1999) Recent advances in the pharmacological treatment of tinnitus. Trends in pharmacological sciences 20:12-18.

Simpson JJ, Gilbert AM, Weiner GM, Davies WE (1999) The assessment of lamotrigine, an antiepileptic drug, in the treatment of tinnitus. The American journal of otology 20:627-631.

Singh NA, Westenskow P, Charlier C, Pappas C, Leslie J, Dillon J, Anderson VE, Sanguinetti MC, Leppert MF, Consortium BP (2003) KCNQ2 and KCNQ3 potassium channel genes in benign familial neonatal convulsions: expansion of the functional and mutation spectrum. Brain : a journal of neurology 126:2726-2737.

Soh H, Tzingounis AV (2010) The specific slow afterhyperpolarization inhibitor UCL2077 is a subtype-selective blocker of the epilepsy associated KCNQ channels. Mol Pharmacol 78:1088-1095.

Soldovieri MV, Miceli F, Taglialatela M (2011) Driving with no brakes: molecular pathophysiology of Kv7 potassium channels. Physiology (Bethesda) 26:365-376.

Suh BC, Hille B (2002) Recovery from muscarinic modulation of M current channels requires phosphatidylinositol 4,5-bisphosphate synthesis. Neuron 35:507-520.

Sun Q, Tu H, Xing GG, Han JS, Wan Y (2005) Ectopic discharges from injured nerve fibers are highly correlated with tactile allodynia only in early, but not late, stage in rats with spinal nerve ligation. Experimental neurology 191:128-136.

Sutherland DP, Masterton RB, Glendenning KK (1998) Role of acoustic striae in hearing: reflexive responses to elevated sound-sources. Behavioural brain research 97:1-12.

Tatulian L, Delmas P, Abogadie FC, Brown DA (2001) Activation of expressed KCNQ potassium currents and native neuronal M-type potassium currents by the anti-convulsant drug retigabine. The Journal of neuroscience : the official journal of the Society for Neuroscience 21:5535-5545.

Taylor J, Jacoby A, Baker GA, Marson AG, Ring A, Whitehead M (2011) Factors predictive of resilience and vulnerability in new-onset epilepsy. Epilepsia 52:610-618.

Tonndorf J (1987) The analogy between tinnitus and pain: a suggestion for a physiological basis of chronic tinnitus. Hear Res 28:271-275.

Turner JG, Parrish J (2008) Gap detection methods for assessing salicylate-induced tinnitus and hyperacusis in rats. American journal of audiology 17:S185-192.

Turner JG, Brozoski TJ, Bauer CA, Parrish JL, Myers K, Hughes LF, Caspary DM (2006a) Gap detection deficits in rats with tinnitus: a potential novel screening tool. In: Behav Neurosci, pp 188-195.

Turner JG, Brozoski TJ, Bauer CA, Parrish JL, Myers K, Hughes LF, Caspary DM (2006b) Gap detection deficits in rats with tinnitus: a potential novel screening tool. Behav Neurosci 120:188-195.

Turrigiano G (2007) Homeostatic signaling: the positive side of negative feedback. Current opinion in neurobiology 17:318-324.

Turrigiano GG (2008) The self-tuning neuron: synaptic scaling of excitatory synapses. Cell 135:422-435.

Tyler RS, Oleson J, Noble W, Coelho C, Ji H (2007) Clinical trials for tinnitus: study populations, designs, measurement variables, and data analysis. Progress in brain research 166:499-509.

Tzingounis AV, Nicoll RA (2008) Contribution of KCNQ2 and KCNQ3 to the medium and slow afterhyperpolarization currents. Proc Natl Acad Sci U S A 105:19974-19979.

Tzounopoulos T, Kim Y, Oertel D, Trussell LO (2004a) Cell-specific, spike timing-dependent plasticities in the dorsal cochlear nucleus. Nature Neuroscience 7:719-725.

Tzounopoulos T, Kim Y, Oertel D, Trussell LO (2004b) Cell-specific, spike timing-dependent plasticities in the dorsal cochlear nucleus. Nature neuroscience 7:719-725.
van Welie I, van Hooft JA, Wadman WJ (2004) Homeostatic scaling of neuronal excitability by synaptic modulation of somatic hyperpolarization-activated Ih channels. Proc Natl Acad Sci U S A 101:5123-5128.
Vartiainen N, Kirveskari E, Kallio-Laine K, Kalso E, Forss N (2009) Cortical reorganization in primary somatosensory cortex in patients with unilateral chronic pain. J Pain 10:854-859.
Vogler DP, Robertson D, Mulders WH (2011) Hyperactivity in the ventral cochlear nucleus after cochlear trauma. The Journal of neuroscience : the official journal of the Society for Neuroscience 31:6639-6645.
von der Behrens W (2014) Animal models of subjective tinnitus. Neural plasticity 2014:741452.
von Hehn CA, Baron R, Woolf CJ (2012) Deconstructing the neuropathic pain phenotype to reveal neural mechanisms. Neuron 73:638-652.
Wahl-Schott C, Biel M (2009) HCN channels: structure, cellular regulation and physiological function. Cellular and molecular life sciences : CMLS 66:470-494.
Wang H, Brozoski TJ, Caspary DM (2011) Inhibitory neurotransmission in animal models of tinnitus: maladaptive plasticity. Hear Res 279:111-117.
Wang H, Brozoski TJ, Turner JG, Ling L, Parrish JL, Hughes LF, Caspary DM (2009) Plasticity at glycinergic synapses in dorsal cochlear nucleus of rats with behavioral evidence of tinnitus. Neuroscience 164:747-759.
Wang HS, Brown BS, McKinnon D, Cohen IS (2000) Molecular basis for differential sensitivity of KCNQ and I(Ks) channels to the cognitive enhancer XE991. Molecular pharmacology 57:1218-1223.
Wang HS, Pan Z, Shi W, Brown BS, Wymore RS, Cohen IS, Dixon JE, McKinnon D (1998) KCNQ2 and KCNQ3 potassium channel subunits: molecular correlates of the M-channel. Science 282:1890-1893.
Wang Y, Hirose K, Liberman MC (2002) Dynamics of noise-induced cellular injury and repair in the mouse cochlea. Journal of the Association for Research in Otolaryngology : JARO 3:248-268.
Weisz N, Wienbruch C, Dohrmann K, Elbert T (2005) Neuromagnetic indicators of auditory cortical reorganization of tinnitus. Brain : a journal of neurology 128:2722-2731.
Wen H, Levitan IB (2002) Calmodulin is an auxiliary subunit of KCNQ2/3 potassium channels. The Journal of neuroscience : the official journal of the Society for Neuroscience 22:7991-8001.
Woolf CJ (1983) Evidence for a central component of post-injury pain hypersensitivity. Nature 306:686-688.
Wu WW, Chan CS, Surmeier DJ, Disterhoft JF (2008) Coupling of L-type Ca2+ channels to KV7/KCNQ channels creates a novel, activity-dependent, homeostatic intrinsic plasticity. Journal of neurophysiology 100:1897-1908.
Wulff H, Castle NA, Pardo LA (2009) Voltage-gated potassium channels as therapeutic targets. Nat Rev Drug Discov 8:982-1001.
Wuttke TV, Jurkat-Rott K, Paulus W, Garncarek M, Lehmann-Horn F, Lerche H (2007) Peripheral nerve hyperexcitability due to dominant-negative KCNQ2 mutations. Neurology 69:2045-2053.

Xie W, Strong JA, Li H, Zhang JM (2007) Sympathetic sprouting near sensory neurons after nerve injury occurs preferentially on spontaneously active cells and is reduced by early nerve block. Journal of neurophysiology 97:492-502.

Xie W, Strong JA, Meij JT, Zhang JM, Yu L (2005) Neuropathic pain: early spontaneous afferent activity is the trigger. Pain 116:243-256.

Xiong Q, Sun H, Zhang Y, Nan F, Li M (2008) Combinatorial augmentation of voltage-gated KCNQ potassium channels by chemical openers. Proc Natl Acad Sci U S A 105:3128-3133.

Yang S, Weiner BD, Zhang LS, Cho SJ, Bao S (2011) Homeostatic plasticity drives tinnitus perception in an animal model. Proc Natl Acad Sci U S A 108:14974-14979.

Yankaskas K (2012) Prelude: Noise-induced tinnitus and hearing loss in the military. Hear Res.

Yankaskas K (2013) Prelude: noise-induced tinnitus and hearing loss in the military. Hear Res 295:3-8.

Yao H, Donnelly DF, Ma C, LaMotte RH (2003) Upregulation of the hyperpolarization-activated cation current after chronic compression of the dorsal root ganglion. The Journal of neuroscience : the official journal of the Society for Neuroscience 23:2069-2074.

Yao X, Rarey KE (1996) Localization of the mineralocorticoid receptor in rat cochlear tissue. Acta oto-laryngologica 116:493-496.

Ying SW, Tibbs GR, Picollo A, Abbas SY, Sanford RL, Accardi A, Hofmann F, Ludwig A, Goldstein PA (2011) PIP2-mediated HCN3 channel gating is crucial for rhythmic burst firing in thalamic intergeniculate leaflet neurons. The Journal of neuroscience : the official journal of the Society for Neuroscience 31:10412-10423.

Young ED, Spirou GA, Rice JJ, Voigt HF (1992) Neural organization and responses to complex stimuli in the dorsal cochlear nucleus. Philosophical transactions of the Royal Society of London Series B, Biological sciences 336:407-413.

Yue C, Yaari Y (2004) KCNQ/M channels control spike afterdepolarization and burst generation in hippocampal neurons. The Journal of neuroscience : the official journal of the Society for Neuroscience 24:4614-4624.

Zacharek MA, Kaltenbach JA, Mathog TA, Zhang J (2002) Effects of cochlear ablation on noise induced hyperactivity in the hamster dorsal cochlear nucleus: implications for the origin of noise induced tinnitus. Hear Res 172:137-143.

Zachos G, Zoumpourlis V, Sekeris C, Spandidos D (1995) Binding of the glucocorticoid and estrogen-receptors to the human h-ras oncogene sequences. International journal of oncology 6:595-600.

Zaika O, Tolstykh GP, Jaffe DB, Shapiro MS (2007) Inositol triphosphate-mediated Ca2+ signals direct purinergic P2Y receptor regulation of neuronal ion channels. The Journal of neuroscience : the official journal of the Society for Neuroscience 27:8914-8926.

Zaydman MA, Cui J (2014) PIP2 regulation of KCNQ channels: biophysical and molecular mechanisms for lipid modulation of voltage-dependent gating. Frontiers in physiology 5:195.

Zaydman MA, Silva JR, Cui J (2012) Ion channel associated diseases: overview of molecular mechanisms. Chemical reviews 112:6319-6333.

Zaydman MA, Silva JR, Delaloye K, Li Y, Liang H, Larsson HP, Shi J, Cui J (2013) Kv7.1 ion channels require a lipid to couple voltage sensing to pore opening. Proc Natl Acad Sci U S A 110:13180-13185.

Zeng C, Yang Z, Shreve L, Bledsoe S, Shore S (2012) Somatosensory projections to cochlear nucleus are upregulated after unilateral deafness. The Journal of neuroscience : the official journal of the Society for Neuroscience 32:15791-15801.

Zhang H, Craciun LC, Mirshahi T, Rohacs T, Lopes CM, Jin T, Logothetis DE (2003) PIP(2) activates KCNQ channels, and its hydrolysis underlies receptor-mediated inhibition of M currents. Neuron 37:963-975.

Zhang JS, Kaltenbach JA (1998) Increases in spontaneous activity in the dorsal cochlear nucleus of the rat following exposure to high-intensity sound.[erratum appears in Neurosci Lett 1998 Aug 14;252(2):668]. Neuroscience Letters 250:197-200.

Zhang JS, Kaltenbach JA, Godfrey DA, Wang J (2006) Origin of hyperactivity in the hamster dorsal cochlear nucleus following intense sound exposure. J Neurosci Res 84:819-831.

Zhao Y, Tzounopoulos T (2011) Physiological activation of cholinergic inputs controls associative synaptic plasticity via modulation of endocannabinoid signaling. The Journal of neuroscience : the official journal of the Society for Neuroscience 31:3158-3168.

Zhao Y, Rubio M, Tzounopoulos T (2011) Mechanisms underlying input-specific expression of endocannabinoid-mediated synaptic plasticity in the dorsal cochlear nucleus. Hear Res 279:67-73.

Zolles G, Klocker N, Wenzel D, Weisser-Thomas J, Fleischmann BK, Roeper J, Fakler B (2006) Pacemaking by HCN channels requires interaction with phosphoinositides. Neuron 52:1027-1036.